

https://dspace.org/

Optimisation and validation of a nanofluidic real-time qPCR assay for the detection and serotyping of Klebsiella pneumoniae

Van Der Merwe, Lara

2025
University of the Witwatersrand, Johannesburg
https://hdl.handle.net/10539/48187

Van Der Merwe, Lara. (2025). Optimisation and validation of a nanofluidic real-time qPCR assay for the detection and serotyping of Klebsiella pneumoniae [Master`s dissertation, University of the Witwatersrand, Johannesburg]. WIReDSpace. https://hdl.handle.net/10539/48187

Downloaded from a DSpace repository. https://dspace.org/

Optimisation and validation of a nanofluidic real-time qPCR assay for the detection and serotyping of *Klebsiella pneumoniae.*

A DISSERTATION BY **LARA VAN DER MERWE (Student no. 827385)**



SUBMITTED IN FULFILMENT OF THE REQUIREMENTS FOR THE DEGREE OF

MASTER OF SCIENCE IN MEDICINE (BY RESEARCH)

FROM THE **FACULTY OF HEALTH SCIENCES**

AT THE **UNIVERSITY OF THE WITWATERSRAND, JOHANNESBURG**

UNDER THE **DEPARTMENT OF CLINICAL MICROBIOLOGY AND INFECTIOUS DISEASES**

IN THE **SCHOOL OF PATHOLOGY**

Project Supervisors:	**Dr. Courtney Olwagen**
	Dr. Vicky Baillie
	Prof. Shabir Madhi
Date of Submission:	**29 May 2025**

DECLARATION

I, **Lara van der Merwe (827385)**, declare that this Dissertation is my own, unaided work. It is being submitted for the Degree of Master of Science in Medicine (Clinical Microbiology and Infectious Diseases) at the University of the Witwatersrand, Johannesburg. It has not been submitted before for any degree or examination at any other University.

L. van der Merwe

Candidate's Signature

29th day of **May 2025** in **Johannesburg**

ABSTRACT

Introduction: *Klebsiella pneumoniae* is a leading cause of neonatal sepsis in Sub-Saharan Africa. Robust surveillance systems and methods that allow for fast and reliable serotype detection are needed to guide research priorities and direct interventions aimed at reducing the burden of *K. pneumoniae* induced disease.

Method: A high throughput nanofluidic qPCR reaction set was developed to detect and serotype thirteen lipopolysaccharide (O) loci (OL: O1/O2v1, O1/O2v2, O1/O2v3, O3/O3a, O3b, O4, O5, O8, O12, OL101, OL102, OL103, OL104), five O-antigen serotypes (O1, O2a, O2ac, O2afg, O2aeh), and fifteen capsular loci (KL: KL2, KL3, KL10, KL15, KL22, KL25, KL28, KL30, KL37, KL39, KL62, KL102, KL110, KL149, KL171) of *K. pneumoniae*. Additional assays to discriminate *K. pneumoniae* from other strains in the Klebsiella Species Complex (KpSC) and *Escherichia coli* were also included in the nanofluidic qPCR reaction set. The optimised reaction set was validated using 77 invasive *K. pneumoniae* isolates from South African infants ≤90 days old, previously serotyped by WGS and the Kaptive v2.3 pipeline, and 83 archived colonisation swab samples (skin, rectal, nasal) enriched in brain heart infusion (BHI) broth. Isolates from the same BHI samples were serotyped using WGS and Kaptive v2.3. Statistical performance of the qPCR method was evaluated against WGS using sensitivity, specificity, and ROC-AUC metrics.

Results: All assays within the nanofluidic qPCR reaction set effectively amplified all 37 targets within the prescribed efficiency range (92-107%). The variance from the linear equation of the regression curve was low (r^2>0.99) while the analytical sensitivity was high (limit of detection: 10-100 gene equivalents). A blind analysis of the 77 invasive isolates and 83 colonisation swab samples enriched in BHI showed perfect concordance (k*appa*=1) between qPCR and WGS for the detection of all O-loci, O antigen types, and K-loci included in the nanofluidic qPCR panel. The nanofluidic qPCR method, which enables the detection of multiple *K. pneumoniae* strains, was applied directly to swab samples (rather than cultured isolates). This *de novo* testing identified concurrent colonisation with two or more K-loci and O-loci in 38% (16/42) and 40% (33/83) of swab samples enriched in BHI broth, respectively.

Conclusion: The nanofluidic qPCR method is a promising method for detecting and serotyping *K. pneumoniae* across multiple sample types (i.e. bacterial isolates and direct swab samples - nasopharyngeal, skin, and rectal). The established qPCR assay may be useful in probing the epidemiology of *K. pneumoniae*, including comprehensive serotyping of temporal changes in colonising and invasive isolates should interventions be established against *K. pneumoniae* invasive disease.

Keywords: *Klebsiella pneumoniae*, Nanofluidic PCR, Serotyping, Neonatal Sepsis, Sub-Saharan Africa

CONFERENCE PRESENTATIONS

1. 10th FIDSSA Congress, 30 May – 01 June 2024

   Development and evaluation of a nanofluidic qPCR technique for *Klebsiella pneumoniae* serotyping.

   Flash Presentations (Winner)

2. Faculty of Health Science Research Day, 5 September 2024

   Optimisation and validation of a nanofluidic qPCR method for serotyping *Klebsiella pneumoniae.*

   Oral Presentation

3. 1st Klebsiella Epidemiology and Biology Symposium, 20th - 22nd November 2024

   Optimisation and validation of a nanofluidic real-time qPCR assay for the detection and serotyping of *Klebsiella pneumoniae*.

   Poster Presentation

ACKNOWLEDGEMENTS

I would like to express my gratitude to the following individuals for their invaluable contributions to the completion of this dissertation.

1. To my co-supervisors, Courtney Olwagen and Vicky Baillie - your guidance and mentorship have been invaluable throughout this journey. Thank you for shaping me into the scientist I am today, for your unwavering support, and for refining my work with patience and precision. I deeply appreciate your keen eye for clarity, your encouragement, and helping me to develop my skill for scientific writing.

2. To Prof. Madhi, thank you for giving me the opportunity to pursue this journey and for fostering such a valuable learning experience.

3. To my parents, René and Piet van der Merwe, thank you for raising me to not be a sheep, and to always strive for more. The blueprint you've given me is strong and has given me the courage to embark on this journey. A special thank you to my mother for her invaluable help in drawing of the figures - I truly appreciate your support and effort.

4. To Jeanine du Plessis - my lab partner, my diatomic molecule, and my friend - thank you for being both a soundboard and a voice of reason. You are a pillar in my life, and I am deeply grateful for your unwavering support over the past decade. Your dedication and brilliance are truly an inspiration to women in science.

5. To Dietrich de Beer, thank you for your constant love and support throughout this journey. You are one of my favourite people, and I'm especially grateful for your keen eye and exceptional proofreading skills in reviewing my dissertation.

6. To my dearest Ouma Baba, thank you for nourishing not just my body, but also my spirit when I was too busy to care for myself. Your unwavering support, endless love, and boundless belief in me have been a source of strength and encouragement. You are my greatest cheerleader and a true blessing in my life. I am forever grateful for you.

7. To all my friends, family, VIDA personnel, and members of the WAM choir, thank you for your support and presence in my life. I wouldn't be the person I am today without you, and you all hold a special place in my heart.

8. Finally, to my husband, Mendy Hymanson - no words can truly capture the depth of your support. Thank you for grounding me when my mind was scattered and for always reminding me how much you believe in me. Your wholehearted love and encouragement mean everything.

TABLE OF CONTENTS

PREAMBLE

Declaration i
Abstract ii
Conference Presentations iii
Acknowledgements iv
Table of Contents v
List of Figures vii
List of Tables ix
Nomenclature x
CHAPTER 1: INTRODUCTION 1
1.1. Background & Study Context 1
1.2. Clinical & Public Health Significance of *K. pneumoniae* 2
1.2.1. Multi-drug resistance 2
1.2.2. Treatment and preventative strategy development 3
1.2.3. Key virulence factors & serotypes of *K. pneumoniae* 3
1.2.4. *K. pneumoniae* phylogenetic complex 10
1.3. Detection and Subtyping Methods of *K. pneumoniae* 11
1.3.1. Culture-based methods: 11
1.3.2. Enzyme-Linked Immunosorbent Assay (ELISA): 11
1.3.3. Whole-Genome Sequencing (WGS): 12
1.3.4. Targeted sequencing of the *wzi* gene: 12
1.3.5. Polymerase Chain Reaction (PCR): 12
1.4. Study Justification 13
CHAPTER 2: METHODOLOGY 16
2.1. Assay Design 16
2.2. Assay Optimisation 23
2.2.1. Specificity and sensitivity controls 23
2.2.2. IFC Standard BioTools BioMark™ HD nanofluidic qPCR loading, sample, and assay preparation 26
2.2.3. Optimisation performance 29
2.3. Assay Validation 29
2.3.1. Samples for validation 29
2.3.2. Extraction and quantification of bacterial isolates and enriched BHI broth from swab samples 30
2.3.3. Sample testing for validation 30

2.4. Statistical Analysis 31
2.5. Ethical Approval 32
CHAPTER 3: RESULTS 33
3.1. Performance of the nanofluidic real-time PCR system 33
3.1.1. Analytical performance of the nanofluidic real-time qPCR 33
3.1.2. Analytical sensitivity and specificity 33
3.2. Diagnostic sensitivity, specificity, and agreement of the nanofluidic qPCR reaction set for the detection of *K. pneumoniae* K-loci, O-loci, and O-types in bacterial cultures compared with whole genome sequencing 37
3.3. Diagnostic sensitivity, specificity, and agreement of the nanofluidic qPCR reaction set for the detection of *K. pneumoniae* K-loci, O-loci, and O-types in swab samples enriched in BHI compared with whole genome sequencing 39
3.4. Observation of *K. pneumoniae* co-colonisation 42
CHAPTER 4: DISCUSSION & CONCLUSION 46
CHAPTER 5: REFERENCES 51
Appendix A: Turnit in Report 61
Appendix B: Ethics Certificate: Correlates of protection study, HREC number: 181110 63
Appendix C Ethics Certificate: Epidemiology of community and hospital-acquired invasive infections in young infants, HREC number: M200932 65
Appendix D Ethics Certificate: Optimisation and validation of a nanofluidic real-time qPCR assay for the detection and serotyping of *Klebsiella pneumoniae*, (M231117). 66

LIST OF FIGURES

Figure 1.1 Structural representation of K. pneumoniae and its surface polysaccharides (45).4

Figure 1.2 The representative CPS locus arrangement adapted from Patro et al. 2019 (58). 5

Figure 1.3 The rfb gene cluster for O3, O4, O5, O8, O12, OL101, OL102, OL103, and OL104 (46). 8

Figure 1.4 Genes present in the O1/O2 locus, and differences among variants. Adapted from Kaptive v2.3 (21). 9

Figure 1.5 Arrangement of the genetic determinants responsible for O-antigen biosynthesis in K. pneumoniae serotypes derived from O2a. Adapted from Clarke et, al. (82). 10

Figure 1.6 Phylogenic Tree exemplifying relationships within the K. pneumoniae species complex (red), Klebsiella genus (black) and Enterobacteriaceae family (grey) (85)..... 11

Figure 1.7 K-loci distribution of invasive K. pneumoniae causing disease in neonates <90 days (N=239) in South Africa between 2018 and 2022. Adapted from Olwagen et. al, (15). K-loci that were targeted highlighted in purple. 14

Figure 2.1 Example of (A) alignment of the wzc gene within the Capsular polysaccharide region from available KL15 strains and (B) the global distribution of the aligned KL15 strains. Sequences were trimmed and processed using the captive pipeline before alignment to ensure accurate identification of the conserved regions between global strains. The conserved region of the KL15 CPS is highlighted in black in Figure A. 17

Figure 2.2 Basic Alignment Mapping of wzc gene in the CPS cluster for the 15 K-loci included in the final nanofluidic qPCR reaction set. 18

Figure 2.3: Screenshot of alignment of the wzc gene of 20 K-loci (KL14-KL33). Locked Nucleic Acid (LNA) probe, highlighted by the black box, targeting the wzc gene of the KL15 capsular polysaccharide synthesis gene cluster. 19

Figure 2.4 Diagram of the STA nano-fluidic high throughput real-time qPCR workflow, within the 96.96 Gene Expression Dynamic Array integrated fluidic circuit (IFC) (Standard BioTools). 27

Figure 3.1 *O-loci detections using 77 cultures tested on a nanofluidic qPCR compared to prediction of Kaptive v2.3. No isolates available for O3/O3a, O8, O12, OL101, OL102, OL103, and OL104 for validation in cohort..* 38

Figure 3.2 *comparison of the nanofluidic real-time PCR and sequencing (Kaptive v2.3) results for typing the O1/O2 complex in 55 isolates. The analysis focused on O1v2, O2afg, O1v1, and O2a, while O2ac and O2aeh isolates were not available in the cohort for validation. Other O-serotypes were represented by different O-loci due to a 1:1 ratio with the O-types, removing the need for additional assays.* 38

Figure 3.3 *K-loci detections using cultures tested on a nanofluidic qPCR compared to prediction of Kaptive v2.3 (N=71). No bacterial isolates available for KL10, KL15, KL22, KL37, KL39, and KL171 in cohort to compare.* 39

Figure 3.4 *Overall distribution of 83 enriched broths of 9 K-loci detected by traditional culturing that were sequenced (purple) compared to direct enrichment tested on nanofluidic real-time qPCR (green) in neonates. The diagnostic performance of the nanofluidic qPCR method could*

not be assessed for assay sets targeting KL2, KL171, KL37, KL22, KL149, and KL28, which were not detected in any clinical isolates by WGS in the TNC study. 40

Figure 3.5 *The overall prevalence of 83 O-loci detected by traditional culturing that were sequenced (purple) compared to direct enrichment tested on nanofluidic real-time qPCR (green) in neonates. The diagnostic performance of the nanofluidic qPCR method could not be assessed for assay sets targeting O1/O2v3, OL104, OL013, OL101, O2aeh, and O2ac, which were not detected in any clinical isolates by WGS in the TNC study.* 41

Figure 3.6 *Overall prevalence of 44 O-types of the O1/O2 complex detected by traditional culturing that were sequenced (purple) compared to direct enrichment tested on nanofluidic qPCR (green) performed using nanofluidic real-time qPCR in neonates. The diagnostic performance of the nanofluidic qPCR method could not be assessed for assay sets targeting, O2aeh and O2ac, which were not detected in any clinical isolates by WGS in the TNC study.* 42

Figure 3.7 *K-locus specific ranking of multiple K. pneumoniae co-colonisers. KL28 and KL37 not included in analysis as broth did not test positive in the TNC study.* 43

Figure 3.8 *Co-colonisation patterns of K. pneumoniae K-locus* 44

Figure 3.9 *O-locus specific ranking of multiple K. pneumoniae co-colonisers. Enriched broth in TNC study did not pick up O8 or OL102, thus excluded from analysis.* 45

Figure 3.10 *Co-colonisation patterns of K. pneumoniae O-locus* 45

LIST OF TABLES

Table 2.1 Algorithm used to detect *K. pneumoniae, K. variicola*, and *E. coli* 18

Table 2.2 Algorithm for typing O1/O2 variants. Adapted from Kaptive v2.3 (21). 20

Table 2.3 Oligonucleotide primer and probe sequences for detection of *K. pneumoniae* capsular (K-) & lipo-polysaccharides (O-) loci and O-antigens. 21

Table 2.4 External synthetic calibrator (gBlock™) sequences. 24

Table 2.5 External synthetic calibrator (gBlock™) properties. 25

Table 2.6 Duplex reactions pairs. 28

Table 3.1 Singleplex vs duplex ct values at serial dilution 34

Table 3.2 Performance of the nanofluidic real-time qPCR 35

Table 3.3 Diagnostic performance of nanofluidic real-time PCR assays compared to whole genome sequencing in the detection of O-loci and O-types in 77 K. pneumoniae strains. 37

Table 3.4 Diagnostic performance of nanofluidic real-time PCR assays compared to whole genome sequencing in the detection of K-loci in 71 K. pneumoniae strains. 37

Table 3.5 Comparative Analysis of K-loci detection between sequencing and nanofluidic real-time qPCR. 39

Table 3.6 Comparative analysis of O-loci detection between sequencing and nanofluidic real time qPCR. 40

Table 3.7 Comparative analysis of O-types in the O1/O2 complex in 44 broth isolates using sequencing and nanofluidic real-time qPCR 41

Table 3.8 Co-colonisation patterns of *K. pneumoniae* with *K. variicola* and *E. coli* in 83 samples. 42

Table 3.9 *K. pneumoniae* K-loci and O-loci co-colonisation as measured by whole genome sequencing and nanofluidic real-time qPCR 43

NOMENCLATURE

Abbreviations	
AMR	Antimicrobial resistance
BHI	Brain heart infusion
BFQ	Black Fluorescent Quencher
BHQ	Black Hole Quencher
BLAST	Basic Local Alignment Search Tool
BSI	Bloodstream infection
CFU/mL	Colony-forming units per milliliter
chuA	Chromosome-encoded heme utilization A
CPS	Capsular polysaccharide
Cq	Quantification cycle
CV	Coefficient of variation
DNA	Deoxyribonucleic acid
dsDNA	Double-stranded DNA
ECO	*Escherichia coli*
ELISA	Enzyme-Linked Immunosorbent Assay
EOS	Early-onset sepsis
ESKAPE	*Enterococcus faecium, Staphylococcus aureus, Klebsiella pneumoniae, Acinetobacter baumannii, Pseudomonas aeruginosa, and Enterobacter species*
GALF	UDP-Galactofuranose Mutase
gBlocks™	Template gene fragments
GBS-CoP study	GBS Correlates of Protection study
GCP	Good Clinical Practice
GE	Gene Expression
gltA	Citrate synthase
gmlABD, gmlB, gmlD	Glycosyltransferase genes involved in capsule biosynthesis
GT	Glycosyltransferase
HAI	Healthcare-associated infection
HIC	High-Income Countries
HKG	Housekeeping Gene
HREC	Human Research Ethics Committee
IABkFQ	Iowa Black® Fluorescent Quencher
IDT	Integrated DNA Technologies
IFC	Integrated fluidic circuit
kb	Kilobase
KL	Capsule locus
KPC	*Klebsiella pneumoniae* Carbapenemase
KPN	*Klebsiella pneumoniae*
KpSC	Klebsiella Species Complex
LMIC	Low-and-middle income countries
LNA	Locked-Nucleic Acid
LOD	Limit of detection
LPS	Lipopolysaccharide
MDR	Multi-drug resistance
MDRE	Multidrug resistant Enterobacteriaceae
MIC	Minimum Inhibitory Concentration

MIQE	Minimum Information for publication of Quantitative real-time PCR Experiments
mL	Millilitre
NTC	No-template control
OL	O-locus
OMP	Outer membrane proteins
PCR	Polymerase Chain Reaction
qPCR	Quantitative Polymerase Chain Reaction
r^2	Correlation coefficient
RNA	Ribonucleic acid
RNP	Ribonuclease P
SD	Standard Deviation
SNP	Single nucleic polymorphism
STA	Specific target amplification
STGG	Skim milk-Tryptone-Glucose-Glycerine
TLR4	Toll-Like Receptor 4
Tm	Melting temperature
TMRH	Thelle Mogoerane Regional Hospital
TNC	Thelle neonatal colonisation study
tyrB	Tyrosine aminotransferase B
VF	Virulence factors
VIDA	Vaccines and Infectious Diseases Analytics Research Unit
wbbL	Galactosyltransferase
wbbM	Mannosyltransferase
wbbY	Glycosyltransferase
wbbZ	Acetyltransferase
wbdA	Glycosyltransferase
wbmVW	O-antigen biosynthesis genes
WGS	Whole genome sequencing
WHO	World Health Organisation
wzc/wzx	Capsular polysaccharide regulation and transport genes
wzm/wzt	Capsular polysaccharide ABC transporter genes
µL	Microlitre

CHAPTER 1: INTRODUCTION

1.1. Background & Study Context

In 2019, there were approximately 5.2 million deaths recorded among children under the age of five worldwide (1). By 2022, this number had decreased to approximately 4.7 million (2). Conversely, deaths from infectious diseases within this age group increased from 1.3 million to 1.43 million over the same timeframe (3–5).

Sepsis, a disseminating infection of the blood and other tissues, is one of the leading causes of neonatal mortality and morbidity globally, accounting for approximately 2,202 cases per 100,000 live births globally, with a case fatality risk of 9% to 11% (2,3,5). Overall, the burden of neonatal sepsis is highest in low-and-middle-income countries (LMIC: 3,930 cases per 100,000 live births) (3). However, infections that lead to sepsis during the first six days of life - early onset sepsis (EOS) - remain amongst the leading causes of infant death for both high-income countries (HIC) and LMIC (6).

During the past decade, there has been an increase in multi-drug resistant (MDR) organisms, defined as resistance to three or more antimicrobial classes (7), being responsible for the majority of neonatal sepsis morbidity and mortality, especially in LMIC (7–10). Infection with MDR bacteria is associated with poor clinical outcomes and a high case fatality risk (20.9% - 35.3%) (11). Healthcare-associated infections (HAI) are critical to control, as the causal organisms are pooled in the same environment allowing for increased opportunities for closely related pathogens to share genetic material enabling rapid evolution and spread of antimicrobial resistance (AMR) (11).

Klebsiella pneumoniae, a gram-negative bacterium belonging to the *Enterobacteriaceae* family, is classified, alongside *Enterobacter* species, as an ESKAPE pathogen (12). These pathogens, a group of six highly virulent and antibiotic-resistant bacteria, are priority targets for new antibiotic development according to the World Health Organisation (WHO), due to their ability to 'escape' the effects of multiple currently available antimicrobial treatments (13,14).

K. pneumoniae commonly colonises mucosal surfaces, particularly the gastrointestinal tract, nasopharynx, and skin (15,16). Colonisation is often asymptomatic but serves as a critical reservoir for subsequent invasive infection, particularly in neonates and immunocompromised individuals (15–17). Transmission can occur via person-to-person contact or through environmental exposure in healthcare settings, with colonised individuals acting as both reservoirs and vectors (17). In neonatal units, colonisation may occur shortly after birth and is often influenced by antibiotic use, delivery mode, and environmental exposure (15). Co-colonisation with multiple *K. pneumoniae* strains is increasingly recognised and may contribute

to horizontal gene transfer, antibiotic resistance, and serotype diversity - factors that are important to consider in both surveillance and vaccine development (15–18).

1.2. Clinical & Public Health Significance of *K. pneumoniae*

Globally, *K. pneumoniae* is a leading cause of AMR HAI, accounting for approximately 8-12% of all nosocomial infections in LMICs (19). In neonatal populations, a multicentre study reported incidences of *K. pneumoniae* sepsis in infants and newborns as 25.3% and 34.2%, respectively (20). In LMIC, *K. pneumoniae* is a leading cause of Gram-negative neonatal sepsis, contributing to 10% of total neonatal sepsis deaths (21). In a neonatal unit at a regional hospital in Johannesburg, South Africa, *K. pneumoniae* was responsible for 66.2% (308/465) of multidrug-resistant *Enterobacteriaceae* (MDRE) bloodstream infections (BSIs) in neonates, with the highest-burden observed in preterm infants (9,22). During an outbreak investigation conducted from January 2017 to August 2018, the incidence of *K. pneumoniae* BSIs increased from 1.6 to 5.0 cases per 100 admissions, with overall healthcare-associated BSI incidence rising from 6.8 to 10.1 cases per 100 admissions (23). The significance of MDR *K. pneumoniae* across LMICs, including South Africa, was highlighted by a multicentre study, which identified it as the leading cause of neonatal sepsis, with MDRE isolates increasing from 0.39 per 1,000 admissions in 2013 to 1.4 per 1,000 admissions in 2015 (4).

1.2.1. Multi-drug resistance

K. pneumoniae infections are treated with common antibiotics including aminoglycosides, piperacillin-tazobactam, and cephalosporins (24,25). However, due to the increase in drug resistance, carbapenems are increasingly used to treat severe infections (26). Carbapenem-resistant *K. pneumoniae*, first identified in the USA in 1996, was detected in South Africa in 2011 with the discovery of carbapenemase enzymes New Delhi Metallo-β-lactamase and *K. pneumoniae* carbapenemase in the Gauteng province (26,27). This resistance has been attributed to the acquisition of carbapenemase enzymes, which hydrolyse carbapenems, and other beta-lactam antibiotics to varying degrees (28–30). An important feature that has facilitated widespread dissemination of carbapenemase genes is that they are associated with mobile elements that can spread horizontally within, and between, bacterial species (30).

Subsequently, treatment of carbapenemase-producing *K. pneumoniae* has shifted towards the use of novel β-lactam/β-lactamase inhibitor combinations such as ceftazidime-avibactam and meropenem-vaborbactam. These agents are administered as single drugs, combining an active β-lactam with a β-lactamase inhibitor to restore activity against resistant strains. Although historically combination therapy - such as meropenem with colistin—was used to treat these infections, current evidence suggests that monotherapy with agents like ceftazidime-avibactam is more effective and associated with better outcomes (31,32).

However, these newer agents remain costly (32), and are often inaccessible in resource-limited settings (33). Moreover, emerging resistance to these therapies has already been reported, raising concerns about their long-term utility (11,34).

1.2.2. Treatment and preventative strategy development

The increasing prevalence of *K. pneumoniae* infections, combined with the bacterium's rapid development of resistance to existing antibiotics and limited new antibiotic options, has intensified the focus on vaccine development as a preventive strategy for invasive *K. pneumoniae* disease (24,25,35). Understanding the distribution of serotypes is essential in the clinical setting, as it informs infection control strategies, aids in tracking outbreaks, and supports the development of targeted treatments (36). Robust surveillance systems that can accurately detect and serotype *K. pneumoniae* are needed to guide research priorities and direct interventions aimed at reducing the burden of *K. pneumoniae* disease (37). Active surveillance and serotyping play a vital role in identifying circulating strains and supporting public health interventions.

1.2.3. Key virulence factors & serotypes of *K. pneumoniae*

K. pneumoniae employs several virulence factors (VF) that enhance its ability to evade the host immune system and establish infections (38). Key VF include the capsular polysaccharide (CPS) and lipopolysaccharide (LPS), which form protective barriers around the bacterium, inhibiting phagocytosis and complement-mediated killing (38,39). The CPS is important for shielding the bacterium from the host's immune defences, while the LPS contributes to the structural integrity of the outer membrane and elicits strong inflammatory responses through endotoxin activity (40). Beyond these, *K. pneumoniae* utilises fimbriae, which facilitate adhesion to host tissues and the formation of biofilms, contributing to persistent infections and antibiotic resistance (41). Moreover, outer membrane proteins (OMPs) and porins, play roles in nutrient acquisition and antimicrobial resistance, while efflux pumps actively remove toxic substances, including antibiotics, from the bacterial cell (42,43). Lastly, iron acquisition systems allow *K. pneumoniae* to thrive in iron-depleted environments within the host (44). Together, these virulence mechanisms not only make *K. pneumoniae* difficult to treat but also capable of causing severe, invasive infections.

1.2.3.1. Clinical significance of serotyping K. pneumoniae

A serotype, in the context of *K. pneumoniae*, refers to the classification of bacterial strains based on the CPS (expressed as K-antigens) or LPS (expressed as O-antigens), expressed as surface polysaccharides as illustrated in **Figure 1.1** (45).

The O-antigen, classified into 14 loci that encode 16 distinct O-types, is the outermost component of the LPS in the bacterial outer membrane (21,46,47). The K-antigen includes 162 types and forms the strain-specific capsular layer that envelops the bacterium (46,48,49). These surface antigens have become crucial for identifying the bacterium's pathogenic potential and characterising interaction with the host immune system (46).

Recent studies have highlighted the genetic diversity of K and O antigens amongst *K. pneumoniae* strains globally and identified significant geographic variability in dominant lineages. The most prevalent K serotypes identified include K1, K2, KL107, KL17, KL106, KL24, KL15, and KL36 (46,50). Notably, K1 and K2 are associated with hypervirulent strains that exhibit a higher abundance of virulence genes. These serotypes are particularly concerning due to their link to severe infections such as liver abscesses and bacteraemia (51–53). On the other hand, the dominant O serotypes identified in clinical isolates are O1, O2, and O3, which together account for approximately 80% of infections (46).

While both K- and O-loci are involved in the expression of surface polysaccharides in *K. pneumoniae*, a clear correlation or fixed association between specific K-loci and O-loci has not been definitively established. Although some trends have been observed - such as the frequent co-occurrence of KL25 with O5, or KL15 with O4 - these associations are not consistent across all isolates and cannot be assumed to be functionally or genetically linked (15). Therefore, each locus must be independently typed to ensure accurate serotype identification and surveillance.

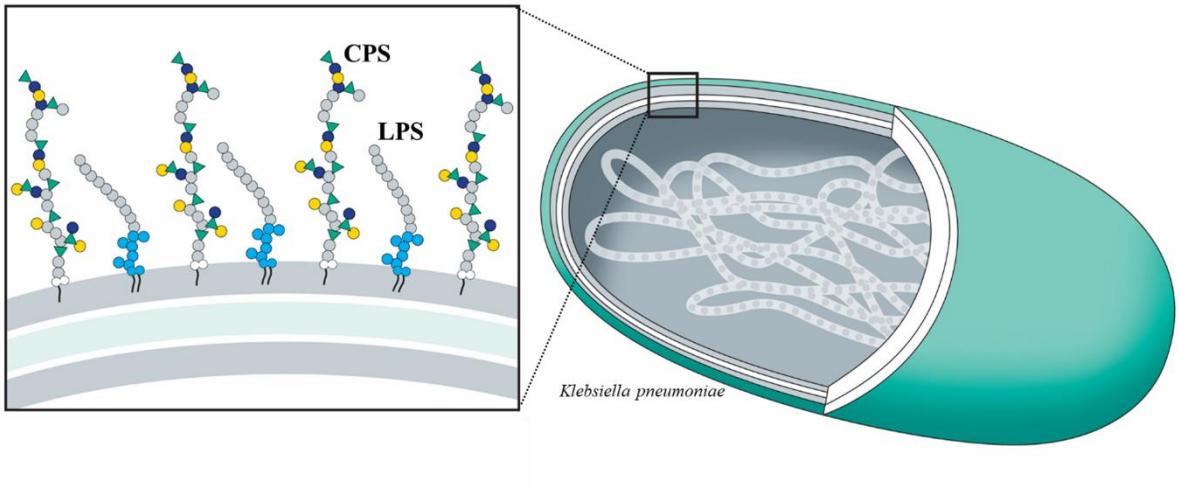


Figure 1.1 *Structural representation of K. pneumoniae and its surface polysaccharides (45).*

1.2.3.2. The capsule polysaccharide (K-antigen)

The polysaccharide capsule is an important virulence factor of *K. pneumoniae* enabling it to evade the immune system during infection (16) by protecting the bacteria from opsonophagocytosis and serum-killing (54,55). The capsule is generated by the CPS locus in

K. pneumoniae and comprises repeated subunits of four to six sugars and uronic acids (56). The central region of the CPS gene clusters, which encodes proteins for the polymerisation and assembly of CPS subunits, is highly divergent (57). This genetic diversity in the CPS biosynthesis pathway can significantly impact the virulence of different *K. pneumoniae* strains (38).

1.2.3.3. The genome of CPS

The genomic architecture of *K. pneumoniae* showcases significant variability within its CPS gene clusters (**Figure 1.2**). These clusters, which start at the *galF* gene and extend to the *ugd* gene, demonstrate diversity in both the quantity of glycosyltransferase (GT) genes and their unique DNA sequences, except for conserved genes *wbaP* and *wcaJ* (48,57). Spanning approximately 21 to 30 kb, the CPS gene clusters encode crucial components of the CPS biosynthesis pathway. Among these, the membrane proteins *wzi*, *wza*, and *wzc*, as well as *wzx*, *wzy*, *wbap*, and *wcaj*, are essential for the production and export of the capsular polysaccharide (**Figure 1.2**) (48,58). While the *wzi*, *wza*, and *wzc* genes are conserved in *E. coli* group 1 and *K. pneumoniae* CPS gene clusters, *wzx* and *wzy* exhibit greater sequence diversity (59). *Wzc*, an inner membrane tyrosine autokinase, forms a channel complex with *wza* to act as a K antigen transporter, regulated by *wzb* (57,60). Genes responsible for K antigen repeat-unit biosynthesis are in the central region of CPS gene clusters, between the *wzc* and *gnd genes*, display substantial diversity (32,46,57).

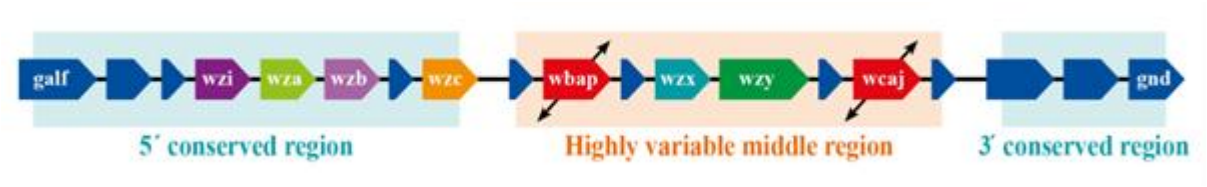


Figure 1.2 *The representative CPS locus arrangement adapted from Patro et al. 2019 (58).*

Strains with the same capsular type demonstrate substantial DNA sequence similarity in the variable region of the *wzc* gene, whereas strains with different capsular types exhibited lower DNA sequence resemblance (60). However, genomic analysis has revealed that some capsular types, such as KL22 and KL37, along with KL9 and KL45, share a high degree of sequence similarity, differing only by a small number of nucleotides or subtle genetic changes (46,49,59). This suggests that these capsular types have nearly identical genetic structures despite being classified separately. Despite this close genetic relationship, each maintains its distinct capsular type, indicating that differentiation is driven by subtle but specific genetic variations (60). While KL52 and KL79 share identical *wzc* DNA sequences, they can be differentiated by variations in other regions of the CPS gene cluster, such as alterations in the promoter sequences, gene presence or absence, point mutations in other glycosyltransferase genes, or differences in the genes responsible for sugar synthesis and transport (58,60).

Variations in other genes within the CPS cluster, the presence of regulatory elements influencing gene expression, and enzymes that uniquely modify polysaccharides all play critical roles in determining capsule composition, structure, and virulence of *K. pneumoniae*. Further, lateral gene transfer and recombination have played a pivotal role in introducing diversity into the *K. pneumoniae* CPS gene clusters (48,61,62). While the CPS operons generally maintain conserved genes at the 5' and 3' ends, exceptions such as the significant genetic variability observed in the *wzb* and *wzc* genes underscore the complexity of this genetic diversity (46,49,57). This diversity is not solely attributed to lateral gene transfer and recombination, as it encompasses a broader range of genetic variabilities within the operons themselves (63). It is also a consequence of the varied genes encoding glycosyltransferases and acetyltransferases, adding layers of complexity to the capsule's structural variety. The interplay of these factors is what gives rise to the observed heterogeneity in the capsule composition of *K. pneumoniae* (49,64).

1.2.3.4. The lipopolysaccharide (O-antigens)

The outer membrane of *K. pneumoniae* is covered with LPS, also known as endotoxins, and are powerful trigger of septic shock, as it activates the host Toll-like receptor 4 (TLR4), leading to an inflammatory cascade that can result in sepsis and septic shock (65,66). The LPS is made up of lipid A, a core domain, and the polysaccharide O-antigen. *K. pneumoniae* isolates with smooth LPS (full-length O-antigen) are resistant to serum complement, while those with rough LPS (shortened or absent O-antigen) are sensitive to serum complement (55). Moreover, variations in LPS can protect bacteria from antimicrobial peptides, including polymyxin antibiotics (32,39).

The O serotypes of *K. pneumoniae* are particularly significant in the context of vaccine development because there are considerably fewer O-types compared to K-types, making them more feasible targets for broad-spectrum vaccines (46). While targeting all O serotypes may offer broad protection, specific O-types such as O1ab, O2afg, and O3b, which are responsible for the majority of invasive disease cases globally, are of particular interest (37,45,67). The structural similarities between *K. pneumoniae* O-antigens and those of other closely related Enterobacteriaceae species, such as *E. coli*, present challenges for the exclusive targeting of these antigens in diagnostics and vaccine development. These shared epitopes can lead to cross-reactivity, reducing the specificity of serological assays and potentially limiting the precision of O-antigen - based vaccines, particularly in distinguishing *K. pneumoniae* from commensal or less pathogenic species (68).

1.2.3.5. The genome of LPS

The LPS is a vital component of the outer membrane in gram-negative bacteria, including *K. pneumoniae*. This complex molecule is synthesised through a coordinated process involving

genes that encode enzymes for LPS assembly (69). While most *Enterobacteriaceae* have a conserved LPS core, *K. pneumoniae* displays two outer core types, distinguished by three specific genes within the *waa* operon, which are independently located in the genome. The *waa* operon is essential for constructing the core oligosaccharide, a critical part of the LPS structure (21,47).

Several genetic components are crucial to the structure and function of *K. pneumoniae'*s lipopolysaccharide (LPS). The lipid A biosynthesis genes (e.g. *lpxA, lpxC, lpxD*) produce the lipid A anchor, essential for LPS structural integrity and endotoxic activity (46,70). Core oligosaccharide biosynthesis genes (e.g. *waaA, waaB, waaC*) assemble the core oligosaccharide, bridging lipid A to the O-antigen (18,46). Additionally, the O-antigen biosynthesis genes (e.g. *wzy, wzz, wzm*) drive the assembly of the variable O-antigen polysaccharide, a region critical to *K. pneumoniae's* serological diversity (47,71).

The *K. pneumoniae* species is distinguished by a variety of O-antigenic types, each denoted by unique lipopolysaccharide compositions on their cell surface. The recognised O-types within *K. pneumoniae* are O1, O2a, O2ac, O2afg, O2aeh, O3/O3a, O3b, O4, O5, O8, O12, OL101, OL102, OL103, and OL104. O-antigen serotypes are each defined by a specific set of genetic arrangements and possess distinct sets of biosynthetic genes, which confer their individual serological properties and characterise the loci (21,47,71,72).

The *rfb* genes are responsible for the synthesis and assembly of the O-antigen, which constitutes a highly variable region of the LPS molecule in *K. pneumoniae* (**Figure 1.3**). The genetic arrangement is responsible for the extensive diversity observed in the LPS of *K. pneumoniae*, with each serotype's gene cluster presenting a unique combination of *manC*, *manB*, *wzm*, *wzt*, *wbd*, and other relevant genes involved in lipopolysaccharide biosynthesis (21,50,70,71). Importantly, these LPS biosynthesis genes are not only vital for the bacterium's survival but also for its pathogenicity and virulence (46). Mutations within this genetic framework can lead to structural alterations in the LPS molecule, ultimately influencing *K. pneumoniae's* capacity to cause infection, evade the host immune system, and contribute to the pathogenic mechanisms of this clinically significant bacterium (40,73).

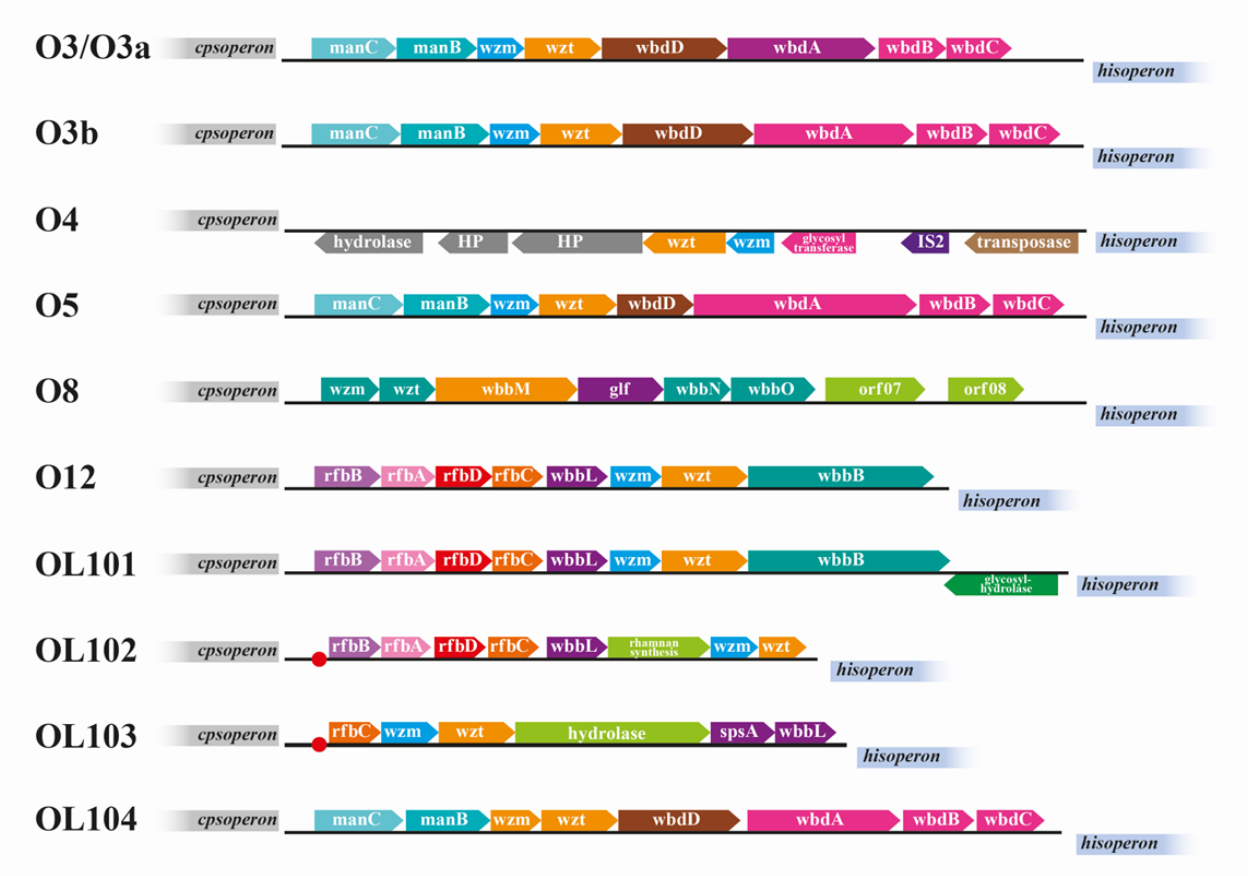


Figure 1.3 *The rfb gene cluster for O3, O4, O5, O8, O12, OL101, OL102, OL103, and OL104 (46).*

Gene cluster with genes coloured according to function and positioned above or below the coding strand based on the direction of transcription (46). In the K. pneumoniae rfb gene clusters, specific genes are color-coded by their functions.

The O serotypes of *K. pneumoniae* exhibit notable genetic and structural diversity, contributing to antigenic variability and influencing pathogenicity. Amongst the most clinically significant are the O1/O2 complex and the O3 serogroup, which account for a substantial proportion of invasive infections globally (74). The O3 serogroup includes the O3, O3a, and O3b variants, with O3b being the most frequently detected. These variations arise from mutations in the *wbdA* glycosyltransferase gene, altering mannose incorporation and producing distinct antigenic profiles (75,76). The O4 and O5 serotypes share structural similarities with the O3 group but are differentiated by specific enzymatic processes. The O4 serotype features galactose and ribofuranose polymers, with unique transposase insertions disrupting gene orientation, while O5 exhibits a mannose chain capped solely by a methyl group, unlike O3, where both phosphate and methyl groups are present (77).

The O8 and O9 serotypes closely resemble O1 due to their shared D-galactan I and II backbone. However, O8 is distinct due to acetylation mediated by the *wbbZ* gene (78). The O9 serotype shares over 95% genetic similarity with O8 and is often classified as a subtype of O2, reflecting their overlapping genetic characteristics (79). Similarly, the O12 serotype and

related variants OL101 and OL102 share genetic elements but are distinguished by gene arrangements involved in rhamnan synthesis (46,77,80). Less common subtypes, such as OL103 and OL104, differ based on modifications in the *wbbL* and *wbdA* genes, contributing to further antigenic variation (51,80).

The O1/O2 complex, comprising O1/O2v1, O1/O2v2, and O1/O2v3, represents one of the most widespread and clinically relevant serogroups. Variability within this complex is driven by differences in the *kfoC*, *gmlB*, and *wbbM* genes, which encode enzymes responsible for sugar linkages in the O-antigen (74).

The variations in specific loci and genes enable the design of assays that accurately capture the diversity and complexity of *K. pneumoniae* O-serotypes, facilitating robust and precise serotyping across clinical isolates.

The relevant gene cluster, illustrated in **Figure 1.4**, highlights the genes responsible for O-antigen biosynthesis. The figure demonstrates the differences in gene composition between the O1/O2 locus variants 1, 2, and 3.

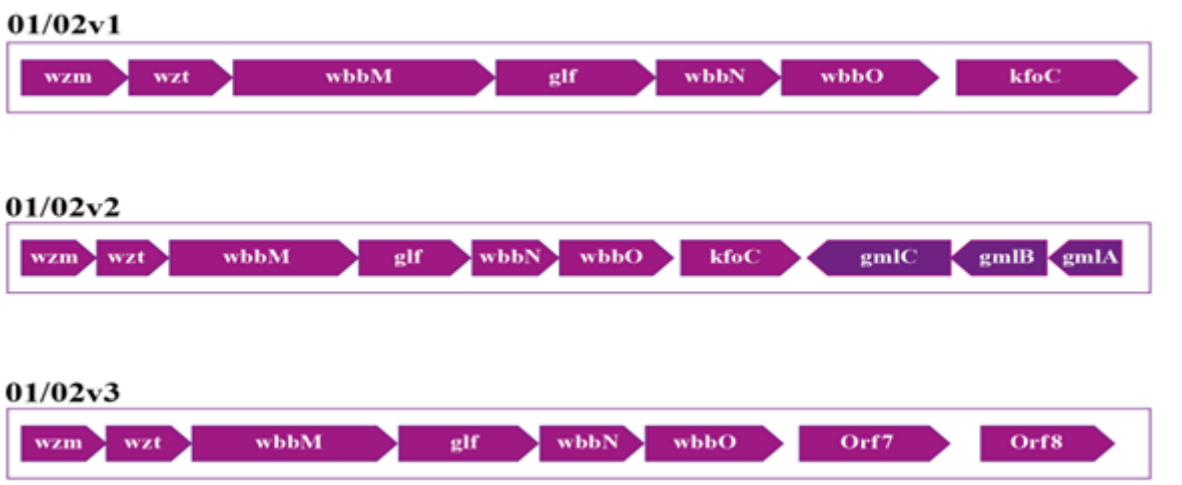


Figure 1.4 *Genes present in the O1/O2 locus, and differences among variants. Adapted from Kaptive v2.3 (21).*

1.2.3.6. Characterisation of the O1 and O2 subtypes

Strains expressing O1 and O2 antigens in *K. pneumoniae* are linked to three main loci: O1/O2v1, O1/O2v2, and O1/O2v3 (**Figure 1.5**). The specific expression of these loci results in the O2 antigen, primarily consisting of D-galactan I or III, which can convert to the O1 antigen through the addition of a D-galactan II repeat, facilitated by the *WbbY* enzyme located downstream in the genome (21).

Four O2 subtypes—O2a, O2afg, O2ac, and O2aeh—each possess unique sugar linkages, adding structural and immunogenic diversity. For instance, O2a features D-galactan I, while O2afg and O2aeh have distinct galactose side chains (68,81). The O1 and O2ac antigens

further modify the O2a backbone with an additional repeat unit, expanding antigenic variation among these subtypes (50,68,82).

Additionally, *K. pneumoniae* O-antigens share genetic homology with *E. coli* serotypes like O9a, particularly in the *wzm* and *wzt* sequences, suggesting horizontal gene transfer. This genetic exchange, especially among mobile O-antigen biosynthesis genes, underscores the evolutionary adaptability of these pathogens, complicating serotyping efforts (68,82–84).

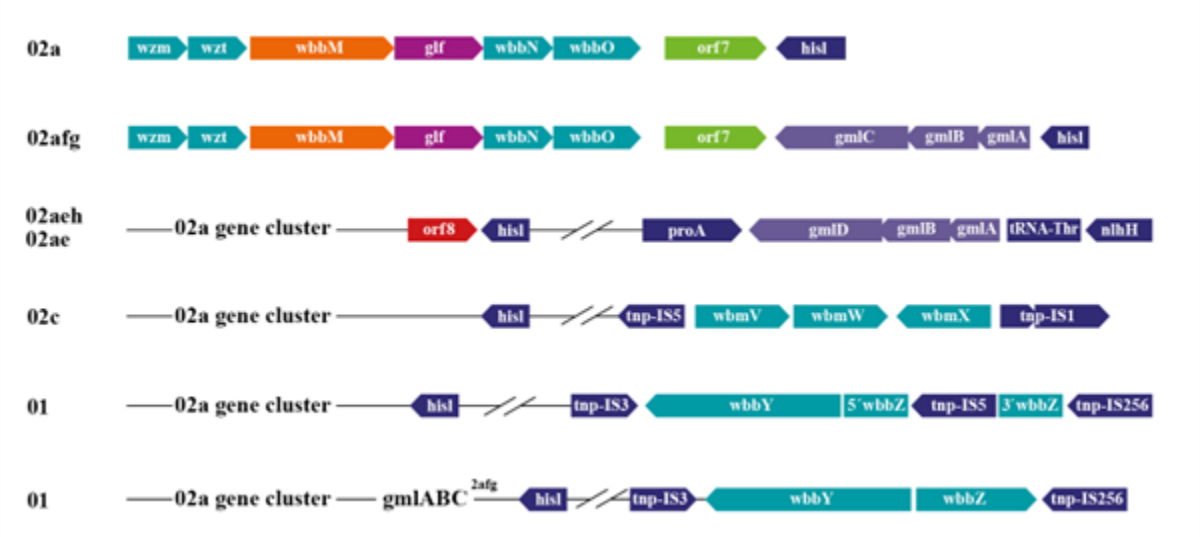


Figure 1.5 *Arrangement of the genetic determinants responsible for O-antigen biosynthesis in K. pneumoniae serotypes derived from O2a. Adapted from Clarke et, al. (82).*

1.2.4. *K. pneumoniae* phylogenetic complex

The *K. pneumoniae* Species Complex (KpSC) includes several subspecies such as *K. quasipneumoniae* and *K. variicola*, which can also cause severe infections (21). Understanding the phylogenetic relationships within this complex is crucial, as these subspecies exhibit diverse pathogenic and resistance profiles that impact infection control strategies and clinical outcomes (50). The use of whole-genome sequencing (WGS) has clarified relationships within *Klebsiella* species, showing that isolates previously identified as *K. pneumoniae* through biochemical or proteomics assays may belong to other members of the KpSC. These subspecies share 95–96% average nucleotide identity, with *K. pneumoniae* showing only 90% identity with other *Klebsiella* species (**Figure 1.6**) (50).

The examination of the entire KpSC is vital for identifying horizontal gene transfer between subspecies, facilitating the spread of antibiotic resistance and virulence factors. This genetic exchange enhances the adaptability of the KpSC, complicating clinical management and infection control. Comprehensive surveillance and accurate identification are necessary to inform effective treatment strategies and limit the spread of resistant strains (50).

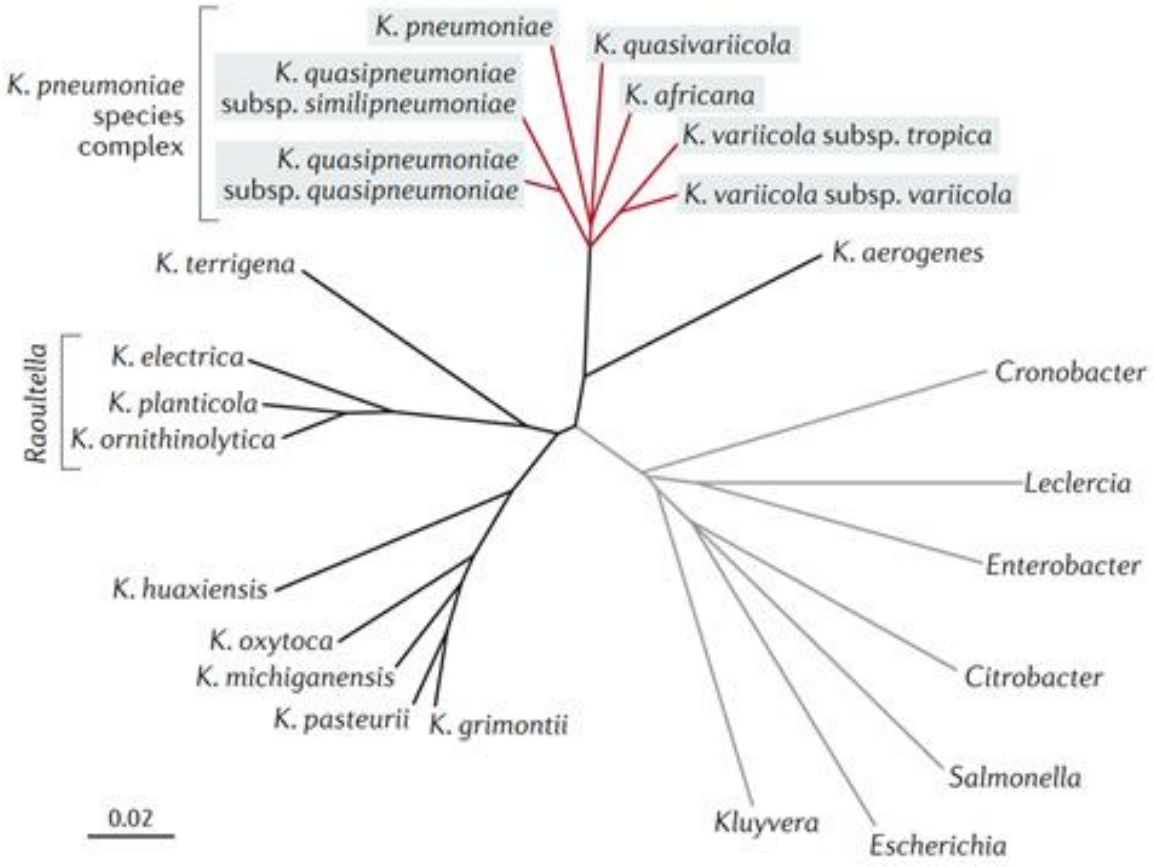


Figure 1.6 *Phylogenic Tree exemplifying relationships within the K. pneumoniae species complex (red), Klebsiella genus (black) and Enterobacteriaceae family (grey) (85).*

1.3. Detection and Subtyping Methods of *K. pneumoniae*

1.3.1. Culture-based methods:

Culture-based methods remain the gold standard for detecting *K. pneumoniae* in a clinical setting (86). However, these methods are time-consuming and incapable of serotyping *K. pneumoniae*.

1.3.2. Enzyme-Linked Immunosorbent Assay (ELISA):

ELISA is a technique that can serotype *K. pneumoniae* by identifying distinct variations of surface-exposed polysaccharides of the K and O types (87). The ELISA method involves coating a microplate with antibodies that capture the specific antigens of *K. pneumoniae*, followed by a detection process that produces a measurable signal. Although ELISA can differentiate between various serotypes, it has limitations in specificity due to cross-reactivity between antigens and poor assay reproducibility (88). Such cross-reactivity not only affects the accuracy of serotyping but also has implications for vaccine design, as shared or similar antigenic epitopes between serotypes may lead to reduced specificity of immune responses, potentially limiting the effectiveness of serotype-targeted vaccines.

1.3.3. Whole-Genome Sequencing (WGS):

WGS is a powerful tool for analysing the genetic diversity of *K. pneumoniae* isolates (89,90) as it provides detailed genetic information and can identify all genes present in an organism. However, WGS relies on an initial culturing step to obtain sufficient bacterial material for sequencing. This requirement means only the dominant strain is sequenced, preventing detection of concurrent colonisation by multiple strains. Additionally, WGS is cost-prohibitive and requires specialised equipment and skilled personnel for data interpretation and bioinformatics analysis, limiting its accessibility in resource-constrained settings (90).

1.3.4. Targeted sequencing of the *wzi* gene:

A more affordable alternative to WGS, according to Brisse *et al.* (59) is the targeted sequencing of the *wzi* gene. This method advances over conventional serological techniques by providing a more precise approximation of capsular serotypes in *K. pneumoniae* isolates. Targeted *wzi* sequencing is quicker and simpler than WGS and can determine K types in most clinical isolates. However, this method has limitations. Approximately 10% of isolates show discrepancies between *wzi* sequencing and K-typing, likely due to the extensive diversity of *wzi* alleles, which do not always correspond to specific K types. Additionally, the method requires a culture step, meaning it may primarily identify the dominant *K. pneumoniae* strain present rather than capturing the full diversity of capsule types within a sample. A 2023 longitudinal analysis found 67% of hospitalised patients carried ≥ 2 distinct *K. pneumoniae* strains (differing by ≥50 SNPs) in gut microbiota, but culture isolated only the dominant strain in 89% of cases (91).

1.3.5. Polymerase Chain Reaction (PCR):

PCR is a highly sensitive and specific nucleic acid amplification technique widely used in clinical settings to detect pathogens like *K. pneumoniae* and *K. variicola* (92). By amplifying target DNA or RNA sequences, PCR allows for rapid and accurate identification, making it a cornerstone of microbial diagnostics due to its affordability and speed (93) which is crucial for effective patient care and controlling the spread of infectious diseases. However, PCR has limitations in differentiating strains within the KpSC (92) and the genetic variability in the K- and O-loci complicates serotyping as typically PCR assays target conserved regions.

Limited studies have applied PCR for *Klebsiella* serotyping, with most focusing on broader species identification (94). This gap reflects the challenge of developing assays that account for the extensive genetic diversity within the species (93). Additionally, PCR can only test for a limited number of serotypes at once, and while multiplex PCR expands capacity, it increases

costs and complexity. High-throughput platforms, such as nanofluidic real-time PCR, provide broader serotype detection but remain expensive and are not yet widely adopted (79).

Despite its limitations, PCR remains a valuable diagnostic tool, and continued refinement is needed to improve serotyping accuracy and expand its applicability to *Klebsiella* epidemiology and infection control.

1.3.6. Nanofluidic qPCR: Principles and Applications

Nanofluidic qPCR is a high-throughput technique that combines microfluidics with quantitative PCR to perform thousands of nanolitre-scale reactions simultaneously. Using Integrated Fluidic Circuits (e.g., 96 assays × 96 samples = 9,216 reactions), it reduces reagent use and processing time while enabling rapid, multiplexed detection. Its compatibility with clinical samples supports direct pathogen detection and strain differentiation without culturing, making it ideal for *K. pneumoniae* serotyping and well-suited for use in resource-limited settings.

1.4. Study Justification

Nosocomial infections and outbreaks caused by *K. pneumoniae* in newborns can lead to pneumonia, sepsis, and meningitis. In South Africa, *K. pneumoniae* is the leading cause of invasive bacterial disease and death in infants younger than 90 days of age. The emergence of MDR strains, particularly carbapenem-resistant *K. pneumoniae*, has further complicated treatment efforts and increased case fatality risk. While vaccines targeting the predominant O and K antigens of *K. pneumoniae* are under consideration, the scarcity of serotype-specific data from Sub-Saharan Africa, including South Africa, could hinder the identification of appropriate antigens and potentially limit vaccine effectiveness against locally prevalent strains. Published studies from HIC have reported geographic variability in dominant *K. pneumoniae* lineages, and preliminary findings from South Africa (**Figure 1.7**) (15) and Malawi have indicated temporal shifts in the dominant lineages. This variability highlights the need for robust regional surveillance systems and methods that enable fast and reliable serotype-specific detection of *K. pneumoniae*. Moreover, if a vaccine is to become licensed then robust surveillance of *K. pneumoniae* will be needed before and after vaccine introduction to measure its effectiveness and determine temporal changes or serotype replacement that could materialise from vaccination.

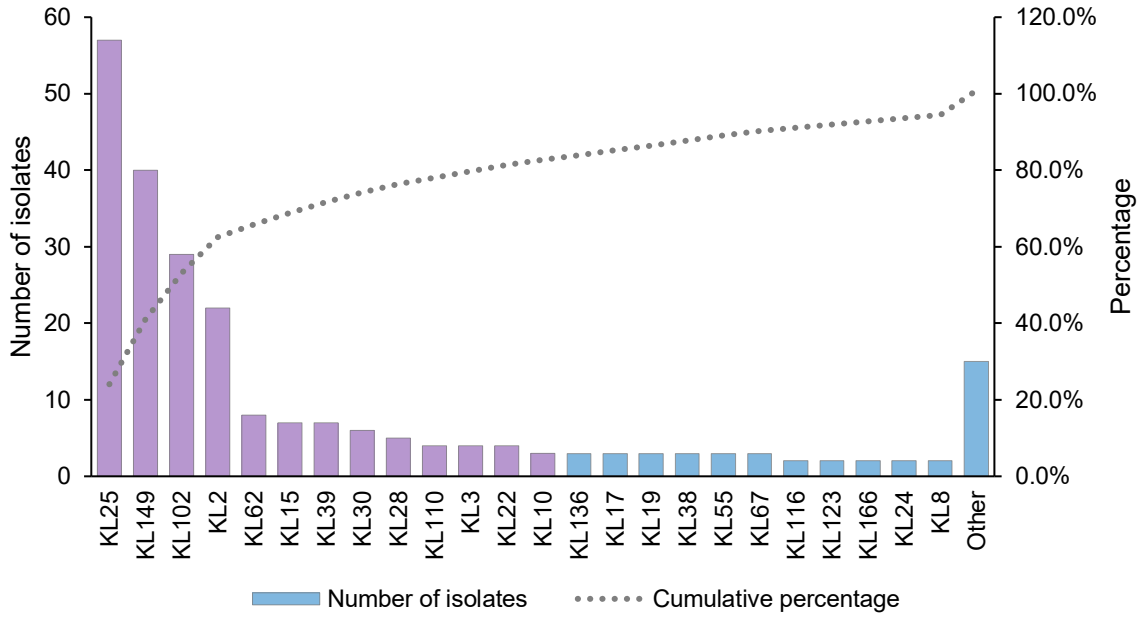


Figure 1.7 *K-loci distribution of invasive K. pneumoniae causing disease in neonates <90 days (N=239) in South Africa between 2018 and 2022. Adapted from Olwagen et. al, (15). K-loci that were targeted highlighted in purple.*

K. pneumoniae has two major surface antigens: O-antigen (16 types), which is the most external or outer component of the lipopolysaccharide outer membrane, and the K-antigen (162 types), which is the strain-specific capsular polysaccharide that makes up the capsule. Current methods used to detect and serotype *K. pneumoniae* include culture, PCR-based techniques (i.e. *wzi* capsular typing), hybridization, mass spectrometry, and ELISA. These methods, however, are limited in that they are time-consuming and lack sensitivity and specificity. While WGS has overcome some challenges, the method is expensive and relies on an initial culturing step to obtain sufficient bacterial material for sequencing. Moreover, detection of multiple *K. pneumoniae* strains of a lower density is often missed and interpretation of the genomic data is difficult and requires skilled personnel.

To overcome these barriers, this study adopted a high-throughput molecular method with the capacity for direct detection and serotyping from enriched clinical samples. This approach was selected for its ability to enhance the resolution of colonisation and invasive strain detection, improve turnaround times, and facilitate large-scale application. The method is particularly well-suited for informing public health strategies and vaccine development efforts, especially in sub-Saharan Africa, where timely, affordable, and accurate tools for *K. pneumoniae* surveillance are urgently needed.

Aims and objectives:

The study aimed to optimise and validate a nanofluidic real-time qPCR method for detecting and serotyping the dominant K-loci and O-antigens of *K. pneumoniae* responsible for causing invasive disease in South African infants.

All available O-loci and O-types were targeted, while the K-loci targets were chosen based on the most frequently isolated K-loci causing invasive *K. pneumoniae* disease in infants in South Africa (based on detection by WGS) at the time of the study design (**Figure 1.7**).

The study objectives included:

1. To design and optimise a nanofluidic qPCR method to differentiate *K. pneumoniae* from other species in the KpSC and *E. coli*.
2. To design and optimise a nanofluidic qPCR method to detect 13 O-loci, 5 O antigens, and 13 K-loci of *K. pneumoniae.*
3. To validate the nanofluidic qPCR assay against invasive isolates previously serotyped by WGS.
4. To validate the nanofluidic qPCR assay using direct swab samples (skin, rectal, and nasal) enriched in BHI media, alongside WGS and serotype prediction of *K. pneumoniae* isolates derived from the same BHI samples using the Kaptive v2.3 pipeline.

CHAPTER 2: METHODOLOGY

2.1. Assay Design

To identify conserved regions within each target, genomic sequences of *K. pneumoniae* LPS O-antigens, LPS O-loci, and the CPS K-loci were sourced from the Pathogenwatch (95) and Kaptive 2.3 (21) databases . Multiple strains accrued globally for each of the targeted K-locus (n=15; KL2, KL3, KL10, KL15, KL22, KL25, KL28, KL30, KL39, KL62, KL102, KL110, KL149 - including KL37 and KL171 due to similarity with KL22), O-locus (n=13; O1/O2v1, O1/O2v2, O1/O2v3, O3/O3a, O3b, O4, O5, O8, O12, OL101, OL102, OL103, OL104) were aligned, including genes that determine the O-antigens, together with all known K-loci (n=162) using Jalview version 2.11.2.6 software (96) (**Figure 2.1**). The sequence for O11 was unavailable in the Pathogenwatch (95) and Kaptive 2.3 (21) databases at the time of assay design and were thus excluded from the final reaction set. To account for the high genetic similarity between *K. pneumoniae* and related *Klebsiella* species, genomic sequences from *K. quasivariicola, K. africana, K. variicola, K. quasipneumoniae, K. oxytoca, K. michiganensis,* and *K. grimontii*, were also sourced and aligned.

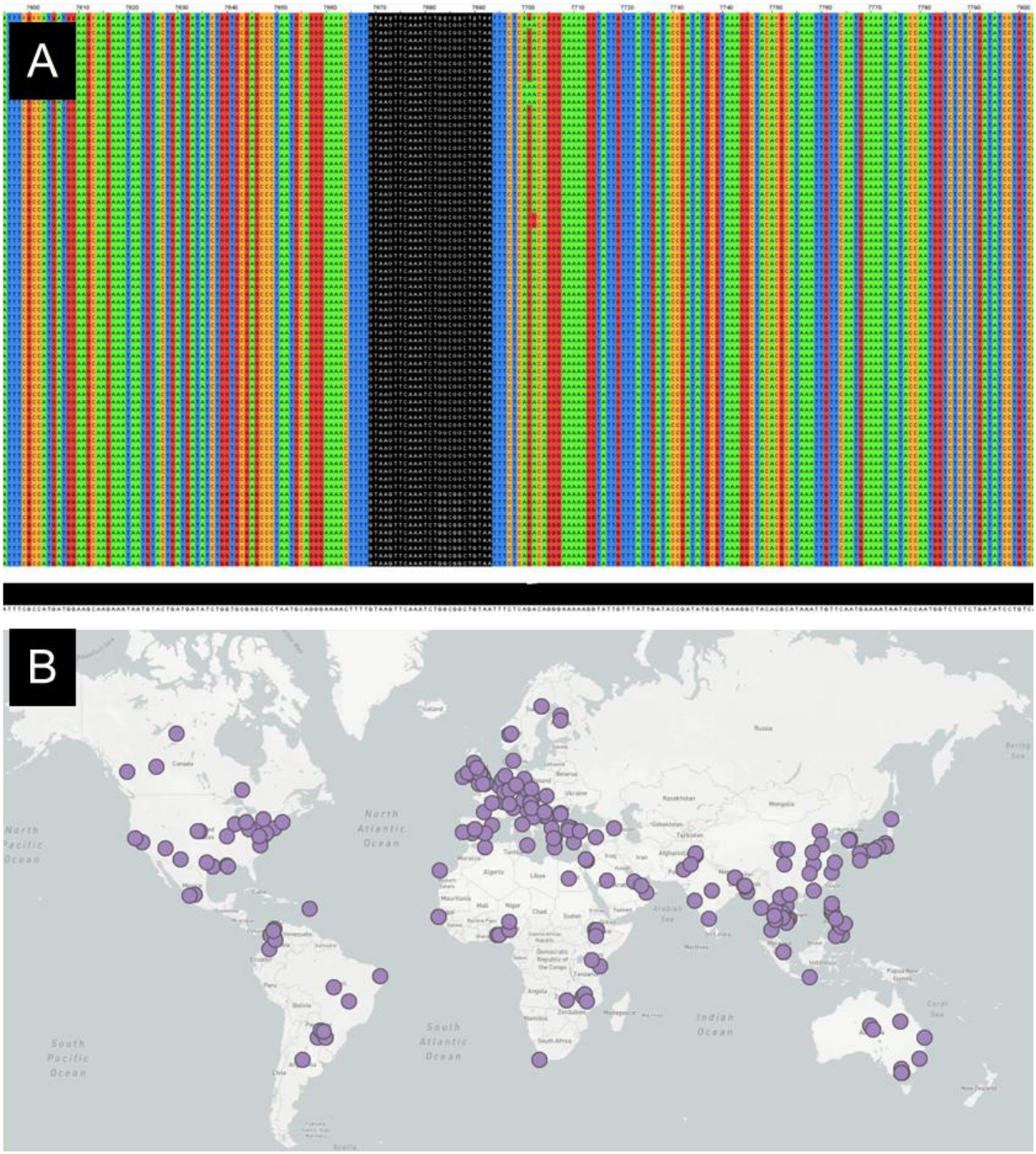


Figure 2.1 *Example of (A) alignment of the wzc gene within the Capsular polysaccharide region from available KL15 strains and (B) the global distribution of the aligned KL15 strains. Sequences were trimmed and processed using the captive pipeline before alignment to ensure accurate identification of the conserved regions between global strains. The conserved region of the KL15 CPS is highlighted in black in Figure A.*

Housekeeping genes for *E. coli* (*chuA*), *K. pneumoniae* (*gltA*), CPS (*GALF*), and *K. variicola* (*tyrB*) were included in the final reaction set to confirm the presence of *K. pneumoniae* (**Table 2.1**)**.** The housekeeping gene for *K variicola* was included as it was the only KpSC member found co-colonising with *K. pneumoniae* (97). Samples were defined as being positive for *K. pneumoniae* if they tested positive for both the *gltA* and *GALF* housekeeping genes and negative for both the *tyrB* and *chuA* genes (**Table 2.2**). Ribonuclease P (RNP), a cellular enzyme involved in tRNA maturation, was included as an internal control to confirm the

presence of human DNA in clinical swab samples and to ensure sample collection and DNA extraction were adequate.

Table 2.1 Algorithm used to detect *K. pneumoniae, K. variicola*, and *E. coli*

	KPN HKG *(gltA)*	CPS HKG *(GALF)*	*K. variicola (tyrB)*	ECO *(chuA)*
K. pneumoniae	+	+	–	–
K. variicola	+	+	+	–
E. coli	–	–	–	+

Abbreviations: chuA – Chromosome-encoded heme utilization A, ECO – Escherichia coli, GALF – Galactofuranosyl transferase, gltA – Glutamate synthase subunit A, HKG – Housekeeping gene, KPN – Klebsiella pneumoniae, tyrB – Tyrosine B. The algorithm is interpreted based on the absence and presence of the gltA, GALF, tyrB, and chuA genes.

For assays targeting the CPS loci, the *wzc* gene was targeted due to the inter-variability of the CPS locus among the different K-loci that were within a conserved region (98,99). There was, however, complete genotypic homology between the *wzc* genes of KL22, KL37, and KL171, except for an additional repeat of the *wzc* gene in KL37. An additional assay targeting the *wzx* gene was thus designed to differentiate KL37 from KL22/KL171; however, the qPCR method was not able to differentiate KL22 from KL171 (**Figure 2.2**).

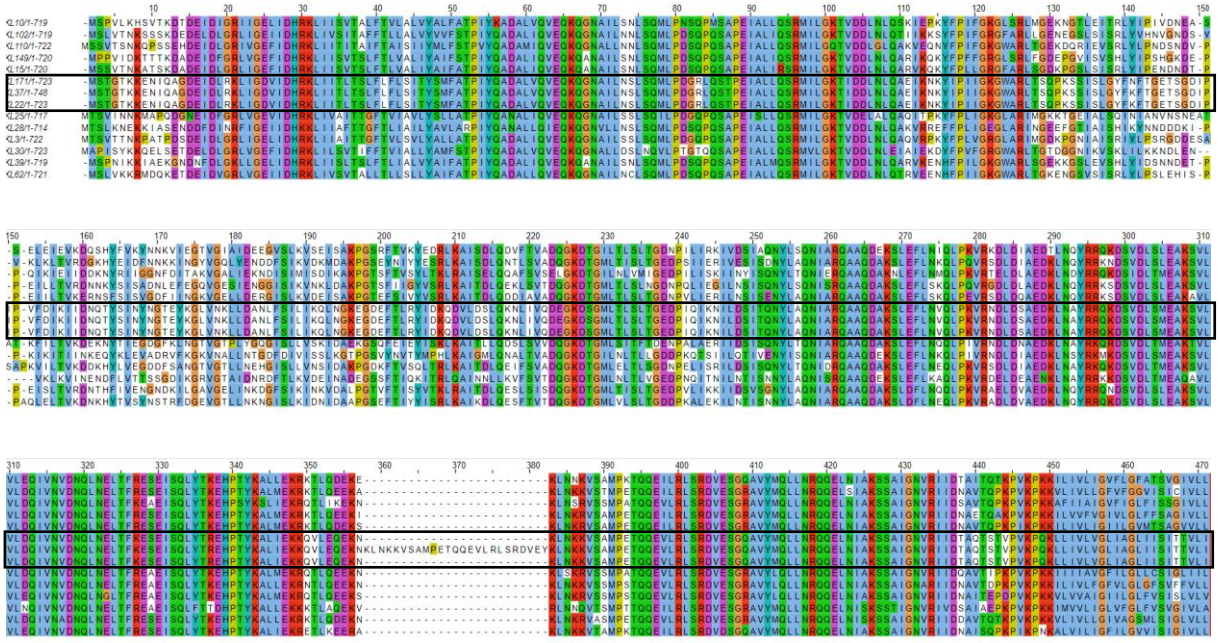


Figure 2.2 *Basic Alignment Mapping of wzc gene in the CPS cluster for the 15 K-loci included in the final nanofluidic qPCR reaction set.*

A specialised locked-nucleic acid (LNA) probe targeting SNP 7699 – 7703 (n=4) of KL15 *wzc* gene was designed to differentiate KL15 from all other K-loci, where there was a high degree of homology within the *wzc* gene, (100). Briefly, LNA-based probes incorporate bases with a

unique methylene bridge, enhancing the probe's affinity for specific sequences, thereby elevating the detection precision of specific genetic variations, including SNPs (101).

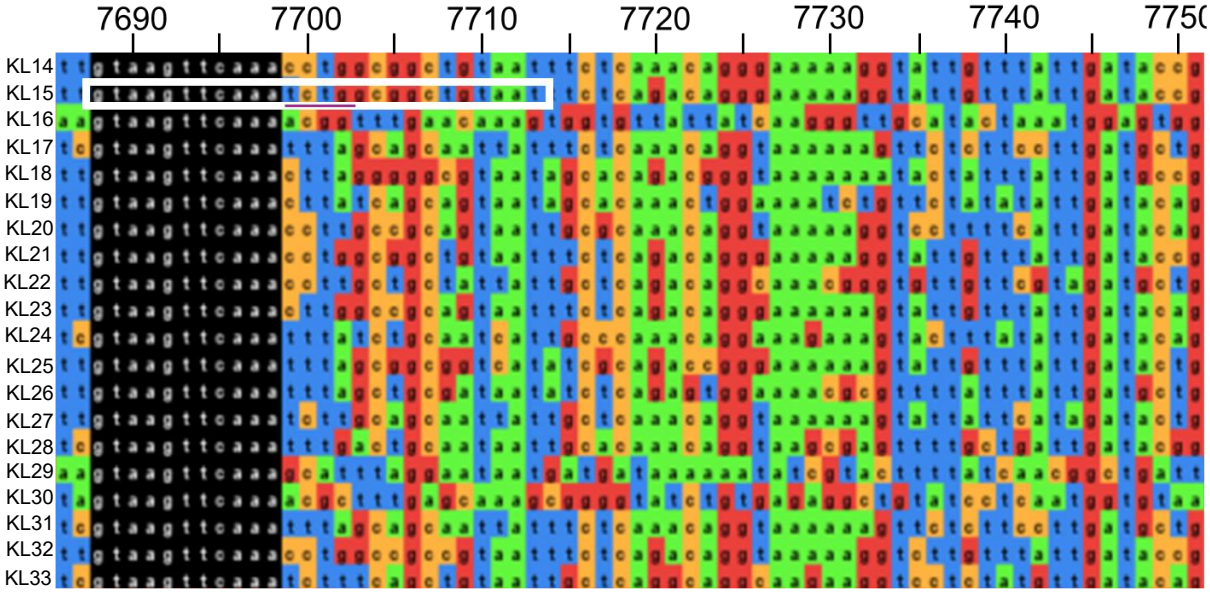


***Figure 2.3**: Screenshot of alignment of the wzc gene of 20 K-loci (KL14-KL33). Locked Nucleic Acid (LNA) probe, highlighted by the black box, targeting the wzc gene of the KL15 capsular polysaccharide synthesis gene cluster.*

Assays targeting the *kfoC* and *gmlB* genes were included to detect the O1/O2v1 and O1/O2v2 loci respectively while assays targeting the *wbbM* gene were included to detect the O1/O2v3 locus. Lastly, assays targeting the *wbbL* (to detect OL103), *WbdA* (to detect O3/O3a, O3b, and OL104), *wzm* (to detect O4, O5, and OL101), *wbbM* (to detect O8), *wbbN* (to detect O12), and the *wzt* (to detect OL102) genes were included to differentiate the remaining O-loci.

Assays were designed based on the discrimination criteria listed by Kaptive v2.3 (21) to differentiate the O1/O2 complex into 5 serotypes (O1, O2a, O2ac, O2agf, and O2aeh), with serotype calls being made based on the presence or absence of four genes targeted (*wbbY*, *wbbZ*, *wbmV*, and *gmlD*) outside of the rfb operon (**Table 2.2**). Samples were defined as positive for the O1/O2v1 locus if positive for both the *wbbY* and *wbbZ* genes, while they were classified as O2aeh if positive for the *gmlABD* gene cluster across the O1/O2v2 loci. For other O-types, the presence of specific loci (e.g. O3b, O4, and O5) was used to directly infer the corresponding O-antigen, as these loci are known to have a one-to-one relationship with their respective O-types.

Table 2.2 Algorithm for typing O1/O2 variants. Adapted from Kaptive v2.3 (21).

Genes	Locus	Type
-	O1/O2v1	O2a
-	O1/O2v2	O2afg
-	O1/O2v3	O2a
wbbY + wbbZ	O1/O2v1	O1
wbbY + wbbZ	O1/O2v2	O1
wbbY + wbbZ	O1/O2v3	O1
wbbY or wbbZ		Non typable
wbbY or wbbZ		Non typable
wbbY or wbbZ		Non typable
wbmVW	O1/O2v1	O2ac
wbmVW	O1/O2v2	O2ac
wbmVW	O1/O2v3	O2ac
gmlABD	O1/O2v1	O2aeh
gmlABD	O1/O2v2	O2aeh
gmlABD	O1/O2v3	O2aeh
wbbY + wbmVW	O1/O2v1	O1 (O2ac)
wbbY + wbmVW	O1/O2v2	O1 (O2ac)
wbbY + wbmVW	O1/O2v3	O1 (O2ac)

Abbreviations: gmlABD – galactosyltransferase and modifying enzymes involved in O2aeh subtype synthesis, wbbY – D-galactan II repeat unit polymerase, wbbZ – D-galactan II transferase, wbmVW – genes encoding enzymes for O2ac subtype modification.

Unmodified primers and Black Fluorescent Quenchers (BFQ) probes were manually designed using the Integrated DNA Technologies (IDT). Oligo-Analyzer (102) and Oligocalc (103) was used to determine the melting temperature (Tm), evaluate secondary structures, and identify self-binding sites of all primers and probes included in the final reaction set. The Basic Local Alignment Search Tool (BLAST) was used to confirm the in silico specificity of the assays included in the final reaction set (**Table 2.3**) and to ensure no cross-reactivity with non-target sequences (104).

Table 2.3 Oligonucleotide primer and probe sequences for detection of *K. pneumoniae* capsular (K-) & lipo-polysaccharides (O-) loci and O-antigens.

Assay-set name	Forward primer (5' to 3')	Reverse primer (5' to 3')	Probe (5' to 3')	Gene target	Accession/ Reference
ECO	CATGCCGCGTGTATGAAGAA	CGGGTAACGTCAATGAGCAAA	5' 6-FAM/TATTAACTT/ZEN/TACTCCCTTCCTCCCCGCTGAA/ 3'IABKFQ	***chuA***	Smati et al, 2013 (105)
gmlABD	GCATCGTTTGTCAGCCATATC	GTCACAATCGCATAACGAGAAC	5' SUN/AACGTCTCG/ZEN/CAGGTAGATTTGCGT/ 3'IABKFQ	***gmlD***	MG458670
gmlB	ACGGTGTAACTGATAATGAGGTAAT	GGTGCAATATAGCCGTGAAGA	5' 6-FAM/CGAGAGCCA/ZEN/GCGCAAGCATTT/ 3'IABKFQ	***gmlB***	LT174602
HKG CPS	CAAAGGCAATTCCAAAGGAG	CCAGCTCGTAGGAGGTATCG	5' 6-FAM/CGAGGAGTG/ZEN/CGTCACCAGAACAAT/ 3'IABKFQ	***GALF***	Panjaitan et al, 2021 (106)
KL10	CGACGATTTGAATCTGCAGTC	TCGGATGCCTCATTATCAACTAT	5' 6-FAM/TGGGAAAGG/ZEN/TTTATCGAGGTTGATGGG/ 3'IABKFQ	***wzc***	LT174532.1
KL102	GGTTATGTTGGCCAGTTGTATG	TCAGCTACCGAAAGCGTATTT	5' 6-FAM/ATTGTACTC/ZEN/GCTACCAGGCTTGGC/ 3'IABKFQ	***wzc***	AB371290
KL110	AAAGACCAACGTATTGAAGTAAGTC	GCACCAACTTTCGCTGTAATATC	5' SUN/CTGAGGAAC/ZEN/ATCGTTGGAATCATTTGGC/ 3'IABKFQ	***wzc***	LT174579.1
KL149	TGAAGGTCAAGTTGGTGAGAG	AAACGTGAAACATAGCCAATGATA	5' 6-FAM/AGATGCGAA/ZEN/ACCCGGGACTTCTTT/ 3'IABKFQ	***wzc***	ERS011792
KL15	TATCTGGTGCGAGCCCTAAT	TACGCATATCGGTATCAATAAACAATA	5' SUN/GTAAGTTCAAAT+C+T+G+GCGGCTGTAA/ 3'IABKFQ	***wzc***	ERS011978
KL171/KL22	GTTGAAGCGCAGAGTTTAATGG	CTGATCGACCGCGAAGTAAA	5' 6-FAM/AGCACCTTC/ZEN/AGCTTGTAATCGGCA/ 3'IABKFQ	***wzx***	LR588412.1
KL2	ACATTACAGGATGAAAGAGGGAAA	GCTCTACCTGACTCAACATCAC	5' SUN/ACAATGCCT/ZEN/GAGACTCAGCAAGAA/ 3'IABKFQ	***wzc***	AB371296
KL22/KL37/ KL171	TGTTCAAGACGAAGGAAAGGA	TTTAGCATCTTGTGCAGCTTG	5' 6-FAM/TGGGATGCT/ZEN/TACTCTTAGTCTGACAGGA/ 3'IABKFQ	***wzc***	LT174543.1
KL25	CCAAGGCAAAGATACGGGAA	CATCTTGTGCGGCTTGTCTA	5' SUN/TCCAGCCTT/ZEN/AGCAGAACGAATCATCG/ 3'IABKFQ	***wzc***	ERS005768
KL28	AGAGCACCCAACATATAAAGCA	CCCTTCCTGATTCAACATCTCTAC	5' 6-FAM/TGCCATCGA/ZEN/CTCAACAAGAAGTATTAAGGT/ 3'IABKFQ	***wzc***	ERS011986
KL3	CATCTACGCAGCAGGAAGTATTA	CTTGCTGACGATTCAACAACTG	5' SUN/TGTAGAGTC/ZEN/CGGTCGTGCTGTGTA/ 3'IABKFQ	***wzc***	ACZD01
KL30	GCCAAATCCCTCTGAACTACTAA	CGTACCTACATATTGCCCGATAA	5' 6-FAM/CCCGCCAAT/ZEN/ATTAGCTGTTACTGATGCA/ 3'IABKFQ	***wzc***	AB924568
KL39	GCTTACAGGTGAAGATCCAGTAT	CAGCCCTGACCTTTGGTAAT	5' SUN/ATATCGCTA/ZEN/GACAAGCTGCGCAGG/ 3'IABKFQ	***wzc***	ERS011815
KL62	GGAAGCGTATCTATTTCGAGATTATA	GCCAACTTCACCATCGAATC	5' 6-FAM/TCTCCTGCT/ZEN/CAACTTGAACTCACTGT/ 3'IABKFQ	***wzc***	AB371295
KPN HKG	AGGCCGAATATGACGAAT	GGTGATCTGCTCATGAA	5' SUN/ACTACCGTC/ZEN/ACCCGCCACA/ 3'IABKFQ	***gltA***	Gadsby et al, 2015 (107)
O1/O2v1	AATTCATCGCCTCATTGGATATTG	AGATACTCTTCCGGCGTTAATC	5' 6-FAM/TATCAAAGC/ZEN/GGCACACTATCGCCT/ 3'IABKFQ	***kfoC***	LT174601
O1/O2v2	TGATGCTCTTGTTGCTCTAAGG	GCTTCACCCGATAGCGTATTT	5' SUN/ACATTGTCG/ZEN/TATTCCTTGAGTGGCACT/ 3'IABKFQ	***kfoC***	LT174602
O1/O2v3	CCTTGCTGACTATGTGGGATTC	GCATTGATGAGCGGGTAGTT	5' SUN/ACCGCAGAC/ZEN/ACTTGAACTTTGCAG/ 3'IABKFQ	***wbbM***	MG280710
O12	CCTGGGAGTTTGTTTCGTTTAC	GCCTCTAAGCCAACACTTGA	5' 6-FAM/AAATTCGAG/ZEN/GCTGTTTGCCGATGC/ 3'IABKFQ	***wbbN***	LT174600
O3a	GAACAAGCTGGCGGAATTTG	GCTGGCGATGTCGGTATATT	5' 6-FAM/ATCTTCGCT/ZEN/ATTTCGCAGTCGGCA/ 3'IABKFQ	***wbdA***	LT174603
O3b	CTATCTGGGCGAACCAAACT	ACTTCCTGCATGGATGATCTG	5' SUN/TCAATACGA/ZEN/AAGGGCGGACGCTAT/ 3'IABKFQ	***wbdA***	LT174604
O4	GGCTAATGCTGGCATGAAATAAA	AACAGGTCAACCAGCCTTATC	5' 6-FAM/ACCTATAGT/ZEN/AAATCTGCTGGCTGC/ 3'IABKFQ	***wzm***	LT174605
O5	GGGATTTATCTGGAGCAGTGTTA	CCAAGATCATAGAGAGCGGTTG	5' 6-FAM/AGGCACGCT/ZEN/ATCAAACCAGTATGCT/ 3'IABKFQ	***wzm***	LT174606.1

O8	ACCTCTGCATGTCGGTAAAG	CGTCAGCTCACAGTAGAATGG	5' 6-FAM/TGGCTGTGC/ZEN/AGGTGATGATACTGG/ 3'IABKFQ	***wbbZ***	AB819963
OL101	CATGTTGACTGTGTATACCTTTGTT	TGGACGATCATACCGACAAATAA	5' 6-FAM/CGACTGGTG/ZEN/GAGATGAAAGCAGAACA/ 3'IABKFQ	***wzm***	LT174596.1
OL102	AAGACGACCTTATTGCGTATGT	CCCAAAGAGATGGAGATCAAAGA	5' 6-FAM/CAGGGAAGG/ZEN/TCACGATTGAGGGTG/ 3'IABKFQ	***wzt***	LT174597
OL103	TTTCGGACGTCGATTTCTCTC	GCGTTATTGCTCACCATCATAAA	5' SUN/ATTCTACGC/ZEN/GCCATCGATGTCAGG/ 3'IABKFQ	***wbbL***	LT174598
OL104	CCACGATCTCATTCCGTTACTT	AGCGTCCGACCTTTCATATTC	5' 6-FAM/TAAAGAACG/ZEN/CTATCTGGGCGAACCG/ 3'IABKFQ	***wbdA***	LT174599
RNP	AGATTTGGACCTGCGAGCG	GAGCGGCTGTCTCCACAAGT	5' 6-FAM/TTCTGACCTGAAGGCTCTGCGCG/ 3'BHQ	***ribonucleaseP***	NM_006413.5
tyrB	GAGTTTGGCGTCTACCTGATTG	TTACATCACCGCAGCAAAGG	5' SUN/TCGTATGTG/ZEN/CGTGGCAGGGTTAAA/ 3'IABKFQ	***tyrB***	CP123430.1
wbby	GTCGTACTTCCATCATCAACCA	CCCGTTAGTTAGCGTGTGTATAA	5' SUN/ATTGATGCG/ZEN/AGTGCTTGCTGAAGC/ 3'IABKFQ	***wbbY***	MG458672
wbbZ	CTCACCTGGAATGGCGATTAT	ATGCAGCCTGTCGGTATTG	5' 6-FAM/TTCTGGCGC/ZEN/GTAATTCTACCCGTT/ 3'IABKFQ	***wbbZ***	KJ451390.1
wbmVW	CTTAATCGCCCTGGACAAGA	ATTGAGGCCCATGGTCTAAC	5' 6-FAM/TGTTGGTGC/ZEN/TACAGATGAACGGCT/ 3'IABKFQ	***wbmV***	MG602074

IABkFQ is an Iowa Black® Fluorescent Quencher and BHQ is Black Hole Quencher ordered from Integrated DNA Technologies

2.2. Assay Optimisation

Assay optimisation involved empirical testing of various parameters, including primer and probe concentrations, annealing temperatures, and reaction conditions, to ensure optimal efficiency, specificity, and minimal cross-reactivity. Optimal conditions were defined as those yielding amplification efficiencies between 90–110%, R^2 values above 0.99, and no amplification in non-target controls. Each assay was initially tested in singleplex format to confirm target specificity and performance. Following successful validation of singleplex reactions, potential duplex combinations were explored to improve throughput. Duplex pairs were selected based on non-overlapping melting temperatures, compatible amplification efficiencies, and minimal interference between assays. Only duplexes that showed comparable Cq values to their respective singleplex reactions and maintained high specificity were retained. This approach ensured that the final assay configuration achieved high sensitivity while maximising the use of the nanofluidic qPCR platform.

2.2.1. Specificity and sensitivity controls

2.2.1.1. Synthetic calibrators (gBlocks™)

Synthetic double-stranded DNA (dsDNA) template gene fragments (gBlocks™) were designed and used as external calibrators to determine the analytical efficacy and diagnostic performance of the assays included in the final reaction set. The gBlocks™ contained equimolar ratios of all templates for the housekeeping genes, K-loci, O-loci, and O-types included in the final reaction set (**Table 2.4 & Table 2.5**). The amount of gBlocks™ synthetic DNA was measured using the Eazydrop quantifier (Anatech, USA) following manufacturer instructions. Briefly, the copy number, representing the number of gene equivalents, was calculated using the following formula:

$$Number\ of\ copies = \frac{Amount\ (ng) \times 6.022\ \times 10^{23}}{Length\ (bp)\ \times 1 \times 10^{9}\ \times 660}$$

The number of copies was determined as the average of three Eazydrop measurements, multiplied by Avogadro's number (6.022×10^{23}). The length in base pairs was multiplied by the average weight of a dsDNA nucleotide (660 Daltons or g/mole) and then converted back to ng (1×10^{9}).

Table 2.4 External synthetic calibrator (gBlock™) sequences.

gBlock™ name	*gBlock™ sequence*
gBlock™ 1	AGCGTTGGTTTATGTTGTTTTTTCTACACCAATCTATCAAGCAGATGCATTAATTCAAGTTGAACAAAAACAAGGCAATGCTATATTAAATAATTTAA GCCAAATGCTTCCTGACAGTCAGCCTCAGTCAGCACCTGAAATTGCTTTAATTCAATCTAGGTAATTTAGAATTTGAAGGTCAAGTTGGTGAGAGC ATTGAAAATGGCGGCATTTCAATAAAAGTTAATAAACTAGATGCGAAACCCGGGACTTCTTTTATCATTGGCTATGTTTCACGTTTAAAAGCAATAA CTGATTTGCAAAGATTCAGCAGGAACAGGAGCTTTAGTTGGTTTTCCTGCTGATCATTCCGCAATAAAAGTATCGGAAAAAAATGGTATTTCCTTA GAGGGCCATAAAGCGACCCAATTCTCATCTAAGCTAGGGAGACAATATGATTTATTACTTGTCATGGAAAAAAAAGGAAAACATTACAGGATGAAA GAGGGAAATTAAATAAGCGTGTTGCAACAATGCCTGAGACTCAGCAAGAAATTTTACGTTTGAGTCGTGATGTTGAGTCAGGTAGAGCTGTATAT ATGCAATGGCGAAAAAGACCAACGTATTGAAGTAAGTCGATTATATTTGCCAAATGATTCCAACGATGTTCCTCAGATTAAGATTGAGATCATTGA TGATAAAAATTATCGCATAATAGGGGGTAACTTCGATATTACAGCGAAAGTTGGTGCTCTAATTGAAAAGAGATCACAAAAAGCGTATGTAACAGG AGAGGTTGTAAAATCAGGCCAGCAGGCTATTACTAACATTCCATTGACCGTGATGGATGCAATCAATGCTGCAAGATAAGTTAAATGCTTATCGCA AACAGAAAGACTCTGTTGACCTAACCATGGAGGCTAAATCAGTTCTGGAGCAAATTGTTAATGTTGACAATCAACTTAACGGCTTGACTTTCCGTG AAGCGGAAATATCACAACTATATACCAAAGAGCACCCGACCTATAAAGCATTAATGGAGAAGCGACAGGTA
gBlock™ 2	TGCTAACTATATCGCTTACAGGTGAAGATCCAGTATTAATAAAAAAAATAATTGATAGTGTTAGTGGTAACTATTTGGCGCAAAATATCGCTAGACA AGCTGCGCAGGATGCAAAAAGTCTTGATTTTTTAAATCAACAATTACCAAAGGTCAGGGCTGAACTAGATGTTGCTGAAGATAAACTATTTGATCT TAGTAGATACCCCGCCAATATTAGCTGTTACTGATGCAGCGATTATCGGGCAATATGTAGGTACGGTATTACTTGTGGCTAGATTTGAATTACGTA CCAGCCTTCATTTCGCCATGATGGAAGCAAGAAATAATGTACTGATGATATCTGGTGCGAGCCCTAATGCAGGGAAAACTTTTGTAAGTTCAAATC TGGCGGCTGTAATTTCTCAGACAGGGAAAAAGGTATTGTTTATTGATACCGATATGCGTAAAGGCTACACGCATAAATTGTTCAATGAAAATTGAT AATGCTGTAACAGATCCTAAACCGGTTAAGCCAAAGAAAATTTTGATTGTACTGTTTGGCTTTGTATTAGGGCTTGGCTTTTCTGTTTTCTTCGTAT TACTACGTGTTTTCATGCACCGTGGAATAGAATCTCCAGAAGAGTTAGAAGCAAAGGCAATTCCAAAGGAGATGCTGCCGATCGTTGATAAGCCA ATGATTCAGTACATTGTTGACGAAATCGTCGCCGCCGGGATCAAAGAGATTGTTCTGGTGACGCACTCCTCGAAGAACGCGGTGGAAAACCACT TCGATACCTCCTACGAGCTGGAATAAATATTCTATTTCAGCAGATAATTTAGAATTTGAAGGTCAAGTTGGTGAGAGCATTGAAAATGGCGGCATT TCAATAAAAGTTAATAAACTAGATGCGAAACCCGGGACTTCTTTTATCATTGGCTATGTTTCACGTTTAAAAGCAATAACTGATTTGCAAGAGAAAC TTTCT
gBlock™ 3	AAATTGGGGCAAGTACCACCAAACCCTGCAGAATTGCTTATGCACCCGCGCTTTGAATCGTTTTTAAAAAATATTTCTGAACGATACGATCTTGTC ATAATTGATACTCCACCTATTTTGGCCGTAACAGATGCAGCAATTATAGGCCGATATTAGGCAAAACGGTCGACGATTTGAATCTGCAGTCAAAAA TTGAACCAAAGTATTTTCCTATTTTTGGGAAAGGTTTATCGAGGTTGATGGGGGAAAAAAATGGTACATTAGAAATCACAAGGTTATATATTCCAAT AGTTGATAATGAGGCATCCGAATTAGAAATAGAAGTCAAAGATCAATCGCATTATTAATTGTTCAAGACGAAGGAAAGGATTCTGGGATGCTTACT CTTAGTCTGACAGGAGAAGATCCTATTCAAATAAAGAACATTCTTGATAGTATAACGCAAAATTATTTAGCACAAAATATTGCTCGGCAAGCTGCA CAAGATGCTAAAAGCTTGGAGTTTCTACAAGTACAGTTCCTGTTAAGCCTCAGAAATTATTGATTGTCCTTGTAGGGTTGATCGCTGGTTTGATTA TCTCTATAACAACTGTGTTAATTAAAGTCTTTCTTAATAGAGGTATTGAATCACCGGAGCAACTGGAAGACGTTGGTAAGATAAGAAAGTTGAAGC GCAGAGTTTAATGGATGCTATAGAGCTTGCAAGTTTAGCACCTTCAGCTTGTAATCGGCAGCCATTTAAATTTTACTTCGCGGTCGATCAGAACAA AGCTGGTTATGTTGGCCAGTTGTATGAAAATGACGACTTTTCCATTAAAGTTGATAAGATGGATGCCAAGCCTGGTAGCGAGTACAATATATATTA TGAAAGTCGTCTCAAAGCTATAAGTGATTTGCAAAATACGCTTTCGGTAGCTGAAAGTGTTGTTGACCAAGGCAAAGATACGGGAATGCTAAGTA TTACTTTTACCGATGAAAATCCAGCCTTAGCAGAACGAATCATCGATAGCATAAGTCAAAATTATTTAACACAAAATATAGCTAGACAAGCCGCAC AAGATGCTCTCGA
gBlock™ 4	GGAAGAATGAACCCCTTGCTGACTATGTGGGATTCATGCATTACCGCAGACACTTGAACTTTGCAGAACAACAAAATCATCCTGAGGATAACTGT GGTCAACTACCCGCTCATCAATGCCGAATACGAAAGCCAGTTTGGTGATGCCATTGATGGCACTCGTGGGATATTGGCGGGTATGGTCATGCTC AGCCATATGTTTGGCAGCTTTATGGGTTGGCCGCAAGTCAGACCATTTAGCGGTGCCTATCTGTGCGTGGTATATTTTGATAAATAAGACTATGA GGCTAATGCTGGCATGAAATAAAGCAGCCAGCAGATTTACTATAGGTAATATCTCAATAGGGAAAACAACTTTTTTGACGAAGTTTACATTTGAGG TGATAAGGCTGGTTGACCTGTTAATACATTCATATTGCTGAGCATTTGCCCTTTGAGGTATTGCAGCAGCTCGTCATGCATACCTTACGGGTGCT GAAACCTGGCGGTTTGCTAATCCTCGAAACGCCGAACCCGGAGAATGTATGGAATGGTTAAAAAACGCTGACCTTCTGCTAACTAACTCCGCTTA TACGGCACAGGAAGCGATTGAGCATCTGCATTTGCAGGGCGACCATGTGCAGAATATTGCAGCTGCAGCCGATCCTCAGTTTTGTATGGCGGAA GTGACAGCGAGCGAGAAAGATCTATTATCCAACCTCTGCATGTCGGTAAAGCAAACTCTTATAATGATATTGGCTGTGCAGGTGATGATACTGGA GATAATATCTCGTTTAAAAATCCATTCTACTGTGAGCTGACGGCCCATTACTGCTTCACGCGAATTCATCGCCTCATTGGATATTGATGAAAGCGA TTTTTATGATGATTTTATCAAAGCGGCACACTATCGCCTGATTCGATTAACGCCGGAAGAGTATCTTTTCTCGTTAAACTATCATTGCGCACTTGAT GCTCTTGTTGCTCTAAGGGATTTTCTTTTTAAAAATGGCATGATGCAAAAGCGACAAAGGGATTTTTATAATTACATTGTCGTATTCCTTGAGTGGC ACTTAAATACGCTATCGGGTGAAGCCTTTAATAAA
gBlock™ 5	CTATTCGTAACGGTGTAACTGATAATGAGGTAATTCCCTCGAGAGCCAGCGCAAGCATTTTTTTAATTGGATATTTTGATTCACCGGCAATTCTTTC TTCACGGCTATATTGCACCTCGATCGAGAGTTTTATATGAACAAGCTGGCGGAATTTGAGCGGGCAGACGCGATCTTCGCTATTTCGCAGTCGG CAGCTCAGGAAGTGATCGAATATACCGACATCGCCAGCGATCGGGTACTGATAAAGAACGCTATCTGGGCGAACCAAACTTCCGTCAGTATTATT ATGATAAACTAGCTCAATACGAAAGGGCGGACGCTATTTTTGCTATTTCCAGATCATCCATGCAGGAAGTTATCGATTACACATCCGGGCGCATC CTGGGAGTTTGTTTCGTTTACGAGATGACATATTTAGCATTGATGCATCGGCAAACAGCCTCGAATTTATTCAAAAATGTCATTCTATTTATACTAT TAACTCAAGTGTTGGCTTAGAGGCGCTTTTATGCCATGTTATAACGAGGAAGAAGTATTCAGTCACTGCTTATCTGAATTACAAGCGGTTCTGGCG GAATTAGTCACGGCAACACTGATTTCAGCTGATAGCTATATTTTATTCGTTGATGATGGCAGCTGTGATTCAACGCCATATCACCGGCATCGTTTG TCAGCCATATCGCCAACGTCTCGCAGGTAGATTTGCGTGATAAGCTGGCTACTGAAGCCTTTAGTTCTCGTTATGCGATTGTGACCGATCCAGCT

gBlock™ 6

CAAACATCTTCTGTCGTACTTCCATCATCAACCAAGATGACCTCAATATTTTGGTACGTCTGAGATTTTATTGATGCGAGTGCTTGCTGAAGCAAAT
GGTGACGTTCGAAGTGAGTTATACACACGCTAACTAACGGGCTGTTAGCTTCGCTTATAGGCTTAATCGCCCTGGACAAGATGTTGGTGCTACAG
ATGAACGGCTTTTTATACATTTTGAAATTTTTGAGTGGCTTTATGAGCAAGTTAGACCATGGGCCTCAATGGCAATCATGTTATCTGTTACCCTGTA
CAAAGTGGCAGGAAGAGGGGCGCTGGGAGGTTACTGATGACGGTCAGAAACGGCTAGGTTACGAACTTCCTGATTTTTCAGCTCGTCAAGATGA
TAACGTCTATATTGTTAGTGAAGATTCATTATCTGAAGCGTTAACTGAGTGTGGCGGTAATAGTAAGCAGGTAAGACGACCTTATTGCGTATGTTC
AGTAAAGTCTATCACCCTACTGCAGGGAAGGTCACGATTGAGGGTGATATCGGTTCTTTGATCTCCATCTCTTTGGGGATCAATCCATTGCCGGC
ACCATTTCAACTTTTCGGACGTCGATTTCTCTCATCATTTTTTCCCAACATAAATAATGAGTATGAATTGCGTAACGCTAATTTTAATGCTGCATTCT
ACGCGCCATCGATGTCAGGATGTTTTATGATGGTGAGCAATAACGCCATTCTACAAGTTTTGTGTTTGCCACGATCTCATTCCGTTACTTAATAAA
GAACGCTATCTGGGCGAACCGAACTTCCGTCAGTATTATCTTGATAAACTTGCTGAATATGAAAGGTCGGACGCTATTTTTGCTATTGCCTGATGC
AGCCATGCCGCGTGTATGAAGAAGGCCTTCGGGTTGTAAAGTACTTTCAGCGGGGAGGAAGGGAGTAAAGTTAATACCTTTGCTCATTGACGTT
ACCCGCAGAAG

gBlock™ 7

GGCTAGACGAGTTTGGCGTCTACCTGATTGCCAGCGGTCGTATGTGCGTGGCAGGGTTAAACTCACGTAATGTTCAGCAGGTGGCGAAAGCCTT
TGCTGCGGTGATGTAAGGCTGAAATATCTCAGTTGTATACAAAAGAGCACCCAACATATAAAGCATTATTAGAAAAAAGGAATACTCTTCAAGAGG
AAAAAAATAAGTTAAACAAAAAAGTTAGTTCTATGCCATCGACTCAACAAGAAGTATTAAGGTTAAGTAGAGATGTTGAATCAGGAAGGGCAGTTT
ATTTACAACTACTCAATAAACGGGTGAGTAGCATGCCATCTACGCAGCAGGAAGTATTACGTTTGAGTAGGGATGTAGAGTCCGGTCGTGCTGTG
TATTTACAGTTGTTGAATCGTCAGCAAGAACTAAATATTGCTAAATCAAATTACTAGAGGACAAGTTCCGCCAAATCCCTCTGAACTACTAATGCAT
GAGAGATTGAAATTATCTTTAGAATCAGTTTCTAAAGAATATGATTTGATCTTAGTAGATACCCCGCCAATATTAGCTGTTACTGATGCAGCGATTA
TCGGGCAATATGTAGGTACGGTATTACTTGTGGCTAGATTCAAGATTAACTGGGAAAGAAAATGGAAGCGTATCTATTTCGAGATTATATTTACCT
AGCTTAGAACATATTTCTCCTGCTCAACTTGAACTCACTGTTAAAGATAATAAACATTATACGGTTTCATATAATAGTACTAGATTCGATGGTGAAG
TTGGCACTCTATTAAACAAAAATGGTATTTCTAGGCCGAATATGACGAATACTACCGTCACCCGCCACATTCATGAGCAGATCACC

Table 2.5 External synthetic calibrator (gBlock™) properties.

gBlock™ name	Assay-Set Targets †	Length (bp)	Amount (ng/µl) ‡	Gene equivalents (Copy no)
gBlock™ 1	KL110, KL149, KL2	1033	11.43	1×10^{10}
gBlock™ 2	*K. pneumoniae* CPS, KL15, KL39	965	13.22	1.25×10^{10}
gBlock™ 3	KL10, KL102, KL171/KL22, KL171/KL22/KL37, KL25	1069	10.83	9.24×10^{9}
gBlock™ 4	O1/O2v1, O1/O2v2, O1/O2v3, O4, O8	1084	15.6	1.31×10^{10}
gBlock™ 5	*gmlABD, gmlB*, O12, O3/O3a, O3b	765	11.48	1.37×10^{10}
gBlock™ 6	ECO, OL102, OL103, OL104, *wbbY, wbmVW*	969	11.8	1.11×10^{10}
gBlock™ 7	KL28, KL3, KL30, KL62, *K. pneumoniae* HKG, *tyrB*	854	12.49	1.33×10^{10}

† Targets in gBlock™ following in order of design.

‡ Average value of 3 successive EzDrop measurements.

Abbreviations: CPS – Capsule polysaccharide, ECO –*Escherichia coli*, *gmlABD* – Galactosyltransferase and modifying enzymes for O2aeh subtype, HKG – Housekeeping gene, KL – Klebsiella capsule locus, OL – O-locus, *tyrB* – Tyrosine aminotransferase B, *wbbY* – D-galactan II repeat unit polymerase, *wbmVW* – Genes encoding enzymes for O2ac subtype modification.

2.2.1.2. Clinical Bacterial validators

Archived bacterial isolates of *K. pneumoniae* K-loci (KL2, KL3, KL10, KL15, KL22, KL25, KL28, KL30, KL39, KL62, KL102, KL110, KL149), O-loci (O1/O2v1, O1/O2v2, O3/O3a, O3b, O4, O5,

O12, OL101, OL103), and O-types (O1, O2a, and O2afg), which previously underwent WGS and typing by Kaptive v2.3, as well as *E. coli, K. grimontii, K. michiganesis, K. oxytoca, K. quasipneumoniae, K. quasivariicola*, and *K. variicola isolates*, which had also undergone WGS, were used to optimise the qPCR assay and assess its specificity. These isolates were selected from various VIDA studies that were collected between 2018 to 2022 that were sequenced and stored. This ensured the assay accurately targeted the desired loci without cross-reactivity between species or loci. Briefly, all isolates were grown according to standard microtiter culture methods to quantify their relative density, measured as colony-forming units per milliliter (CFU/mL) (108).

Bacterial isolates for KL171, KL37, O1/O2v3, OL102, OL104, O2ac, and O2aeh were not available at the time of study design; therefore, we could not validate these assays against clinical samples. Nevertheless, assays were still optimised using gBlocks™.

2.2.1.3. Extraction and quantification of bacterial isolates

Genomic DNA was extracted from all bacterial isolates, including control strains and clinical isolates, using the Whitesci Tanbead® Nucleic Acid Extraction System Maelstrom 4800 (Taiwan Advanced Nanotech) according to the manufacturer's instructions. Briefly, 50 µL of bacterial samples stored in Skim milk-Tryptone-Glucose-Glycerine (STGG) were combined with 200 µL of lysis buffer and incubated at 56ºC for 30 minutes. Following incubation, the lysate was processed using the Whitesci Tanbead® Nucleic Acid Extraction System Maelstrom 4800 and eluted in 100 µL of elution buffer. The extracted DNA was quantified using the Anatech EzDrop 1000 Micro-Volume Spectrophotometer (Blue-Ray Biotech, Taiwan) and stored at -80°C until further analysis.

2.2.2. IFC Standard BioTools BioMark™ HD nanofluidic qPCR loading, sample, and assay preparation

Extracts from culture controls and gBlocks™ underwent specific target amplification (STA) as an initial pre-amplification of DNA step for the Biomark™ HD system (Standard BioTools Incorporated, formerly Fluidigm™) following the manufacturer's instructions. Briefly, 100nM of both the forward and reverse primers for each of the 37 assays were mixed to create a primer pool and diluted with 10 mM Tris/HCL and 0.1 mM EDTA (pH 8) to give a final concentration of 18nM of each primer. The primer pool (1.25 µL) was then added to 1.25 µL of extracted DNA (10^5 CFU/mL), 1 µL TaqMan PreAmp Master Mix (Standard BioTools Incorporated, CA, USA), and diluted to a final volume of 5 µL with ultrapure distilled H_2O, then amplified with the T100 Thermal Cycler (Bio-Rad Laboratories, CA, USA). Cycling conditions included an initial activation at 95ºC for 10 minutes followed by 14 two-step cycles (denaturation at 95ºC for 15 seconds and annealing/extension at 60ºC for 4 minutes). Following pre-amplification, 20 µL of molecular-grade H_2O was added to each 5 µL sample (**Figure 2.4**).

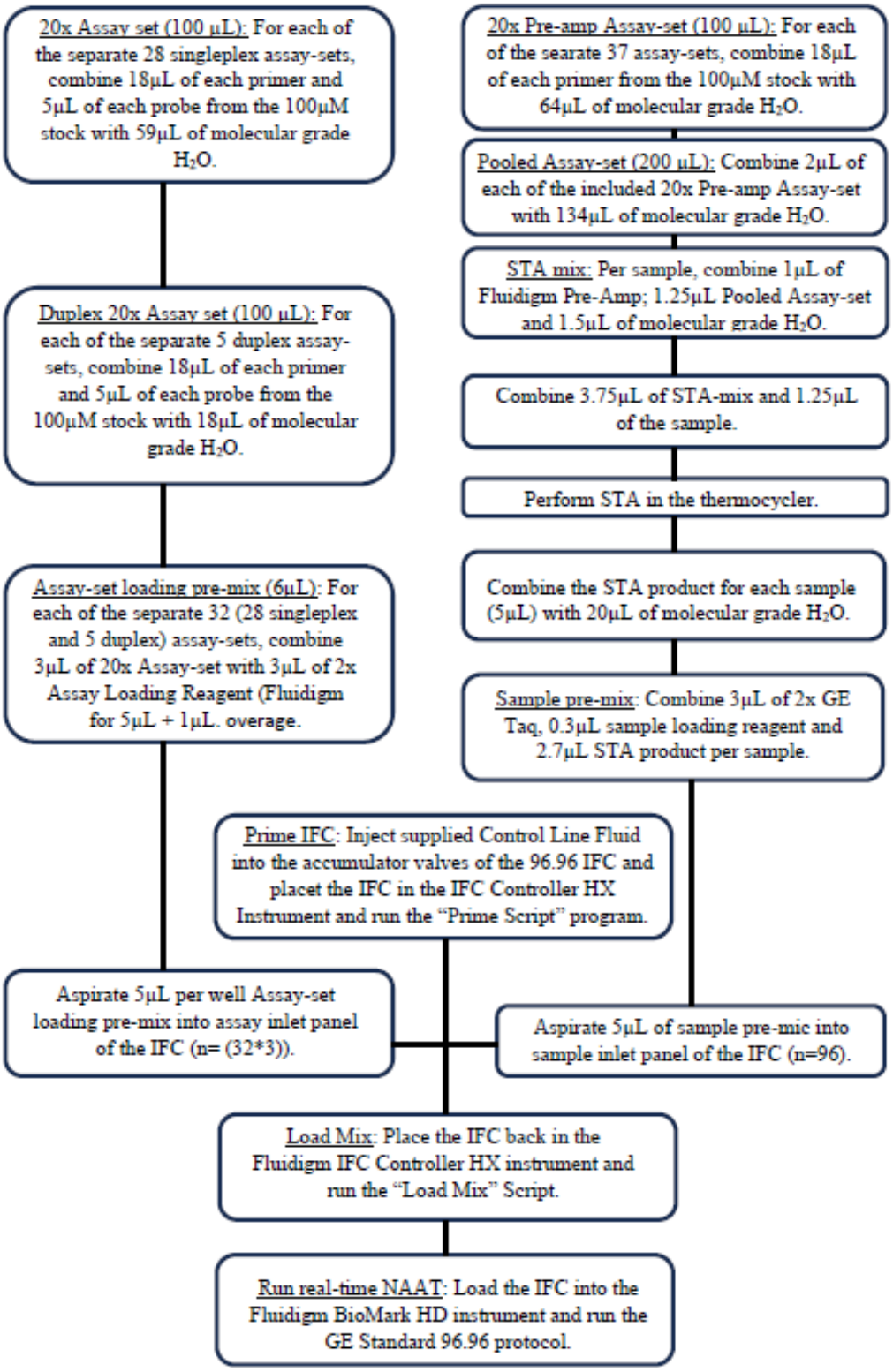


Figure 2.4 *Diagram of the STA nano-fluidic high throughput real-time qPCR workflow, within the 96.96 Gene Expression Dynamic Array integrated fluidic circuit (IFC) (Standard BioTools).*
Abbreviations: GE – gene expression, IFC – integrated fluidic circuit, STA – Specific target amplification

Following pre-amplification, qPCR was performed with the Standard BioTools 96.96 Gene Expression (GE) Dynamic Array Integrated Fluidic Circuit (IFC: product number: IFLUBMK-M10-96.96) according to manufacturer's instructions. In addition to the singleplex reactions, the assay design included five duplex reactions to increase throughput and cost-effectiveness

(**Table 2.6**). The decision to include five duplex reactions was based on practical and technical considerations to maximise the use of the 96-assay IFC platform while allowing triplicate testing of 32 reactions per sample; the selected duplexes, chosen from 216 possible combinations (excluding housekeeping genes), showed comparable Cq values to singleplex formats, ensuring assay performance was maintained.

Loading was done as follows: assay mixture and sample pre-mix were prepared separately, with each assay set [27 singleplex and 5 duplex reactions (**Table 2.6**)], prepared in triplicate making a total of 96 assays. Each assay included 2.5 µL of a diluted assay mix (IDT, Whitehead Scientific, Cape Town), which was constituted by combining the forward and reverse primers with the probe. The final concentrations of the dilution were 9 µM for each primer and 2.5 µM for the probe. Additionally, 2.5 µL of 2X Assay Loading Reagent (Standard BioTools Incorporated, Catalog No. 85000736) was added to each reaction mixture. The sample pre-mixture was prepared by mixing 2.5µL of TaqMan™ Fast Advanced PCR Master Mix (2X) (Life Technologies, Catalog No. 4444555), 0.25 µL of 20X GE Sample Loading Reagent (Standard BioTools Incorporated, Catalog No. 85000746), and 2.25 µL of the already diluted pre-amplified DNA for each sample/control across the 96 inlets.

Table 2.6 Duplex reactions pairs.

Prime/probe duplex combinations	
Primer/probe combination	**Duplex reaction**
O1/O2v3 (O2aeh) & OL102	A
wbbY & KL28	B
KL62 & KL110	C
KL22/KL171 & KL15	D
gmID & OL104	E

The 96.96 dynamic arrays IFC Chip (Standard BioTools Incorporated, CA, USA) were primed with control line fluid using an IFC controller HD (Standard BioTools Incorporated, CA, USA) as per the manufacturers instructions. Subsequently, 5 µL of each prepared assay and sample mixture was pipetted into the designated inlets on the primed chip, which was then loaded using the IFC controller HD. The loaded chip was then placed in the Biomark™ HD system for nucleic acid amplification tests, initiating with a 10-minute incubation at 95ºC, the cycle conditions were as follows: 40 cycles of 15 seconds at 95ºC and 1 minute at 60ºC.

Data was analysed using the Real-Time PCR Analysis Software on the Biomark™ system (Standard BioTools Incorporated, CA, USA), with thresholds manually defined. Samples were defined as negative if the Cq values were ≥35 for each tested assay.

2.2.3. Optimisation performance

All assays were optimised according to the minimum information for publication of quantitative real-time PCR experiments (MIQE) guidelines (109). Briefly, calibration curves were prepared using ten-fold serial dilutions of the targeted positive culture control strains or gBlocks™ in triplicate for each assay set across the linear dynamic range of 10^8-10^1 GE/mL. To establish the linear dynamic range and the correlation coefficient (r^2), a minimum of five data points were used, and extreme outliers that failed to show a linear trend in Cq values were excluded. For each assay set, the efficiency (formula below) was calculated based on the slope (m) of the linear relationship (represented as y = mx + c) delineated by the standard curves (ideally between 90–110%).

$$E = \left[-1 + 10^{\left(-\frac{1}{m}\right)}\right] \times 100$$

To establish the analytical sensitivity or limit of detection (LOD), which is defined as the lowest copies of bacteria detectable in triplicate using the Standard BioTools Biomark™ HD system, bacterial control strains or gBlocks™ at the lower end of the linear dynamic range (10^3–10^0 copies per µL) were utilised.

The repeatability (intra-assay variance) was assessed by determining the standard deviation (SD) for the variance in Cq of gBlocks™ (at 10^3 gene equivalents) run in triplicate within the same IFC (qPCR plates). Reproducibility (inter-assay variance) was defined as the standard deviation for Cq variance for the gBlocks™ in triplicate across four different IFCs. To determine the accuracy of the assay sets, a ratio was calculated between the observed copy numbers, derived from the standard curves, and the expected copy numbers, calculated from the known input concentrations of the template DNA.

2.3. Assay Validation

2.3.1. Samples for validation

Archived *K. pneumoniae* bacterial cultures collected between March 2019 February 2021 from infants 0-90 days as part of an observational study of invasive bacterial disease were retrospectively tested (110). Briefly, all *K. pneumoniae* isolates were sequenced and serotyped using Kaptive v2.3.

Samples collected from infants up to 90 days of age in a longitudinal microbial surveillance of infants hospitalised post-delivery were retrospectively tested. The study has been described (111). In brief, 102 neonates were enrolled in the Thelle neonatal colonisation (TNC) study within 24 hours of birth at Thelle Mogoerane Regional Hospital (TMRH) in Johannesburg,

South Africa, from 25 October 2021 to 30 April 2022. Rectal, nasal, and skin swab samples were collected from all infants at enrolment and then again at intervals between 48 to 96 hours until discharge or death. All swab samples were enriched in Brain-Heart Infusion (BHI) for 24 hours at 37ºC and then subsequently sub-cultured on a non-selective chromogenic medium. The enriched broth was stored with 10% glycerol at -80 ºC for downstream testing and 83 *K. pneumoniae* isolates underwent WGS for serotyping (15).

In this study, archived BHI broth samples were retrospectively tested on the nanofluidic qPCR panel, and the findings were compared to genomic data from sequencing of the *K. pneumoniae* isolates cultured from the same BHI broth sample.

2.3.2. Extraction and quantification of enriched BHI broth from swab samples

DNA extraction and quantification from swab samples enriched in BHI media (Product code: 53286-100G, Sigma-Aldrich Corp, USA) followed a similar protocol to section 2.2.2. Samples were thawed, vortexed at low speed for 30 seconds, and 200 µL of the enriched broth was used for nucleic acid extraction. DNA was eluted into 100 µL of elution buffer using the Whitesci Tanbead® Nucleic Acid Extraction System Maelstrom 4800, following the manufacturer's instructions. A no-template control (NTC) was included with each batch of 47 clinical samples to ensure quality and accuracy during extraction.

2.3.3. Sample testing for validation

A total of 77 archived *K. pneumoniae* cultured isolates were retrospectively tested. The remaining 19 positions on the 96-well plate were filled with control samples and KpSC isolates to evaluate assay specificity.

For the BHI samples, 83 DNA extracts were tested that had been obtained directly from BHI-enriched swab specimens (skin, rectal, or nasal). Previously, cultured isolates obtained from these same BHI-enriched broth samples had undergone whole-genome sequencing (WGS) at the time of the study. The results from the BHI extracts were compared to the WGS data from the corresponding cultured isolates to evaluate assay concordance. The remaining 13 positions on the plate were filled with assay controls.

Positive controls included pooled archived bacterial isolates of *K. pneumoniae* representing a range of K-loci (KL2, KL3, KL10, KL15, KL22, KL25, KL28, KL30, KL39, KL62, KL102, KL110, KL149), O-loci (O1/O2v1, O1/O2v2, O3/O3a, O3b, O4, O5, O12, OL101, OL103), and O-types (O1, O2a, and O2afg). Additional controls comprised isolates of *E. coli*, *K. grimontii*, *K. michiganensis*, *K. oxytoca*, *K. quasipneumoniae*, *K. quasivariicola*, and *K. variicola*, along with seven synthetic gBlocks containing target sequences. These controls were included to confirm that the assay was functioning correctly. Extraction NTC were also added to each panel to confirm that no contamination or primer cross-reactivity took place.

All samples were pre-treated using STA and were tested and analysed on the Standard BioTools qPCR platform, as previously described in Section 2.2.2.

2.3.4. Co-colonisation detection, classification, and visualisation

Co-colonisation was defined as the detection of more than one *K. pneumoniae* serotype (K- or O-locus) within a single BHI-enriched swab sample, as identified by the nanofluidic qPCR assay. Detection was based on serotype-specific amplification curves with valid Cq values (≤24) in at least two out of three replicates. When multiple serotypes were detected in a single sample, their relative abundance was estimated using Cq values, under the assumption that lower Cq values reflect higher template concentrations.

The primary coloniser was defined as the serotype with the lowest average Cq value across replicates, indicating the highest relative abundance. Secondary and tertiary colonisers were classified as additional serotypes detected with progressively higher Cq values. Only serotypes with clear, reproducible amplification across replicates were included in the classification.

Figures were generated as chord diagrams using Flourish (version 8.6.6, 2024), a data visualisation platform developed by Canva UK Operations Limited. These diagrams were used to illustrate serotype diversity and co-colonisation patterns among *K. pneumoniae* strains detected in BHI-enriched samples.

2.4. Statistical Analysis

Cohen's kappa coefficient was used to evaluate the agreement between the nanofluidic qPCR method and Kaptive v2.3 (using WGS data as the reference standard) for detecting Klebsiella pneumoniae K- and O-loci. The interpretation of kappa values followed standard thresholds: values <0.20 indicated slight agreement, 0.21–0.40 fair agreement, 0.41–0.60 moderate agreement, 0.61–0.80 substantial agreement, and 0.81–1.00 denoted almost perfect or perfect agreement.

For cultured isolates, a direct 1:1 comparison was conducted, as each isolate was individually sequenced and tested on the qPCR platform. When assessing K-locus agreement, isolates with loci not represented in the qPCR assay panel (e.g., KL46) were excluded, resulting in 71 isolates analysed out of the original 77.

For the BHI broth swab samples, kappa was calculated by comparing the WGS-derived K-loci from cultured isolates to the K-loci detected in the corresponding enriched samples using the qPCR assay. Of the 83 samples tested, only 42 were included in the kappa analysis; the remaining 41 were excluded due to detection of K-loci not included in the qPCR panel. In samples where multiple *K. pneumoniae* strains were detected by qPCR, co-colonisation was

not grounds for exclusion. Instead, the strain with the highest relative density (based on Cq values) was considered the dominant strain and used for comparison with the WGS result.

To assess diagnostic performance, sensitivity, specificity, positive predictive value (PPV), and negative predictive value (NPV) were calculated using 2×2 contingency tables, with WGS as the gold standard. Sensitivity was defined as the proportion of true positives correctly identified by the assay, and specificity as the proportion of true negatives. PPV and NPV were calculated using standard definitions.

Additionally, receiver operating characteristic (ROC) curves were generated, and the area under the curve (AUC) was calculated to evaluate the overall discriminatory power of the qPCR assay. An AUC ≥0.99 was considered indicative of excellent assay accuracy. All statistical analyses were performed using STATA version 18 SE (2024).

.

2.5. Ethical Approval

Ethics consent for the parent studies was obtained from the Medical Human Research Ethics Committee (HREC) of the University of Witwatersrand: Correlates of protection study, HREC number: 181110 (**Appendix B**) and the Epidemiology of community and hospital-acquired invasive infections in young infants, HREC number: M200932 (**Appendix C**). Approval for further testing of these samples for this study was obtained from the HREC (M231117) (**Appendix D**). Written, informed consent had been obtained from the parents/guardians of all the study participants at the time of initial enrolment. All procedures adhered to the relevant local and international guidelines and regulations for Good Clinical Practice.

CHAPTER 3: RESULTS

3.1. Performance of the nanofluidic real-time PCR system

3.1.1. Analytical performance of the nanofluidic real-time qPCR

All 28 singleplex and 5 duplex assays were efficient in amplifying their respective targets with high sensitivity and specificity, with amplification efficiencies of the assays ranging between 92.1% and 107.3% (**Table 3.2**). Within the dynamic range, the correlation coefficient (r^2) of all assays was high (r^2 >= 0.99), allowing for precise relative quantification of the bacterial load through the slope of the linear equation.

3.1.2. Analytical sensitivity and specificity

The analytical sensitivity was high for all 36 included assays, with a LOD equivalent to >100 gene equivalents (GE) for 75% (n=27/36) of the assays, and >10 GE for assays targeting OL103, KPN HKG, KL25, *E. coli*, O1/O2v2, O12, KL28, KL62, O3/O3a and O3b. Furthermore, all the assays performed consistently with the inter-assay (reproducibility) and intra-assay (repeatability) variability within ± 0.1 SD of the mean, and the accuracy within ± 0.1 (**Table 3.2**). Furthermore, the Cq values for all duplex assays differed by no more than one Cq compared with their singleplex counterpart, and all assay sets demonstrated specificity to their respective target bacterial control calibrators, with no cross-reactivity observed between the assay sets.

Table 3.1 Singleplex vs duplex ct values at serial dilution

	OL104		gmlD		OL102		KL62		wbbY	
gBlock concentration	Singleplex	Multiplex	Singleplex	Multiplex	Singleplex	Multiplex	Singleplex	Multiplex	Singleplex	Multiplex
1 x 10-1 ng/µl	2,50	2,50	2,50	2,50	2,74	2,50	2,50	2,50	2,50	2,50
1 x 10-2 ng/µl	4,74	4,75	4,32	4,37	4,71	4,84	4,21	4,28	4,17	4,08
1 x 10-3 ng/µl	7,83	7,93	7,50	7,49	7,83	7,97	7,40	7,41	7,38	7,30
1 x 10-4 ng/µl	10,93	10,96	10,42	10,38	10,95	11,19	10,38	10,41	10,33	10,29
1 x 10-5 ng/µl	14,46	14,54	14,17	14,10	14,40	14,68	14,00	13,87	14,07	13,95
1 x 10-6 ng/µl	17,50	17,41	17,44	17,35	17,48	17,65	17,12	17,09	17,18	17,25
1 x 10-7 ng/µl	21,16	21,33	20,57	20,93	21,11	21,11	20,66	20,33	20,64	20,15
	KL22/KL171		**O2aeh**		**KL28**		**KL110**		**KL15**	
gBlock concentration	Singleplex	Multiplex	Singleplex	Multiplex	Singleplex	Multiplex	Singleplex	Multiplex	Singleplex	Multiplex
1 x 10-1 ng/µl	2,50	2,74	2,50	2,50	3,80	2,76	2,50	2,50	2,50	2,50
1 x 10-2 ng/µl	4,98	4,83	4,17	4,08	4,72	4,82	4,87	4,70	5,80	5,63
1 x 10-3 ng/µl	8,15	8,11	7,38	7,30	7,95	7,96	8,01	7,83	9,07	8,89
1 x 10-4 ng/µl	11,34	11,14	10,33	10,29	10,99	11,15	11,18	10,53	11,91	11,72
1 x 10-5 ng/µl	14,88	14,76	14,07	13,95	14,59	14,73	14,81	14,58	15,50	15,56
1 x 10-6 ng/µl	17,80	17,25	17,18	17,25	17,58	17,78	18,04	17,71	18,90	18,72
1 x 10-7 ng/µl	22,55	22,28	20,64	20,15	21,17	20,97	23,06	21,84	21,97	22,26

Table 3.2 Performance of the nanofluidic real-time qPCR

BACTERIAL TARGET	Gene	Standard Curve formula	Slope	Y-intercept	Coefficient correlation (r^2)	Efficiency (%)	Limit of detection (GE/PCR)	Intra-assay variation (CV)	Accuracy	Inter-assay variation (CV)
***Klebsiella pneumoniae* gene**	*gltA*	y = -3.3127x + 26.03	-3.31	26.03	0.99	100.39	10	0.0062	0.05	0.0083
Escherichia coli	*chuA*	y = -3.1586x + 24.489	-3.16	24.49	1.00	107.30	10	0.0048	-0.04	0.0349
Klebsiella Specie Complex	*tyrB*	y = -3.2482x + 28,13	-3.25	28.13	1.00	103.17	100	0.0044	-0.11	0.0215
***Klebsiella pneumoniae* Capsule polysaccharide**	*GALF*	y = -3.2524x + 29,309	-3.25	28.31	1.00	102.99	100	0.0054	0.00	0.0094
***Klebsiella pneumoniae* Capsule polysaccharide serotype KL10**	*GALF*	y = -3.2696x + 27,861	-3.27	27.86	1.00	102.23	100	0.0045	0.05	0.0286
***Klebsiella pneumoniae* Capsule polysaccharide serotype KL102**	*wzc*	y = -3.3244x + 28,496	-3.32	28.50	0.99	99.90	100	0.0063	0.06	0.0037
***Klebsiella pneumoniae* Capsule polysaccharide serotype KL110**	*wzc*	y = -3,3995x + 28.222	-3.40	24.80	1.00	96.86	100	0.0057	-0.14	0.0073
***Klebsiella pneumoniae* Capsule polysaccharide serotype KL149**	*wzc*	y = -3.3052x + 26,819	-3.31	26.82	1.00	100.70	100	0.0061	0.04	0.0291
***Klebsiella pneumoniae* Capsule polysaccharide serotype KL15**	*wzc*	y = -3.5161x + 29.644	-3.52	29.64	1.00	92.49	100	0.0031	-0.03	0.0295
***Klebsiella pneumoniae* Capsule polysaccharide serotype KL171/KL22**	*wzx*	y = -3,218x + 27.677	-3.22	27.68	0.99	104.53	100	0.0042	0.07	0.0269
***Klebsiella pneumoniae* Capsule polysaccharide serotype KL171/KL22/KL37**	*wzc*	y = -3.3166x + 28,468	-3.32	28.47	0.99	100.22	100	0.0079	0.06	0.0235
***Klebsiella pneumoniae* Capsule polysaccharide serotype KL2**	*wzc*	y = -3.3823x + 24,237	-3.38	24.24	1.00	97.54	100	0.0070	0.02	0.0158
***Klebsiella pneumoniae* Capsule polysaccharide serotype KL25**	*wzc*	y = -3.414x + 24.38	-3.41	24.38	0.99	96.30	10	0.0021	-0.05	0.0347
***Klebsiella pneumoniae* Capsule polysaccharide serotype KL28**	*wzc*	y = -3,2512x + 27.532	-3.25	27.53	1.00	103.04	100	0.0052	-0.03	0.0339
***Klebsiella pneumoniae* Capsule polysaccharide serotype KL3**	*wzc*	y = -3,1693x + 25,603	-3.17	25.60	1.00	106.79	100	0.0029	-0.01	0.0261
***Klebsiella pneumoniae* Capsule polysaccharide serotype KL30**	*wzc*	y = -3.1993x + 26,874	-3.20	26.87	1.00	105.38	100	0.0035	0.00	0.0283
***Klebsiella pneumoniae* Capsule polysaccharide serotype KL39**	*wzc*	y = -3.3575x + 27,835	-3.36	27.84	1.00	98.54	100	0.0035	0.05	0.0296
***Klebsiella pneumoniae* Capsule polysaccharide serotype KL62**	*wzc*	y = -3.2979x + 27.136	-3.30	27.14	1.00	101.01	10	0.0064	0.04	0.0218
***Klebsiella pneumoniae* Lipopolysaccharide Serotype O1/O2V1**	*kfoC*	y = -3.2755x + 27,51	-3.28	27.51	1.00	101.97	100	0.0064	0.05	0.0233
***Klebsiella pneumoniae* Lipopolysaccharide Serotype O1/O2V2**	*kfoC*	y = -3.3479x + 23.706	-3.35	23.71	1.00	98.93	10	0.0025	0.02	0.0093
***Klebsiella pneumoniae* Lipopolysaccharide Serotype O1/O2v3**	*wbbM*	y = -3.1805x + 26,9	-3.18	27.35	1.00	106.26	10	0.0067	-0.02	0.0180
***Klebsiella pneumoniae* Lipopolysaccharide Serotype O3/O3a**	*wbdA*	y = -3.4327x + 31,704	-3.43	31.70	1.00	95.58	100	0.0052	0.10	0.0213
***Klebsiella pneumoniae* Lipopolysaccharide Serotype O3b**	*wbdA*	y = -3.3067x + 27.271	-3.31	27.27	1.00	100.64	10	0.0056	-0.04	0.0043

***Klebsiella pneumoniae* Lipopolysaccharide Serotype O4**	*wzm*	y = -3.2563x + 28.254	-3.26	28.25	1.00	102.81	100	0.0055	0.09	0.0277
***Klebsiella pneumoniae* Lipopolysaccharide Serotype O5**	*wzm*	y = -3.5266x + 28.803	-3.53	28.80	1.00	92.11	100	0.0090	0.10	0.0187
***Klebsiella pneumoniae* Lipopolysaccharide Serotype O8**	*wbbM*	y = -3.3989x + 24.36	-3.40	24.36	1.00	96.89	10	0.0075	0.06	0.0236
***Klebsiella pneumoniae* Lipopolysaccharide Serotype O12**	*wbbN*	y = -3.2592x + 26,832	-3.26	26.83	1.00	102.69	100	0.0047	0.00	0.0184
***Klebsiella pneumoniae* Lipopolysaccharide Serotype OL101**	*wzm*	y = -3.3754x + 26.823	-3.38	26.82	1.00	97.82	100	0.0040	0.01	0.0158
***Klebsiella pneumoniae* Lipopolysaccharide Serotype OL102**	*wzt*	y = -3.2645x + 27.609	-3.26	27.61	1.00	102.45	100	0.0039	0.04	0.0246
***Klebsiella pneumoniae* Lipopolysaccharide Serotype OL103**	*wbbL*	y = -3.173x + 23.516	-3.17	23.52	0.99	106.61	10	0.0077	-0.08	0.0154
***Klebsiella pneumoniae* Lipopolysaccharide Serotype OL104**	*wbdA*	y = -3.2964x + 27.628	-3.30	27.63	1.00	101.08	100	0.0008	0.01	0.0229
***Klebsiella pneumoniae* Lipopolysaccharide**	*gmlD*	y = -3.3168x + 27,362	-3.32	27.36	1.00	100.21	100	0.0031	-0.04	0.0256
***Klebsiella pneumoniae* Lipopolysaccharide**	*gmlB*	y = -3,3284x + 28,777	-3.33	28.78	1.00	99.72	100	0.0056	-0.14	0.0292
***Klebsiella pneumoniae* Lipopolysaccharide**	*wbbY*	y = -3.2531x + 26,809	-3.25	26.81	1.00	102.95	100	0.0086	-0.04	0.0260
***Klebsiella pneumoniae* Lipopolysaccharide**	*wbbZ*	y = -3.383x + 27,957	-3.38	27.96	1.00	97.51	100	0.0064	0.05	0.0100
***Klebsiella pneumoniae* Lipopolysaccharide**	*wbmVW*	y = -3.2615x + 27,102	-3.26	27.10	1.00	102.59	100	0.0042	0.08	0.0143

Abbreviations: *CV: Coefficient of Variation, GALF: Capsule Polysaccharide gene in Klebsiella pneumoniae, gltA: Citrate Synthase, a housekeeping gene for K. pneumoniae, GGE/PCR: Gene Equivalents per Polymerase Chain Reaction, gmlD/gmlB/wbmVW: Genes involved in O-antigen synthesis in K. pneumoniae, kfoC: Gene involved in O-antigen synthesis (O1/O2) in K. pneumoniae, tyrB: Tyrosine aminotransferase, a housekeeping gene for the Klebsiella species complex, chuA: Heme transport protein gene in Escherichia coli, wbbM/wbbZ/wbbY/wbbL: Glycosyltransferase genes involved in O-antigen synthesis in K. pneumoniae, wbdA: Glycosyltransferase gene involved in O-antigen synthesis (O3) in K. pneumoniae, wzm/wzt: ABC transporter genes involved in O-antigen transport in K. pneumoniae, wzc/wzx: Genes involved in Capsule Polysaccharide (CPS) synthesis in K. pneumoniae*

3.2. Diagnostic sensitivity, specificity, and agreement of the nanofluidic qPCR reaction set for the detection of *K. pneumoniae* K-loci, O-loci, and O-types in bacterial cultures compared with whole genome sequencing

The nanofluidic qPCR method accurately classified *K. pneumoniae* LPS and capsular serotypes compared to WGS, demonstrating perfect concordance with a ROC-AUC greater than 0.99 for all assays (**Table 3.3**, **Figure 3.1, Figure 3.2, Table 3.4,** and **Figure 3.3**). For O-loci and O-types, 77 isolates were tested, while K-loci were assessed in 71 isolates. The remaining six isolates expressed K-loci that were not covered by the panel, preventing their inclusion in the analysis.

Table 3.3 Diagnostic performance of nanofluidic real-time PCR assays compared to whole genome sequencing in the detection of O-loci and O-types in 77 *K. pneumoniae* strains.

Target	*WGS* (n=77)*	*Nanofluidic real-time PCR (n=77)*	*Sensitivity (%)*	*Specificity (%)*	*Kappa*	*Agreement*	*PPV (%)*	*NPV (%)*	*ROC-AUC*
O1/O2v2	41 (53%)	41 (53%)	100%	100%	1	Perfect	100%	100%	1.0
O1/O2v1	14 (18%)	14 (18%)	100%	100%	1	Perfect	100%	100%	1.0
O3b	5 (6%)	5 (6%)	100%	100%	1	Perfect	100%	100%	1.0
O4	5 (6%)	5 (6%)	100%	100%	1	Perfect	100%	100%	1.0
O5	12 (16%)	12 (16%)	100%	100%	1	Perfect	100%	100%	1.0
O1v1	12 (16%)	12 (16%)	100%	100%	1	Perfect	100%	100%	1.0
O1v2	25 (32%)	25 (32%)	100%	100%	1	Perfect	100%	100%	1.0
O2afg	16 (21%)	16 (21%)	100%	100%	1	Perfect	100%	100%	1.0
O2a	2 (3%)	2 (3%)	100%	100%	1	Perfect	100%	100%	1.0

**The diagnostic performance of the nanofluidic qPCR method could not be assessed for assay sets targeting O1/O2v3, O8, O12, OL101, OL102, OL103, OL104, O2ac, and O2eah which were not detected in any clinical isolates by WGS in the GBS-CoP study.*

Table 3.4 Diagnostic performance of nanofluidic real-time PCR assays compared to whole genome sequencing in the detection of K-loci in 71 *K. pneumoniae* strains.

Target	WGS* (n=71)	Nanofluidic real-time PCR (n=71)	Sensitivity (%)	Specificity (%)	Kappa	Agreement	PPV (%)	NPV (%)	ROC-AUC
KL149	25 (35%)	25 (35%)	100%	100%	1	Perfect	100%	100%	1.0
KL25	15 (21%)	15 (21%)	100%	100%	1	Perfect	100%	100%	1.0
KL102	13 (18%)	13 (18%)	100%	100%	1	perfect	100%	100%	1.0
KL2	6 (8%)	6 (8%)	100%	100%	1	Perfect	100%	100%	1.0
KL110	4 (6%)	4 (6%)	100%	100%	1	Perfect	100%	100%	1.0
KL62	3 (4%)	3 (4%)	100%	100%	1	Perfect	100%	100%	1.0
KL28	2 (3%)	2 (3%)	100%	100%	1	Perfect	100%	100%	1.0
KL3	2 (3%)	2 (3%)	100%	100%	1	Perfect	100%	100%	1.0
KL30	1 (1%)	1 (1%)	100%	100%	1	Perfect	100%	100%	1.0

**The diagnostic performance of the nanofluidic qPCR method could not be assessed for assay sets targeting KL10, KL15, KL22, KL37, KL39, and KL171 which were not detected in any clinical isolates by WGS in the GBS-CoP study.*

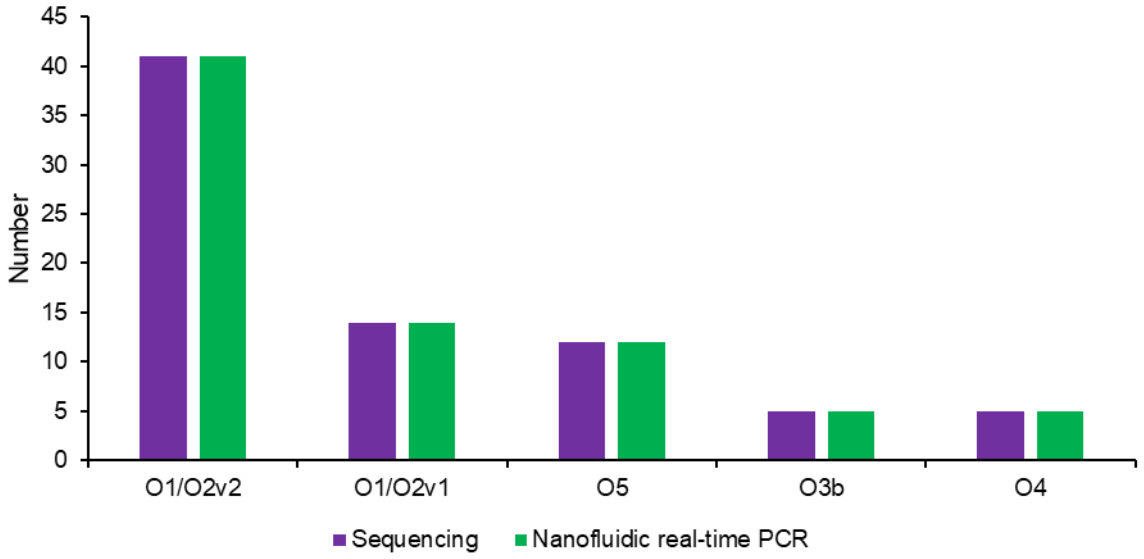


Figure 3.1 *O-loci detections using 77 cultures tested on a nanofluidic qPCR compared to prediction of Kaptive v2.3. No isolates available for O3/O3a, O8, O12, OL101, OL102, OL103, and OL104 for validation in cohort..*

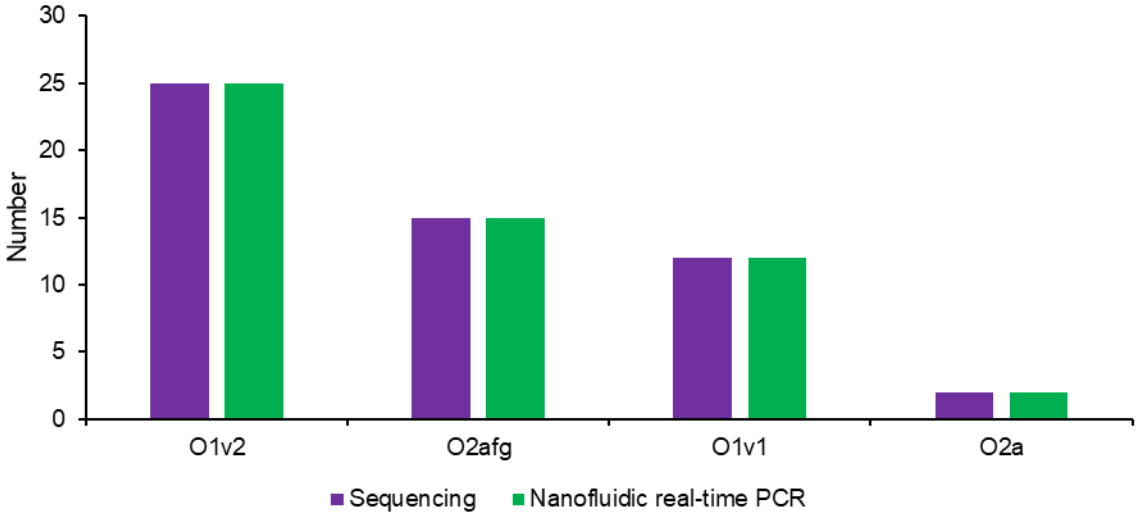


Figure 3.2 *comparison of the nanofluidic real-time PCR and sequencing (Kaptive v2.3) results for typing the O1/O2 complex in 55 isolates. The analysis focused on O1v2, O2afg, O1v1, and O2a, while O2ac and O2aeh isolates were not available in the cohort for validation. Other O-serotypes were represented by different O-loci due to a 1:1 ratio with the O-types, removing the need for additional assays.*

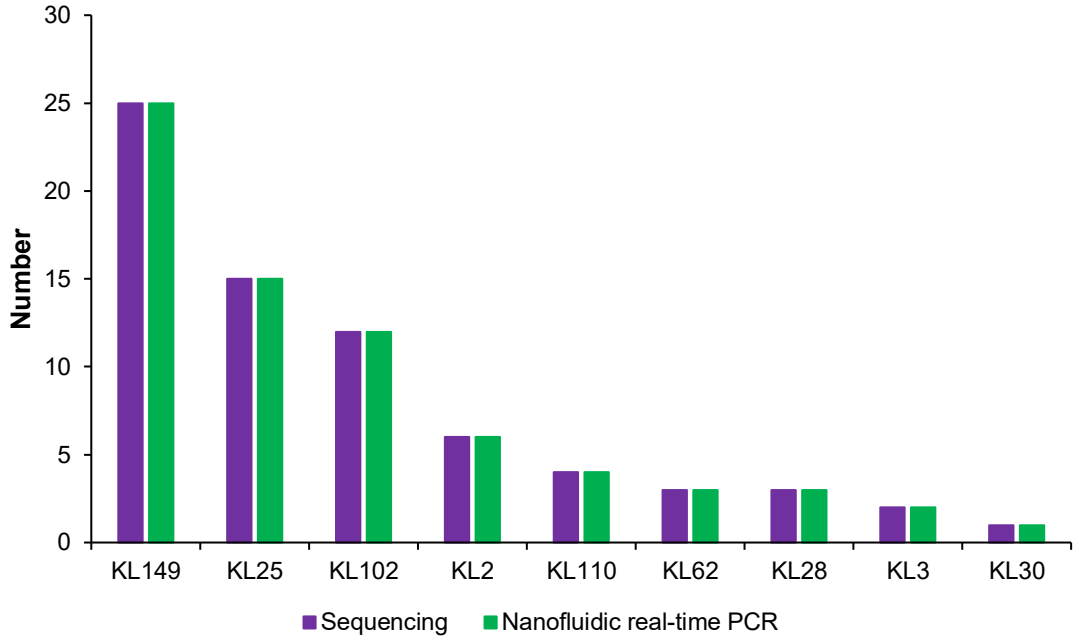


Figure 3.3 *K-loci detections using cultures tested on a nanofluidic qPCR compared to prediction of Kaptive v2.3 (N=71). No bacterial isolates available for KL10, KL15, KL22, KL37, KL39, and KL171 in cohort to compare.*

3.3. Diagnostic sensitivity, specificity, and agreement of the nanofluidic qPCR reaction set for the detection of *K. pneumoniae* K-loci, O-loci, and O-types in swab samples enriched in BHI compared with whole genome sequencing

A blind analysis of 83 enriched broth samples targeting O-loci demonstrated perfect concordance (kappa = 1) between nanofluidic real-time qPCR and WGS, achieving 100% sensitivity and specificity across all the assays for detecting K- and O-loci. In this analysis, 42 K-loci were tested, as the remaining samples expressed K-loci not covered by the panel, consistent with previous testing limitations.

Table 3.5 Comparative Analysis of K-loci detection between sequencing and nanofluidic real-time qPCR.

Target	KL25	KL15	KL102	KL10	KL110	KL39	KL62	KL3	KL30
***Sequencing (42)**	25 (60%)	3 (7%)	5 (12%)	1 (2%)	2 (5%)	1 (2%)	1 (2%)	2 (5%)	2 (5%)
Nanofluidic real-time qPCR (42)	25 (60%)	3 (7%)	5 (12%)	1 (2%)	2 (5%)	1 (2%)	1 (2%)	2 (5%)	2 (5%)
Sensitivity (%)	100%	100%	100%	100%	100%	100%	100%	100%	100%
Specificity (%)	100%	100%	100%	100%	100%	100%	100%	100%	100%
Kappa	1.00	1.00	1.00	1.00	1.00	1.00	1.00	1.00	1.00
Concordance	Perfect	Perfect	Perfect	Perfect	Perfect	Perfect	Perfect	Perfect	Perfect
PPV (%)	100%	100%	100%	100%	100%	100%	100%	100%	100%

NPV (%)	100%	100%	100%	100%	100%	100%	100%	100%	100%
ROC-AUC	1	1	1	1	1	1	1	1	1

**The diagnostic performance of the nanofluidic qPCR method could not be assessed for assay sets targeting KL2, KL171, KL37, KL22, KL149, and KL28, which were not detected in any clinical isolates by WGS in the TNC study.*

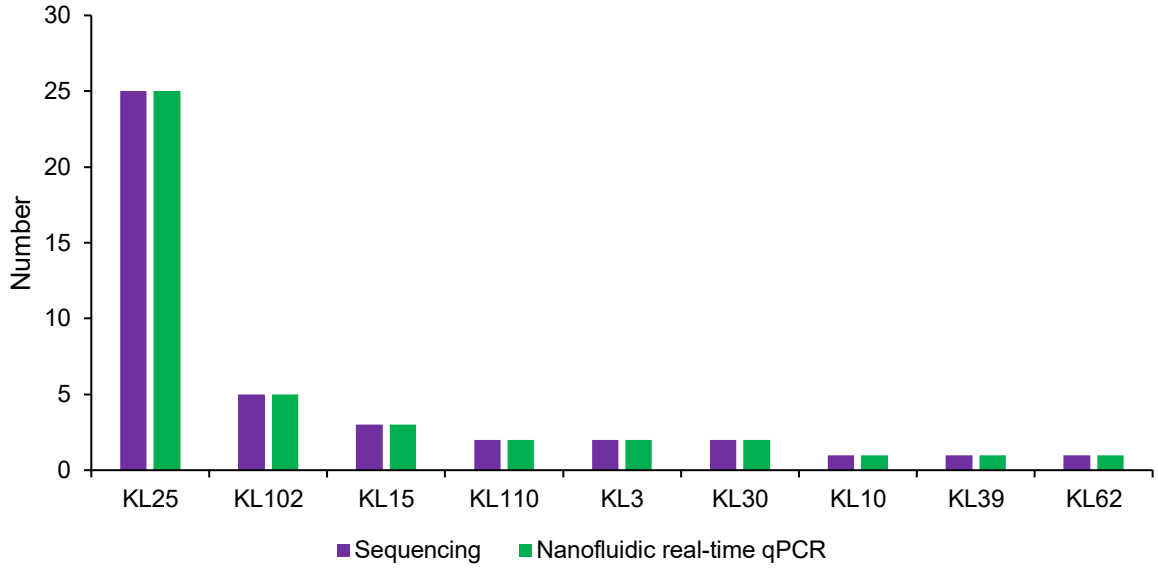


Figure 3.4 *Overall distribution of 83 enriched broths of 9 K-loci detected by traditional culturing that were sequenced (purple) compared to direct enrichment tested on nanofluidic real-time qPCR (green) in neonates. The diagnostic performance of the nanofluidic qPCR method could not be assessed for assay sets targeting KL2, KL171, KL37, KL22, KL149, and KL28, which were not detected in any clinical isolates by WGS in the TNC study.*

Table 3.6 Comparative analysis of O-loci detection between sequencing and nanofluidic real time qPCR.

Target	O1/O2v1	O1/O2v2	O5	O3/O3a	O4	O3b	O12	OL102
Sequencing	30	14	25	1	7	3	2	1
(83)	(36%)	(17%)	(30%)	(1%)	(8%)	(4%)	(2%)	(1%)
Nanofluidic	30	14	25	1	7	3	2	1
real-time qPCR	(36%)	(17%)	(30%)	(1%)	(8%)	(4%)	(2%)	(1%)
(83)								
Sensitivity (%)	100%	100%	100%	100%	100%	100%	100%	100%
Specificity (%)	100%	100%	100%	100%	100%	100%	100%	100%
Kappa	1.00	1.00	1.00	1.00	1.00	1.00	1.00	1.00
Concordance	Perfect	Perfect	Perfect	Perfect	Perfect	Perfect	Perfect	Perfect
PPV (%)	100%	100%	100%	100%	100%	100%	100%	100%
NPV (%)	100%	100%	100%	100%	100%	100%	100%	100%
ROC-AUC	1	1	1	1	1	1	1	1

**The diagnostic performance of the nanofluidic qPCR method could not be assessed for assay sets targeting O1/O2v3, OL104, OL013, and OL101, which were not detected in any clinical isolates by WGS in the TNC study.*

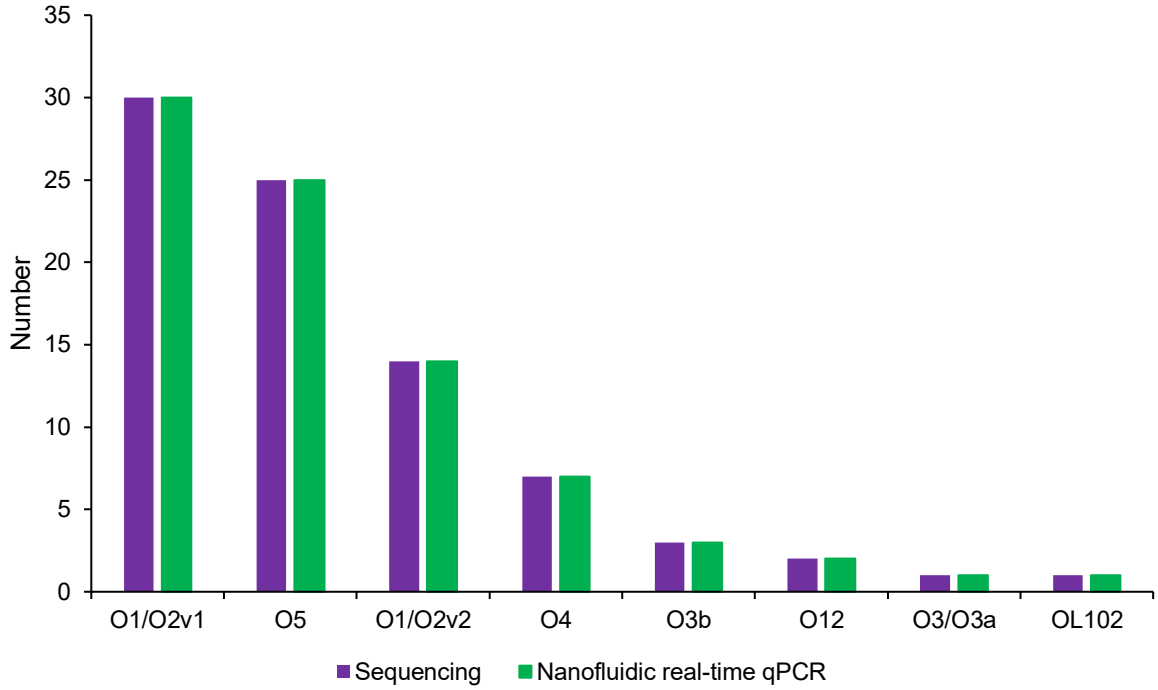


Figure 3.5 *The overall prevalence of 83 O-loci detected by traditional culturing that were sequenced (purple) compared to direct enrichment tested on nanofluidic real-time qPCR (green) in neonates. The diagnostic performance of the nanofluidic qPCR method could not be assessed for assay sets targeting O1/O2v3, OL104, OL013, OL101, O2aeh, and O2ac, which were not detected in any clinical isolates by WGS in the TNC study.*

A blind analysis of 44 enriched broth samples from the O1/O2 complex showed varying agreement between nanofluidic real-time qPCR and WGS. For O1v1, qPCR detected 36 positives compared to 33 by sequencing, with 100% sensitivity and 72.7% specificity (kappa = 0.8). For O2afg, qPCR detected 4 positives versus 8 by sequencing, resulting in 50% sensitivity, 100% specificity, and moderate concordance (kappa = 0.69). For O1v2 and O2a, qPCR and sequencing results were identical, showing 100% sensitivity and specificity with perfect concordance (kappa = 1.00).

Table 3.7 Comparative analysis of O-types in the O1/O2 complex in 44 broth isolates using sequencing and nanofluidic real-time qPCR.

Target	O1v1	O2afg	O1v2	O2a
Sequencing (44)	33	8	2	1
Nanofluidic real-time qPCR (44)	36	5	2	1
Sensitivity (%)	100%	50%	100%	100%
Specificity (%)	72.7%	100%	100%	100%
Kappa	0.8	0.69	1.00	1.00
Concordance	Strong	Moderate	Perfect	Perfect
PPV (%)	97.7%	100%	100%	100%
NPV (%)	100%	90%	100%	100%
ROC-AUC	0.86	0.75	1	1

**The diagnostic performance of the nanofluidic qPCR method could not be assessed for assay sets targeting O2aeh and O2ac which were not detected in any clinical isolates by WGS in the TNC study.*

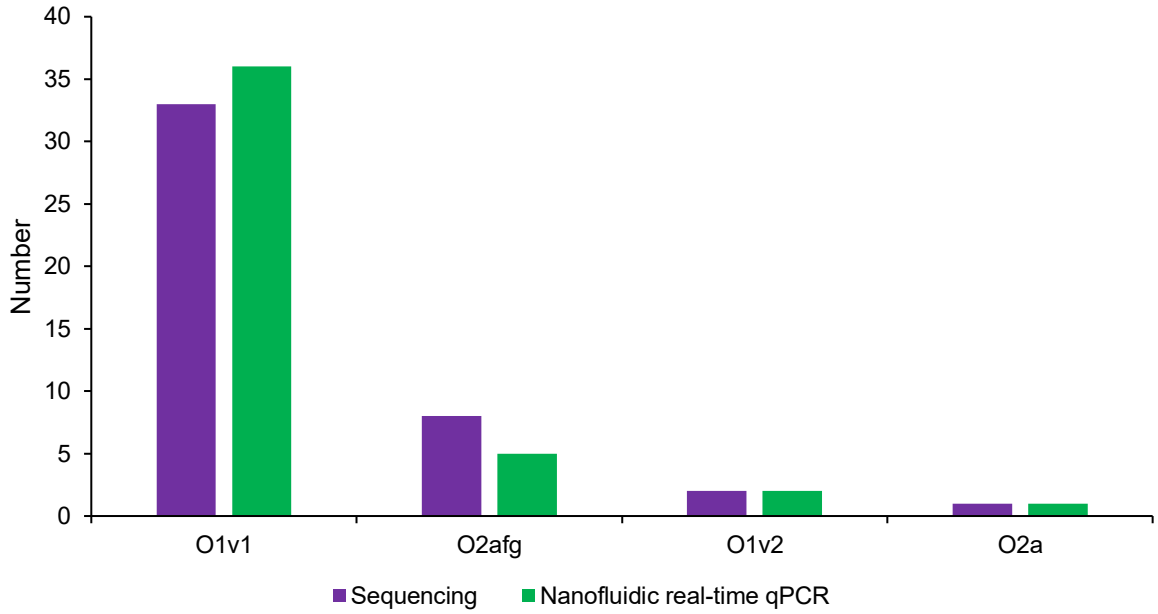


Figure 3.6 *Overall prevalence of 44 O-types of the O1/O2 complex detected by traditional culturing that were sequenced (purple) compared to direct enrichment tested on nanofluidic qPCR (green) performed using nanofluidic real-time qPCR in neonates. The diagnostic performance of the nanofluidic qPCR method could not be assessed for assay sets targeting, O2aeh and O2ac, which were not detected in any clinical isolates by WGS in the TNC study.*

3.4. Observation of *K. pneumoniae* co-colonisation

Overall, the nanofluidic qPCR method detected co-colonisation of *K. pneumoniae* and *K. variicola* in 12.1% (10/83) and K. *pneumoniae* and *E. coli* in ~~and~~ 50.1% (42/83) of the archived swab samples enriched in BHI broth, respectively (**Table 3.8**).

Table 3.8 Co-colonisation patterns of *K. pneumoniae* with *K. variicola* and *E. coli* in 83 samples.

Co-colonisation Status	Number of Samples
K. pneumoniae only	24 (29%)
K. pneumoniae + *K. variicola*	10 (12%)
K. pneumoniae + *E. coli*	42 (51%)
K. pneumoniae + *K. variicola* + *E. coli*	7 (8%)
Total	**83**

Moreover, of the samples colonised with *K. pneumoniae*, 38% (16/42), and 40% (33/83), of the samples were co-colonised with two K-loci and O-loci, respectively (**Table 3.9**). Only 42 samples were included for K-loci co-colonising analysis. Nineteen percent of the samples (11/42) were colonised with three or more K-loci, and 28% (23/83) with three or more O-loci. O-types were excluded from this analysis because the O-loci had a 1:1 correspondence with

O-types, except for the O1/O2 complex. However, due to validation limitations in the O1/O2 complex, no conclusions can be drawn regarding co-colonisation of O-types.

Table 3.9 *K. pneumoniae* K-loci and O-loci co-colonisation as measured by whole genome sequencing and nanofluidic real-time qPCR.

	Colonised	Nanofluidic Real-time PCR
K-loci	1 Serotype	42 (100%)
	2 serotypes	16 (38%)
	3+ serotypes	11 (26%)
O-loci	1 Serotype	83 (100%)
	2 serotypes	33 (40%)
	3+ serotypes	23 (28%)

Values are number (%).

Overall, KL25 (81%, 34/42) was most frequently found as a the primary isolate (defined as having the highest density), with other co-colonising serotypes, while KL39 (7%, 3/42) and KL149 (2%, 1/42) were identified as primary isolates only, and KL2 (2%, 1/42) and KL62 (7%, 3/42) were respectively identified as second and third colonisers (**Figure 3.7**).

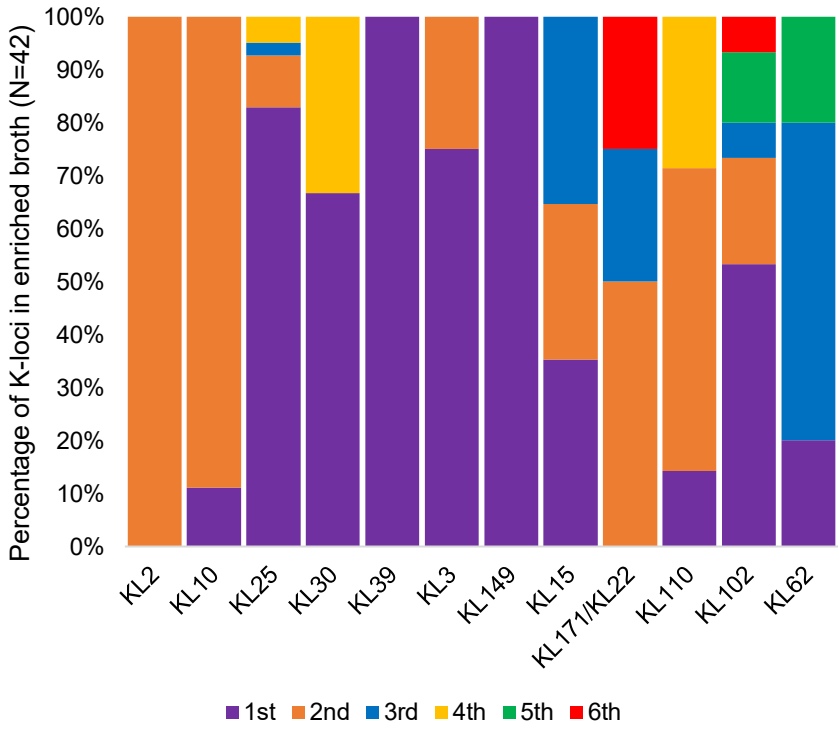


Figure 3.7 *K-locus specific ranking of multiple K. pneumoniae co-colonisers. KL28 and KL37 not included in analysis as broth did not test positive in the TNC study.*

K-loci 25 and KL15 were the most common co-colonisers (24%, 10/42), followed by KL25 and KL102 (19%, 8/42), KL10 and KL15 (7%, 3/42), KL110 and KL15 (7%, 3/42), KL102 and KL3 (7%, 3/42), as well as KL15 and KL62 (7%, 3/42) (**Figure 3.8**).

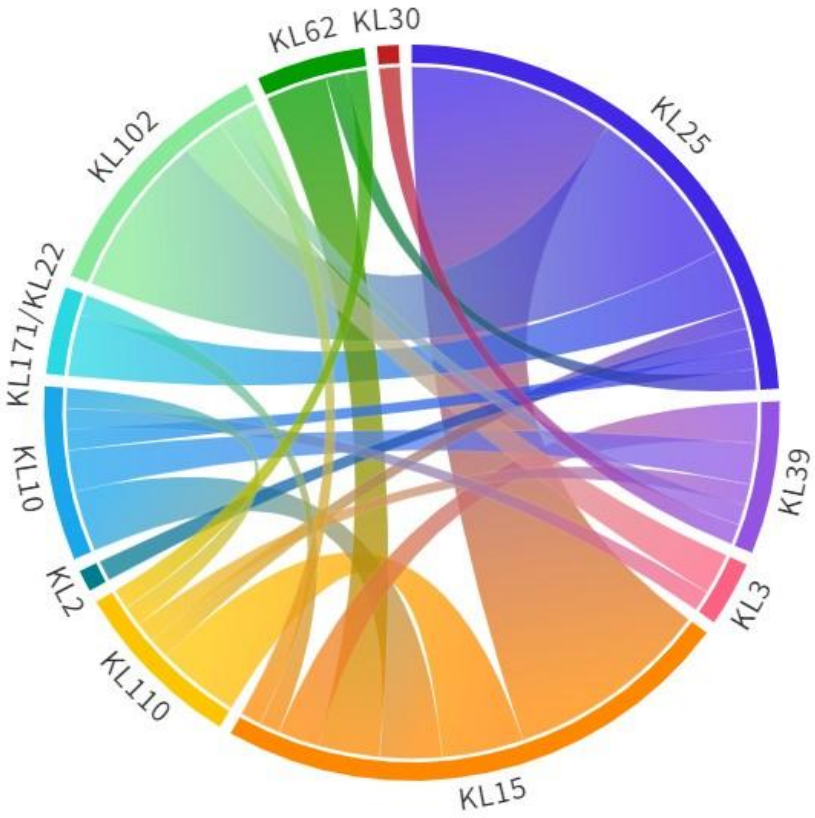


Figure 3.8 *Co-colonisation patterns of K. pneumoniae K-locus*

Overall, O5 (31%, 26/83) was most frequently found as the primary isolate (defined as having the highest density), with other co-colonising serotypes. O1/O2v1 (30%, 25/83) was also frequently identified as a primary coloniser. O1/O2v3 (2%, 2/83) and O12 (2%, 2/83) were identified as primary isolates only, while O3/O3a (10%, 8/83) and OL101 (2%, 2/83) were most frequently identified as second and third colonisers, respectively (**Figure 3.9**).

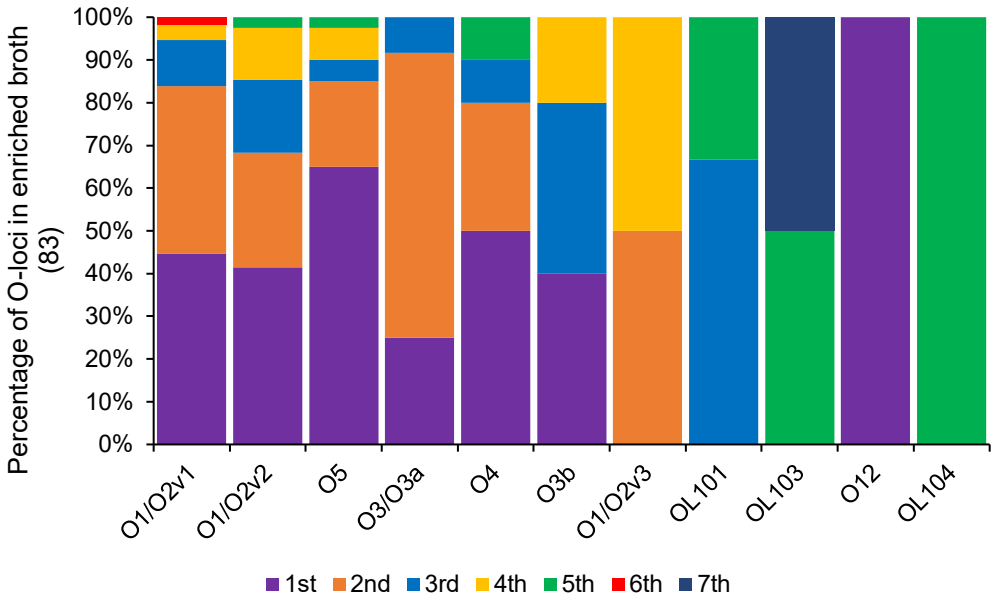


Figure 3.9 *O-locus specific ranking of multiple K. pneumoniae co-colonisers. Enriched broth in TNC study did not pick up O8 or OL102, thus excluded from analysis.*

Among the O-loci, O1/O2v1 and O5 were the most common co-colonisers (24%, 20/38), followed by O1/O2v2 and O5 (14%, 12/83), O1/O2v2 and O4 (5%, 4/83), O4 and O5 (5%, 4/83), as well as O1/O2v2 and O4 (5%, 4/83) (**Figure 3.10**).

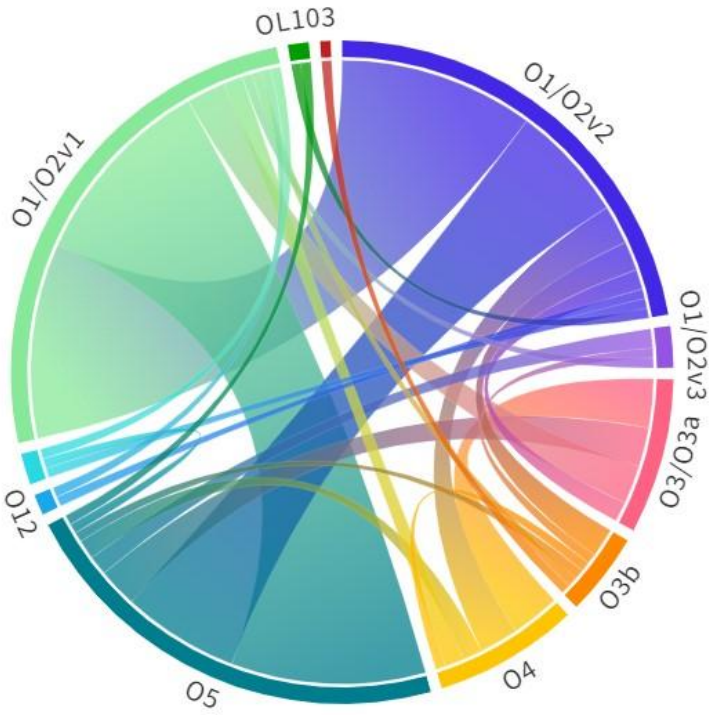


Figure 3.10 *Co-colonisation patterns of K. pneumoniae O-locus*

CHAPTER 4: DISCUSSION & CONCLUSION

This study successfully developed and validated a novel nanofluidic qPCR assay capable of simultaneously detecting 13 O-loci, five O-antigens within the O1/O2 cluster, and 15 K-loci of *K. pneumoniae* with high accuracy across multiple sample types, including bacterial isolates and nasopharyngeal, skin, and rectal swab samples. The nanofluidic qPCR method offers a reliable, rapid, and cost-effective alternative to WGS for serotyping, particularly in LMICs where resources are limited. Unlike WGS, which requires culturing, DNA extraction, and complex bioinformatics, qPCR provides a streamlined workflow for rapid, multiplex detection directly from enriched clinical specimens. Further, multiplex qPCR's simplified data output reduces the need for specialised personnel and infrastructure, making it more scalable and practical for high-throughput surveillance, especially in LMICs. In this study, the nanofluidic platform enabled over 10,000 reactions per run - significantly enhancing time efficiency - supporting its suitability for routine surveillance, outbreak response, and monitoring vaccine-related serotype shifts.

Nanofluidic qPCR platforms have been increasingly adopted in various countries for high-throughput pathogen detection. In South Africa, the technology has been successfully used for serotyping *Streptococcus pneumoniae* from nasopharyngeal and urine samples (93,100,112). In China, nanofluidic chip digital PCR (cdPCR) has been applied to detect African swine fever virus, norovirus, and bacterial pathogens with high sensitivity (113). Japanese researchers have evaluated nanofluidic qPCR for diagnosing pneumococcal pneumonia in adults, demonstrating its clinical utility (114). In Europe, high throughput nanofluidic real-time PCR systems have been used for detecting human enteric viruses in both clinical and environmental settings (115). These studies underscore the adaptability and global relevance of nanofluidic platforms for infectious disease surveillance. However, to our knowledge, this study represents the first application of nanofluidic qPCR for comprehensive *K. pneumoniae* K- and O-locus typing from colonisation samples.

PCR-based methods have been developed for O-locus typing of *K. pneumoniae*, including conventional and multiplex qPCR assays. However, these are typically limited to a small number of serotypes and often require cultured isolates as input. For example, studies by Fang et al. (2016) developed multiplex PCR panels targeting a handful of common O-types, but lacked the scalability and resolution required for comprehensive surveillance (79). In contrast, the nanofluidic qPCR assay presented here enables simultaneous detection of 32 loci (including 13 O-loci, 5 O-antigens, and 15 K-loci) and is capable of direct testing from enriched clinical samples. This enhances its suitability for large-scale epidemiological studies and real-time surveillance, particularly in resource-limited settings where culturing may be impractical.

Concurrent *K. pneumoniae* colonisation remains poorly characterised, with only two prior studies reporting on co-colonisation. A year-long prospective surveillance study (April 2013 – March 2014) in Melbourne, Australia, found that five out of 26 adult patients (19%) admitted to various hospital wards, carried two distinct *K. pneumoniae* strains simultaneously (116), while a study in Shanghai, China, reported concurrent *K. pneumoniae* carriage in 15.2% (37/243) of ICU-admitted adults (117). In contrast, our nanofluidic qPCR method detected co-colonisation of multiple K- and O-loci in 27% and 56% of swab samples, respectively, with 28% and 26% harbouring three or more O- and K-loci. The most common co-colonisers were KL25 and KL15 (12%) for K-loci, and O1/O2v1 and O5 (24%) for O-loci. The higher co-colonisation rates observed in our study are likely due to the culture-independent nature of qPCR, which does not rely on pure isolate recovery as WGS does. Additionally, other studies were conducted in adult populations, whereas colonisation rates in children might be higher due to differences in exposure, immune development, and microbiome composition. However, other factors, such as geographical variation, host-specific influences, and healthcare settings, may also contribute. The high rate of concurrent colonisation underscores the dynamic nature of *K. pneumoniae* transmission and the necessity for highly sensitive techniques to track these patterns, particularly in neonates, where maternal vaccines are being developed to protect against invasive *K. pneumoniae* disease (118). Localised surveillance will be essential for optimising vaccine formulations and monitoring serotype shifts post-vaccination. While invasive isolates are typically assumed to represent single strains, understanding colonisation dynamics is crucial for vaccine development. Colonisation precedes invasive disease, especially in neonates, and represents the primary reservoir for transmission. Co-colonisation increases the potential for genetic exchange and the emergence of novel serotypes. Therefore, characterising sero-epidemiology at the colonisation level complements invasive isolate data by informing both transmission dynamics and the full spectrum of serotype diversity that vaccines must target to be effective.

Although the qPCR method is culture independent, the use of a 24-hour BHI enrichment step prior to testing may have influenced the observed strain profiles. Enrichment can favour the growth of faster-replicating strains, potentially skewing the relative abundance of co-colonising *K. pneumoniae* types. Nevertheless, this approach still offers improved detection of mixed colonisation compared to traditional culture-isolate workflows and allows for serotyping from samples that may otherwise yield insufficient DNA for direct analysis. Future studies may explore DNA extraction directly from raw swab material to further minimise this potential bias.

An additional advantage of this nanofluidic qPCR method is its ability to differentiate *K. pneumoniae* from closely related species such as *K. quasipneumoniae* and *K. variicola*, which are frequently misidentified due to their genetic and phenotypic similarities. Studies using standard culture-based identification methods have shown that up to 7.2% of *K.*

pneumoniae isolates are *K. quasipneumoniae* or *K. variicola* (119). This misclassification may have significant implications for infection control and epidemiological studies. The ability of the qPCR assay to rapidly and accurately detect *K. pneumoniae* serotypes - directly from clinical and colonisation samples - holds significant value for infection prevention and control (IPC) programmes. Early identification of colonised patients, including those carrying high-risk or MDR strains, can inform timely implementation of isolation precautions and targeted interventions. Additionally, the detection of co-colonisation and strain diversity enhances outbreak tracking, allowing for more precise mapping of transmission pathways within healthcare settings. Compared to WGS, which has longer turnaround times and requires isolate recovery, this qPCR platform enables near real-time surveillance, making it highly suitable for routine IPC monitoring in neonatal units and other high-risk environments. While the initial capital investment for nanofluidic qPCR instrumentation is substantial, comparable to or slightly higher than that of conventional qPCR systems, the long-term operational cost is significantly lower than WGS. Once established in a centralised laboratory, the platform enables high-throughput testing at a per-sample cost of approximately R800, including reagents and consumables, compared to R1600 for WGS. This calculation accounts for batching efficiency and reduced personnel time due to simplified workflows. A cost analysis was conducted using internal laboratory costing data and supplier pricing, including primers, probes, gBlocks, and nanofluidic PCR plates, to calculate the cost per sample for testing 90 samples with 6 controls across 37 assays, although the assay doesn't cover all K - loci. Furthermore, nanofluidic systems require less computational infrastructure and expertise than WGS, making them more sustainable for use in LMICs when implemented at referral or national public health laboratories. While the upfront costs of nanofluidic platforms are not negligible, they are generally lower than the substantial outlay required for high-throughput sequencing equipment, making them a more accessible option for resource-limited settings.

Given the high sensitivity of nanofluidic qPCR, there is an inherent risk of cross-contamination between samples or from amplified products (amplicon carryover), which could lead to false-positive results. To mitigate this, strict laboratory workflows should be followed, including physical separation of pre- and post-amplification areas, use of unidirectional workflow, and incorporation of appropriate negative controls throughout the process. Additionally, the closed-system format of the nanofluidic platform reduces manual handling, thereby lowering contamination risk compared to conventional qPCR setups. Nonetheless, routine quality assurance measures remain critical to maintain assay reliability, particularly in high-throughput surveillance applications.

While the current assay configuration includes five duplex reactions and 27 singleplex to balance throughput and reliability, further duplexing could potentially reduce reagent use and enhance cost-effectiveness. Some primer-probe sets in the assay showed reduced sensitivity

or inconsistent amplification, which likely reflects differences in target gene copy number, GC content, secondary structure, or suboptimal primer-probe interactions. In attempts to increase duplexing, interference between certain reactions further impacted performance. While these limitations affected the uniformity of detection across all loci, careful assay design and threshold optimisation helped mitigate false negatives. Nonetheless, reduced sensitivity for some targets may underestimate the prevalence of certain K- or O-types, particularly in samples with low bacterial load. Ongoing refinement of primer-probe sets, and the incorporation of newly validated duplex combinations will be essential for improving assay robustness and coverage.

While shotgun metagenomic sequencing theoretically offers the ability to detect *K. pneumoniae* K- and O-loci directly from clinical samples, several barriers limit its practical implementation. These include high sequencing costs, the requirement for deep coverage to detect low-abundance pathogens, and the substantial presence of host DNA, which can obscure bacterial signal. Moreover, metagenomic data interpretation requires advanced bioinformatics infrastructure and expertise that are often unavailable in low-resource settings.

Despite its advantages, this study had some limitations. The assay did not include all known K-loci, potentially underestimating co-colonisation prevalence. Future improvements should incorporate additional K-loci, such as KL24, KL136, and KL38, which are relevant in adult populations in South Africa (15). The inability to distinguish certain closely related loci, such as KL22 and KL171, arises from their high genetic similarity, particularly within the conserved capsule synthesis regions targeted by qPCR. This limits the assay's resolution and may lead to under- or overestimation of individual serotype prevalence. In surveillance and vaccine monitoring contexts, such ambiguity could obscure the detection of serotype-specific trends or replacement dynamics. The impact can be mitigated by periodically refining target regions or incorporating additional discriminatory markers as they are identified.

Additionally, the assay was not validated for direct clinical samples like blood or cerebrospinal fluid, limiting its current application in invasive disease diagnostics. Another limitation was its inability to establish direct associations between co-colonising K- and O-loci, making it difficult to identify high-risk clonotypes. The reliance on genetic algorithms to detect O1/O2 complex serotypes may also introduce misclassification errors, particularly when multiple O1/O2 variants are present. These discrepancies are likely due to the genetic similarity among O1/O2 loci and the presence of multiple allelic variants that complicate the distinction between serotypes such as O1, O2a, O2afg, and O2aeh. Additionally, the genetic detection of serotype-specific markers does not always reflect functional expression, especially in the case of phase-variable or recombined loci. Similar challenges have been reported in WGS-based typing pipelines, suggesting that this limitation is not unique to qPCR but is inherent to current

molecular approaches targeting the O1/O2 complex (50). Incorporating additional genetic markers or expression-based validation could improve future assay resolution. Furthermore, as the assay detects predefined gene targets, newly evolved serotypes or genetic recombinants may go undetected, highlighting the need for periodic updates to the assay design.

Beyond serotyping, the nanofluidic qPCR platform has strong potential for expansion to include AMR gene targets. Incorporating primers for key resistance determinants - such as bla_{KPC}, bla_{NDM}, bla_{OXA-48}, and *mcr* genes - would enable simultaneous detection of MDR *K. pneumoniae* strains from colonisation samples. This would enhance infection prevention strategies by identifying high-risk carriers in near real-time, informing isolation protocols and empirical treatment decisions. Given the platform's multiplexing capacity and culture-independent workflow, integrating AMR detection would significantly broaden its utility for comprehensive surveillance and outbreak response.

In conclusion, the nanofluidic qPCR method represents a significant advancement in *K. pneumoniae* surveillance, offering a rapid, accurate, and cost-effective alternative to WGS. Its ability to detect co-colonisation, differentiate closely related species, and function independently of culture-based methods may makes it particularly valuable for epidemiological studies and vaccine development efforts. As maternal vaccines progress, this assay could be used to monitor vaccine-induced shifts in *K. pneumoniae* serotype distribution, ensuring comprehensive coverage and preventing the emergence of replacement serotypes. As our understanding of antigenic cross-protection between K- and O-loci improves, this information could be leveraged to refine the qPCR panel to focus on vaccine-included serotypes and those with demonstrated cross-reactivity. This would enhance the assay's utility in post-vaccine surveillance by allowing for targeted monitoring of both direct and indirect vaccine effects, such as cross-protection or serotype replacement. The modular design of the nanofluidic qPCR platform supports the rapid inclusion or substitution of loci, making it adaptable to evolving vaccine formulations and public health priorities. Future work should focus on expanding the assay's genetic targets, validating its use in clinical infections, and integrating it into broader surveillance programs to inform global infection control strategies.

CHAPTER 5: REFERENCES

1. World Health Organization. Children: improving survival and well-being. 2020 Sep 8 [cited 2024 Sep 29]; Available from: https://www.who.int/news-room/fact-sheets/detail/child-mortality-under-5-years#:~:text=Substantial%20global%20progress%20has%20been,1990%20to%2038%20in%202019

2. World Health Organization. Global report on the epidemiology and burden of sepsis: current evidence, identifying gaps and future directions [Internet]. http://apps.who.int/iris.; 2020. Available from: https://apps.who.int/iris/bitstream/handle/10665/334216/9789240010789-eng.pdf

3. Fleischmann C, Reichert F, Cassini A, Horner R, Harder T, Markwart R, et al. Global incidence and mortality of neonatal sepsis: a systematic review and meta-analysis. Arch Dis Child. 2021 Aug;106(8):745.

4. Sands K, Carvalho MJ, Portal E, Thomson K, Dyer C, Akpulu C, et al. Characterization of antimicrobial-resistant Gram-negative bacteria that cause neonatal sepsis in seven low- and middle-income countries. Nat Microbiol. 2021 Mar 29;6(4):512.

5. Afsharpaiman S, Torkaman M, Saburi A, Farzaampur A, Amirsalari S, Kavehmanesh Z. Trends in incidence of neonatal sepsis and antibiotic susceptibility of causative agents in two neonatal intensive care units in Tehran, I.R Iran. J Clin Neonatol. 2012;1(3):124.

6. Schrag SJ, Farley MM, Petit S, Reingold A, Weston EJ, Pondo T, et al. Epidemiology of Invasive Early-Onset Neonatal Sepsis, 2005 to 2014. Pediatrics. 2016 Dec 1;138(6):e20162013.

7. Wattal C, Kler N, Oberoi JK, Fursule A, Kumar A, Thakur A. Neonatal Sepsis: Mortality and Morbidity in Neonatal Sepsis due to Multidrug-Resistant (MDR) Organisms: Part 1. Indian J Pediatr. 2020 Feb;87(2):117.

8. Flannery DD, Chiotos K, Gerber JS, Puopolo KM. Neonatal multidrug-resistant gram-negative infection: epidemiology, mechanisms of resistance, and management. Pediatr Res. 2022 Jan;91(2):380.

9. Ballot DE, Bandini R, Nana T, Bosman N, Thomas T, Davies VA, et al. A review of - multidrug-resistant Enterobacteriaceae in a neonatal unit in Johannesburg, South Africa. BMC Pediatr. 2019 Dec;19(1):320.

10. Rahman S. Multidrug resistant neonatal sepsis in Peshawar, Pakistan. Arch Dis Child - Fetal Neonatal Ed. 2002 Jul 1;87(1):52F.

11. Murray CJL, Ikuta KS, Sharara F, Swetschinski L, Robles Aguilar G, Gray A, et al. Global burden of bacterial antimicrobial resistance in 2019: a systematic analysis. The Lancet. 2022 Feb;399(10325):629.

12. Santajit S, Indrawattana N. Mechanisms of Antimicrobial Resistance in ESKAPE Pathogens. BioMed Res Int. 2016;2016:1.

13. Mancuso G, Midiri A, Gerace E, Biondo C. Bacterial Antibiotic Resistance: The Most Critical Pathogens. Pathogens. 2021 Oct 12;10(10):1310.

14. Priyanka A, Akshatha K, Deekshit VK, Prarthana J, Akhila DS. Klebsiella pneumoniae Infections and Antimicrobial Drug Resistance. In: Siddhardha B, Dyavaiah M, Syed A, editors. Model Organisms for Microbial Pathogenesis, Biofilm Formation and Antimicrobial Drug Discovery [Internet]. Singapore: Springer Singapore; 2020 [cited 2023 Dec 29]. p. 195–225. Available from: http://link.springer.com/10.1007/978-981-15-1695-5_12

15. Olwagen CP, Izu A, Khan S, Van Der Merwe L, Dean NJ, Mabena FC, et al. Genomic relatedness of colonizing and invasive disease Klebsiella pneumoniae isolates in South African infants. Sci Rep. 2025 Mar 7;15(1):8043.

16. Martin RM, Bachman MA. Colonization, Infection, and the Accessory Genome of Klebsiella pneumoniae. Front Cell Infect Microbiol. 2018 Jan 22;8:4.

17. Hu Y, Anes J, Devineau S, Fanning S. *Klebsiella pneumoniae* : Prevalence, Reservoirs, Antimicrobial Resistance, Pathogenicity, and Infection: A Hitherto Unrecognized Zoonotic Bacterium. Foodborne Pathog Dis. 2021 Feb 1;18(2):63.

18. Lewis JM, Mphasa M, Banda R, Beale MA, Mallewa J, Heinz E, et al. Genomic and antigenic diversity of colonizing Klebsiella pneumoniae isolates mirrors that of invasive isolates in Blantyre, Malawi. Microb Genomics [Internet]. 2022 Mar 1 [cited 2025 May 19];8(3). Available from: https://www.microbiologyresearch.org/content/journal/mgen/10.1099/mgen.0.000778

19. Ashurst JV, Dawson A. Klebsiella Pneumonia. In: StatPearls [Internet]. Treasure Island (FL): StatPearls Publishing; 2025 [cited 2025 May 18]. Available from: http://www.ncbi.nlm.nih.gov/books/NBK519004/

20. Gadisa E, Egyir B, Fekede E, Adu B, Danso J, Oclu A, et al. Epidemiology, antimicrobial resistance profile, associated risk factors and management of carbapenem resistant Klebsiella pneumoniae in children under 5 with suspected sepsis in Ethiopia. BMC Infect Dis. 2024 Dec 23;24(1):1458.

21. Lam MMC, Wick RR, Judd LM, Holt KE, Wyres KL. Kaptive 2.0: updated capsule and LPS locus typing for the *Klebsiella pneumoniae* species complex [Internet]. Genomics; 2021 Nov [cited 2023 Oct 13]. Available from: http://biorxiv.org/lookup/doi/10.1101/2021.11.05.467534

22. Mashau RC, Meiring ST, Dramowski A, Magobo RE, Quan VC, Perovic O, et al. Culture-confirmed neonatal bloodstream infections and meningitis in South Africa, 2014–19: a cross-sectional study. Lancet Glob Health. 2022 Aug;10(8):e1170.

23. Essel V, Tshabalala K, Ntshoe G, Mphaphuli E, Feller G, Shonhiwa AM, et al. A multisectoral investigation of a neonatal unit outbreak of Klebsiella pneumoniae bacteraemia at a regional hospital in Gauteng Province, South Africa. S Afr Med J. 2020 Jul 29;110(8):783.

24. Li Y, Kumar S, Zhang L. Mechanisms of Antibiotic Resistance and Developments in Therapeutic Strategies to Combat Klebsiella pneumoniae Infection. Infect Drug Resist. 2024 Mar;Volume 17:1107.

25. Sharma A, Thakur A, Thakur N, Kumar V, Chauhan A, Bhardwaj N. Changing Trend in the Antibiotic Resistance Pattern of Klebsiella Pneumonia Isolated From Endotracheal Aspirate Samples of ICU Patients of a Tertiary Care Hospital in North India. Cureus [Internet]. 2023 Mar 17 [cited 2024 Apr 21]; Available from:

https://www.cureus.com/articles/136634-changing-trend-in-the-antibiotic-resistance-pattern-of-klebsiella-pneumonia-isolated-from-endotracheal-aspirate-samples-of-icu-patients-of-a-tertiary-care-hospital-in-north-india

26. Marais G, Moodley C, Claassen-Weitz S, Patel F, Prentice E, Tootla H, et al. Carbapenem-resistant *Klebsiella pneumoniae* among hospitalized patients in Cape Town, South Africa: molecular epidemiology and characterization. JAC-Antimicrob Resist. 2024 Mar 5;6(2):dlae050.

27. Zhu J, Li Q, Li X, Kang J, Song Y, Song J, et al. Successful control of the first carbapenem-resistant Klebsiella pneumoniae outbreak in a Chinese hospital 2017–2019. Antimicrob Resist Infect Control. 2020 Dec;9(1):91.

28. Pitout JDD, Nordmann P, Poirel L. Carbapenemase-Producing Klebsiella pneumoniae, a Key Pathogen Set for Global Nosocomial Dominance. Antimicrob Agents Chemother. 2015 Oct;59(10):5873.

29. Arnold RS, Thom KA, Sharma S, Phillips M, Kristie Johnson J, Morgan DJ. Emergence of Klebsiella pneumoniae Carbapenemase-Producing Bacteria: South Med J. 2011 Jan;104(1):40.

30. Pu D, Zhao J, Chang K, Zhuo X, Cao B. “Superbugs” with hypervirulence and carbapenem resistance in Klebsiella pneumoniae: the rise of such emerging nosocomial pathogens in China. Sci Bull. 2023 Sep;S2095927323006758.

31. Nordmann P, Bouvier M, Poirel L. Efficacy of ceftazidime-avibactam, meropenem-vaborbactam, and imipenem-relebactam combinations against carbapenemase-producing Enterobacterales in Switzerland. Eur J Clin Microbiol Infect Dis. 2023 Sep;42(9):1145–52.

32. Cheng YH, Lin TL, Pan YJ, Wang YP, Lin YT, Wang JT. Colistin Resistance Mechanisms in Klebsiella pneumoniae Strains from Taiwan. Antimicrob Agents Chemother. 2015 May;59(5):2909.

33. Pogue JM, Bonomo RA, Kaye KS. Ceftazidime/Avibactam, Meropenem/Vaborbactam, or Both? Clinical and Formulary Considerations. Clin Infect Dis. 2019 Jan 18;68(3):519–24.

34. Lee GC, Burgess DS. Treatment of Klebsiella Pneumoniae Carbapenemase (KPC) infections: a review of published case series and case reports. Ann Clin Microbiol Antimicrob. 2012;11(1):32.

35. Hafiz TA, Alanazi S, Alghamdi SS, Mubaraki MA, Aljabr W, Madkhali N, et al. Klebsiella pneumoniae bacteraemia epidemiology: resistance profiles and clinical outcome of King Fahad Medical City isolates, Riyadh, Saudi Arabia. BMC Infect Dis. 2023 Sep 5;23(1):579.

36. Chang D, Sharma L, Dela Cruz CS, Zhang D. Clinical Epidemiology, Risk Factors, and Control Strategies of Klebsiella pneumoniae Infection. Front Microbiol. 2021 Dec 22;12:750662.

37. Assoni L, Girardello R, Converso TR, Darrieux M. Current Stage in the Development of Klebsiella pneumoniae Vaccines. Infect Dis Ther. 2021 Dec;10(4):2157.

38. Zhu J, Wang T, Chen L, Du H. Virulence Factors in Hypervirulent Klebsiella pneumoniae. Front Microbiol. 2021 Apr 8;12:642484.

39. Papo N, Shai Y. A Molecular Mechanism for Lipopolysaccharide Protection of Gram-negative Bacteria from Antimicrobial Peptides. J Biol Chem. 2005 Mar;280(11):10378.

40. Bengoechea JA, Sa Pessoa J. *Klebsiella pneumoniae* infection biology: living to counteract host defences. FEMS Microbiol Rev. 2019 Mar 1;43(2):123.

41. Guerra MES, Destro G, Vieira B, Lima AS, Ferraz LFC, Hakansson AP, et al. Klebsiella pneumoniae Biofilms and Their Role in Disease Pathogenesis. Front Cell Infect Microbiol. 2022 May 11;12:877995.

42. Fernández L, Hancock REW. Adaptive and Mutational Resistance: Role of Porins and Efflux Pumps in Drug Resistance. Clin Microbiol Rev. 2012 Oct;25(4):661.

43. Gaurav A, Bakht P, Saini M, Pandey S, Pathania R. Role of bacterial efflux pumps in antibiotic resistance, virulence, and strategies to discover novel efflux pump inhibitors. Microbiology [Internet]. 2023 May 24 [cited 2024 Jun 25];169(5). Available from: https://www.microbiologyresearch.org/content/journal/micro/10.1099/mic.0.001333

44. Paczosa MK, Mecsas J. Klebsiella pneumoniae: Going on the Offense with a Strong Defense. Microbiol Mol Biol Rev. 2016 Sep;80(3):629.

45. Opoku-Temeng C, Kobayashi SD, DeLeo FR. Klebsiella pneumoniae capsule polysaccharide as a target for therapeutics and vaccines. Comput Struct Biotechnol J. 2019;17:1360.

46. Follador R, Heinz E, Wyres KL, Ellington MJ, Kowarik M, Holt KE, et al. The diversity of Klebsiella pneumoniae surface polysaccharides. Microb Genomics [Internet]. 2016 Aug 25 [cited 2023 Mar 12];2(8). Available from: https://www.microbiologyresearch.org/content/journal/mgen/10.1099/mgen.0.000073

47. Singh S, Wilksch JJ, Dunstan RA, Mularski A, Wang N, Hocking D, et al. LPS O Antigen Plays a Key Role in Klebsiella pneumoniae Capsule Retention. Rendueles Garcia O, editor. Microbiol Spectr. 2022 Aug 31;10(4):e01517.

48. Arakawa Y, Wacharotayankun R, Nagatsuka T, Ito H, Kato N, Ohta M. Genomic organization of the Klebsiella pneumoniae cps region responsible for serotype K2 capsular polysaccharide synthesis in the virulent strain Chedid. J Bacteriol. 1995 Apr;177(7):1788.

49. Wyres KL, Wick RR, Gorrie C, Jenney A, Follador R, Thomson NR, et al. Identification of Klebsiella capsule synthesis loci from whole genome data. Microb Genomics [Internet]. 2016 Dec 1 [cited 2023 Oct 13];2(12). Available from: https://www.microbiologyresearch.org/content/journal/mgen/10.1099/mgen.0.000102

50. Lam MMC, Wick RR, Watts SC, Cerdeira LT, Wyres KL, Holt KE. A genomic surveillance framework and genotyping tool for Klebsiella pneumoniae and its related species complex. Nat Commun. 2021 Jul 7;12(1):4188.

51. Follador R, Heinz E, Wyres KL, Ellington MJ, Kowarik M, Holt KE, et al. The diversity of Klebsiella pneumoniae surface polysaccharides. Microb Genomics [Internet]. 2016 Aug 25 [cited 2023 Mar 12];2(8). Available from: https://www.microbiologyresearch.org/content/journal/mgen/10.1099/mgen.0.000073

52. Chuang YP, Fang CT, Lai SY, Chang SC, Wang JT. Genetic Determinants of Capsular Serotype K1 of Klebsiella pneumoniae Causing Primary Pyogenic Liver Abscess [Internet]. 2006 p. 645. Available from: http://genomeold.wustl.edu/projects/bacterial/

53. Jun JB. *Klebsiella pneumoniae* Liver Abscess. Infect Chemother. 2018;50(3):210.

54. Domenico P, Salo RJ, Cross AS, Cunha BA. Polysaccharide capsule-mediated resistance to opsonophagocytosis in Klebsiella pneumoniae. Infect Immun. 1994 Oct;62(10):4495.

55. Merino S, Camprubí S, Albertí S, Benedí VJ, Tomás JM. Mechanisms of Klebsiella pneumoniae resistance to complement-mediated killing. Infect Immun. 1992 Jun;60(6):2529.

56. Podschun R, Ullmann U. *Klebsiella* spp. as Nosocomial Pathogens: Epidemiology, Taxonomy, Typing Methods, and Pathogenicity Factors. Clin Microbiol Rev. 1998 Oct;11(4):589.

57. Shu HY, Fung CP, Liu YM, Wu KM, Chen YT, Li LH, et al. Genetic diversity of capsular polysaccharide biosynthesis in Klebsiella pneumoniae clinical isolates. Microbiology. 2009 Dec 1;155(12):4170.

58. Patro LPP, Rathinavelan T. Targeting the Sugary Armor of Klebsiella Species. Front Cell Infect Microbiol. 2019 Nov 8;9:367.

59. Brisse S, Passet V, Haugaard AB, Babosan A, Kassis-Chikhani N, Struve C, et al. *wzi* Gene Sequencing, a Rapid Method for Determination of Capsular Type for Klebsiella Strains. J Clin Microbiol. 2013 Dec;51(12):4073.

60. Pan YJ, Lin TL, Chen YH, Hsu CR, Hsieh PF, Wu MC, et al. Capsular Types of Klebsiella pneumoniae Revisited by wzc Sequencing. Forestier C, editor. PLoS ONE. 2013 Dec 9;8(12):e80670.

61. Rahn A, Drummelsmith J, Whitfield C. Conserved Organization in the *cps* Gene Clusters for Expression of *Escherichia coli* Group 1 K Antigens: Relationship to the Colanic Acid Biosynthesis Locus and the *cps* Genes from *Klebsiella pneumoniae*. J Bacteriol. 1999 Apr;181(7):2307.

62. Kaszowska M, Majkowska-Skrobek G, Markwitz P, Lood C, Jachymek W, Maciejewska A, et al. The Mutation in wbaP cps Gene Cluster Selected by Phage-Borne Depolymerase Abolishes Capsule Production and Diminishes the Virulence of Klebsiella pneumoniae. Int J Mol Sci. 2021 Oct 26;22(21):11562.

63. Wyres KL, Gorrie C, Edwards DJ, Wertheim HFL, Hsu LY, Van Kinh N, et al. Extensive Capsule Locus Variation and Large-Scale Genomic Recombination within the Klebsiella pneumoniae Clonal Group 258. Genome Biol Evol. 2015 May;7(5):1267.

64. Mike LA, Stark AJ, Forsyth VS, Vornhagen J, Smith SN, Bachman MA, et al. A systematic analysis of hypermucoviscosity and capsule reveals distinct and overlapping genes that impact Klebsiella pneumoniae fitness. Mecsas J, editor. PLOS Pathog. 2021 Mar 15;17(3):e1009376.

65. Roger T, Froidevaux C, Le Roy D, Reymond MK, Chanson AL, Mauri D, et al. Protection from lethal Gram-negative bacterial sepsis by targeting Toll-like receptor 4. Proc Natl Acad Sci. 2009 Feb 17;106(7):2348.

66. Hotchkiss RS, Moldawer LL, Opal SM, Reinhart K, Turnbull IR, Vincent JL. Sepsis and septic shock. Nat Rev Dis Primer. 2016 Jun 30;2(1):16045.

67. Rodrigues MX, Yang Y, De Souza Meira EB, Do Carmo Silva J, Bicalho RC. Development and evaluation of a new recombinant protein vaccine (YidR) against Klebsiella pneumoniae infection. Vaccine. 2020 Jun;38(29):4640.

68. Kelly SD, Clarke BR, Ovchinnikova OG, Sweeney RP, Williamson ML, Lowary TL, et al. Klebsiella pneumoniae O1 and O2ac antigens provide prototypes for an unusual strategy for polysaccharide antigen diversification. J Biol Chem. 2019 Jul;294(28):10863.

69. Farhana A KY. Biochemistry, Lipopolysaccharide. [Internet]. StatPearls Publishing; 2023. Available from: https://www.ncbi.nlm.nih.gov/books/NBK554414/

70. Zhou H, Liu W, Qin T, Liu C, Ren H. Defining and Evaluating a Core Genome Multilocus Sequence Typing Scheme for Whole-Genome Sequence-Based Typing of Klebsiella pneumoniae. Front Microbiol [Internet]. 2017 Mar 8 [cited 2023 May 7];8. Available from: http://journal.frontiersin.org/article/10.3389/fmicb.2017.00371/full

71. Raetz CRH, Whitfield C. Lipopolysaccharide Endotoxins. Annu Rev Biochem. 2002 Jun;71(1):635.

72. Regué M, Izquierdo L, Fresno S, Piqué N, Corsaro MM, Naldi T, et al. A Second Outer-Core Region in *Klebsiella pneumoniae* Lipopolysaccharide. J Bacteriol. 2005 Jun 15;187(12):4198.

73. Bulati M, Busà R, Carcione C, Iannolo G, Di Mento G, Cuscino N, et al. Klebsiella pneumoniae Lipopolysaccharides Serotype O2afg Induce Poor Inflammatory Immune Responses Ex Vivo. Microorganisms. 2021 Jun 17;9(6):1317.

74. Fitzgerald C, Sherwood R, Gheesling LL, Brenner FW, Fields PI. Molecular Analysis of the *rfb* O Antigen Gene Cluster of *Salmonella enterica* Serogroup O:6,14 and Development of a Serogroup-Specific PCR Assay. Appl Environ Microbiol. 2003 Oct;69(10):6099.

75. Wick RR, Heinz E, Holt KE, Wyres KL. Kaptive Web: User-Friendly Capsule and Lipopolysaccharide Serotype Prediction for Klebsiella Genomes. Diekema DJ, editor. J Clin Microbiol. 2018 Jun;56(6):e00197.

76. Motley MP, Fries BC. A New Take on an Old Remedy: Generating Antibodies against Multidrug-Resistant Gram-Negative Bacteria in a Postantibiotic World. Achkar JM, editor. mSphere. 2017 Oct 25;2(5):e00397.

77. Vinogradov E, Frirdich E, MacLean LL, Perry MB, Petersen BO, Duus JØ, et al. Structures of Lipopolysaccharides from Klebsiella pneumoniae. J Biol Chem. 2002 Jul;277(28):25070.

78. Kelly RF, Severn WB, Richards JC, Perry MB, MacLean LL, Tomás JM, et al. Structural variation in the O-specific polysaccharides of *Klebsiella pneumoniae* serotype O1 and O8 lipopolysaccharide: evidence for clonal diversity in *rfb* genes. Mol Microbiol. 1993 Nov;10(3):615.

79. Fang CT, Shih YJ, Cheong CM, Yi WC. Rapid and Accurate Determination of Lipopolysaccharide O-Antigen Types in Klebsiella pneumoniae with a Novel PCR-Based O-Genotyping Method. Munson E, editor. J Clin Microbiol. 2016 Mar;54(3):666.

80. Greenfield LK, Whitfield C. Synthesis of lipopolysaccharide O-antigens by ABC transporter-dependent pathways. Carbohydr Res. 2012 Jul;356:12.

81. Whitfield C, Richards JC, Perry MB, Clarke BR, MacLean LL. Expression of two structurally distinct D-galactan O antigens in the lipopolysaccharide of Klebsiella pneumoniae serotype O1. J Bacteriol. 1991 Feb;173(4):1420.

82. Clarke BR, Ovchinnikova OG, Kelly SD, Williamson ML, Butler JE, Liu B, et al. Molecular basis for the structural diversity in serogroup O2-antigen polysaccharides in Klebsiella pneumoniae. J Biol Chem. 2018 Mar;293(13):4666.

83. Hsieh PF, Wu MC, Yang FL, Chen CT, Lou TC, Chen YY, et al. D-galactan II is an immunodominant antigen in O1 lipopolysaccharide and affects virulence in Klebsiella pneumoniae: implication in vaccine design. Front Microbiol [Internet]. 2014 Nov 19 [cited 2023 Dec 13];5. Available from: http://journal.frontiersin.org/article/10.3389/fmicb.2014.00608/abstract

84. Kelly RF, Perry MB, MacLean LL, Whitfield C. Structures of the O-antigens of Klebsiella serotypes 02 (2a,2e), 02 (2a,2e,2h), and 02 (2a,2f,2g), members of a family of related D-galactan O-antigens in Klebsiella spp. J Endotoxin Res. 1995 Apr;2(2):131.

85. Wyres KL, Lam MMC, Holt KE. Population genomics of Klebsiella pneumoniae. Nat Rev Microbiol. 2020 Jun;18(6):344.

86. Wang Y, Liang X, Jiang Y, Dong D, Zhang C, Song T, et al. Novel fast pathogen diagnosis method for severe pneumonia patients in the intensive care unit: randomized clinical trial. Kana BD, editor. eLife. 2022 Oct;11:e79014.

87. Grazioli S, Ferris NP, Dho G, Pezzoni G, Morris AS, Mioulet V, et al. Development and validation of a simplified serotyping ELISA based on monoclonal antibodies for the diagnosis of foot-and-mouth disease virus serotypes O, A, C and Asia 1. Transbound Emerg Dis. 2020 Nov;67(6):3005.

88. Ludi AB, Morris A, Gubbins S, Asfor A, Afzal M, Browning CF, et al. Cross-Serotype Reactivity of ELISAs Used to Detect Antibodies to the Structural Proteins of Foot-and-Mouth Disease Virus. Viruses. 2022 Jul 8;14(7):1495.

89. Long SW, Linson SE, Ojeda Saavedra M, Cantu C, Davis JJ, Brettin T, et al. Whole-Genome Sequencing of Human Clinical Klebsiella pneumoniae Isolates Reveals Misidentification and Misunderstandings of Klebsiella pneumoniae, Klebsiella variicola, and Klebsiella quasipneumoniae. D'Orazio SEF, editor. mSphere. 2017 Aug 30;2(4):e00290.

90. Alkan C, Sajjadian S, Eichler EE. Limitations of next-generation genome sequence assembly. Nat Methods. 2011 Jan;8(1):61.

91. Heinz E, Pearse O, Zuza A, Bilima S, Msefula C, Musicha P, et al. Longitudinal analysis within one hospital in sub-Saharan Africa over 20 years reveals repeated replacements of dominant clones of Klebsiella pneumoniae and stresses the importance to include temporal patterns for vaccine design considerations. Genome Med. 2024 May 6;16(1):67.

92. Barbier E, Rodrigues C, Depret G, Passet V, Gal L, Piveteau P, et al. The ZKIR Assay, a Real-Time PCR Method for the Detection of *Klebsiella pneumoniae* and Closely Related

Species in Environmental Samples. Dudley EG, editor. Appl Environ Microbiol. 2020 Mar 18;86(7):e02711.

93. Downs SL, Madhi ShabirA, Van Der Merwe L, Nunes MartaC, Olwagen CP. Optimization of a high-throughput nanofluidic real-time PCR to detect and quantify of 15 bacterial species and 92 Streptococcus pneumoniae serotypes. Sci Rep. 2023 Mar 21;13(1):4588.

94. Slater D, Hutt Vater K, Sridhar S, Hwang W, Bielawski D, Turbett SE, et al. Multiplexed real-time PCR for the detection and differentiation of *Klebsiella pneumoniae* O-antigen serotypes. Manning SD, editor. Microbiol Spectr. 2024 Sep 3;12(9):e00375.

95. Argimón S, David S, Underwood A, Abrudan M, Wheeler NE, Kekre M, et al. Rapid Genomic Characterization and Global Surveillance of *Klebsiella* Using Pathogenwatch. Clin Infect Dis. 2021 Dec 1;73(Supplement_4):S325.

96. Clamp M, Cuff J, Searle SM, Barton GJ. The Jalview Java alignment editor. Bioinformatics. 2004 Feb 12;20(3):426.

97. Huang L, Fu L, Hu X, Liang X, Gong G, Xie C, et al. Co-occurrence of Klebsiella variicola and Klebsiella pneumoniae Both Carrying blaKPC from a Respiratory Intensive Care Unit Patient. Infect Drug Resist. 2021 Oct; Volume 14:4503.

98. Pan YJ, Lin TL, Chen YH, Hsu CR, Hsieh PF, Wu MC, et al. Capsular Types of Klebsiella pneumoniae Revisited by wzc Sequencing. 2013; Available from: www.plosone.org

99. Brisse S, Issenhuth-Jeanjean S, Grimont PAD. Molecular Serotyping of *Klebsiella* Species Isolates by Restriction of the Amplified Capsular Antigen Gene Cluster. J Clin Microbiol. 2004 Aug;42(8):3388.

100. Downs SL, Madhi SA, Van Der Merwe L, Nunes MC, Olwagen CP. High-throughput nanofluidic real-time PCR to discriminate Pneumococcal Conjugate Vaccine (PCV)-associated serogroups 6, 18, and 22 to serotypes using modified oligonucleotides. Sci Rep. 2021 Dec 9;11(1):23728.

101. Jacobsen N. LNA-enhanced detection of single nucleotide polymorphisms in the apolipoprotein E. Nucleic Acids Res. 2002 Oct 1;30(19):100e.

102. Integrated DNA Technologies [Internet]. [cited 2024 Sep 20]. OligoAnalyzer Tool - Primer analysis and Tm Calculator | IDT. Available from: https://eu.idtdna.com/pages/tools/oligoanalyzer

103. Kibbe W. OligoCalc: an online oligonucleotide properties calculator. 2007 [cited 2024 Sep 20]. OligoCalc: Oligonucleotide Properties Calculator. Available from: http://biotools.nubic.northwestern.edu/OligoCalc.html

104. Basic Local Alignment Search Tool [Internet]. [cited 2024 Sep 20]. BLAST: Basic Local Alignment Search Tool. Available from: https://blast.ncbi.nlm.nih.gov/Blast.cgi

105. Smati M, Clermont O, Bleibtreu A, Fourreau F, David A, Daubié A, et al. Quantitative analysis of commensal *Escherichia coli* populations reveals host-specific enterotypes at the intra-species level. MicrobiologyOpen. 2015 Aug;4(4):604.

106. Panjaitan NSD, Horng YT, Chien CC, Yang HC, You RI, Soo PC. The PTS Components in Klebsiella pneumoniae Affect Bacterial Capsular Polysaccharide

Production and Macrophage Phagocytosis Resistance. Microorganisms. 2021 Feb 8;9(2):335.

107. Gadsby NJ, McHugh MP, Russell CD, Mark H, Conway Morris A, Laurenson IF, et al. Development of two real-time multiplex PCR assays for the detection and quantification of eight key bacterial pathogens in lower respiratory tract infections. Clin Microbiol Infect. 2015 Aug;21(8):788.e1-788.e13.

108. Rosanna Hartline. Determination of Bacterial Numbers. In LibreTexts Biology; p. 1.15: Determination of Bacterial Numbers. (CC BY-NC-SA 4.0). Available from: https://bio.libretexts.org/Bookshelves/Microbiology/Microbiology_Laboratory_Manual_(Hartline)/01%3A_Labs/1.15%3A_Determination_of_Bacterial_Numbers

109. Bustin SA, Benes V, Garson JA, Hellemans J, Huggett J, Kubista M, et al. The MIQE Guidelines: Minimum Information for Publication of Quantitative Real-Time PCR Experiments. Clin Chem. 2009 Apr 1;55(4):611.

110. Madhi SA, Anderson AS, Absalon J, Radley D, Simon R, Jongihlati B, et al. Potential for Maternally Administered Vaccine for Infant Group B Streptococcus. N Engl J Med. 2023 Jul 20;389(3):215.

111. Mabena FC, Olwagen CP, Phosa M, Ngwenya IK, Van Der Merwe L, Khan A, et al. Bacterial and Candida Colonization of Neonates in a Regional Hospital in South Africa. Pediatr Infect Dis J [Internet]. 2023 Nov 20 [cited 2024 Feb 20]; Available from: https://journals.lww.com/10.1097/INF.0000000000004177

112. Olwagen CP, Jeche TR, Van Der Merwe L, Nunes MC, Madhi SA, Baillie VL. Nanofluidic qPCR unable to detect and serotype Streptococcus pneumoniae in urine samples of hospitalized South African patients with community-acquired pneumonia. Sci Rep. 2023 Dec 4;13(1):21332.

113. Jia R, Zhang G, Liu H, Chen Y, Zhou J, Liu Y, et al. Novel Application of Nanofluidic Chip Digital PCR for Detection of African Swine Fever Virus. Front Vet Sci. 2021 Feb 5;7:621840.

114. Kakiuchi S, Suzuki M, Dhoubhadel BG, Furumoto A, Ito H, Matsuki K, et al. Accuracy of High-Throughput Nanofluidic PCR-Based Pneumococcal Serotyping and Quantification Assays Using Sputum Samples for Diagnosing Vaccine Serotype Pneumococcal Pneumonia: Analyses by Composite Diagnostic Standards and Bayesian Latent Class Models. Bourbeau P, editor. J Clin Microbiol. 2018 May;56(5):e01874.

115. Coudray-Meunier C, Fraisse A, Martin-Latil S, Delannoy S, Fach P, Perelle S. A Novel High-Throughput Method for Molecular Detection of Human Pathogenic Viruses Using a Nanofluidic Real-Time PCR System. Sakamoto N, editor. PLOS ONE. 2016 Jan 29;11(1):e0147832.

116. Gorrie CL, Mirčeta M, Wick RR, Judd LM, Lam MMC, Gomi R, et al. Genomic dissection of Klebsiella pneumoniae infections in hospital patients reveals insights into an opportunistic pathogen. Nat Commun. 2022 May 31;13(1):3017.

117. Qin X, Wu S, Hao M, Zhu J, Ding B, Yang Y, et al. The Colonization of Carbapenem-Resistant Klebsiella pneumoniae: Epidemiology, Resistance Mechanisms, and Risk Factors in Patients Admitted to Intensive Care Units in China. J Infect Dis. 2020 Mar 16;221(Supplement_2):S206.

118. Dangor Z, Benson N, Berkley JA, Bielicki J, Bijsma MW, Broad J, et al. Vaccine value profile for Klebsiella pneumoniae. Vaccine. 2024 Jul;42(19):S125.

119. Heinz E, Pearse O, Zuza A, Bilima S, Msefula C, Musicha P, et al. Longitudinal analysis within one hospital in sub-Saharan Africa over 20 years reveals repeated replacements of dominant clones of Klebsiella pneumoniae and stresses the importance to include temporal patterns for vaccine design considerations. Genome Med. 2024 May 6;16(1):67.

APPENDIX A: TURNIT IN REPORT

turnitin

Digital Receipt

This receipt acknowledges that Turnitin received your paper. Below you will find the receipt information regarding your submission.

The first page of your submissions is displayed below.

Submission author:	Lara van der Merwe
Assignment title:	Final submission (all, regardless of course/programme)
Submission title:	Final_Turnitin_MSc Dissertation_(827385).pdf
File name:	Final_Turnitin_MSc_Dissertation__28827385_29.pdf
File size:	1.89M
Page count:	48
Word count:	13,426
Character count:	79,529
Submission date:	24-Feb-2025 02:34PM (UTC+0200)
Submission ID:	2597246331



Optimisation and validation of a nanofluidic real-time qPCR assay for the detection and serotyping of *Klebsiella pneumoniae*.

A DISSERTATION BY **LARA VAN DER MERWE** (Student no. 827385)

UNIVERSITY OF THE WITWATERSRAND JOHANNESBURG 1922 2022

SUBMITTED IN FULFILMENT OF THE REQUIREMENTS FOR THE DEGREE OF

MASTER OF SCIENCE IN MEDICINE (BY RESEARCH)

FROM THE FACULTY OF HEALTH SCIENCES

AT THE UNIVERSITY OF THE WITWATERSRAND, JOHANNESBURG

UNDER THE DEPARTMENT OF CLINICAL MICROBIOLOGY AND INFECTIOUS DISEASES

IN THE SCHOOL OF PATHOLOGY

Project Supervisors	Dr. Courtney Olivier Dr. Vicky Bellie Prof. Shabir Madhi
Date of Submission	25 February 2025

Copyright 2025 Turnitin. All rights reserved.

Final_Turnitin_MSc Dissertation_(827385).pdf

ORIGINALITY REPORT

14%	9%	12%	5%
SIMILARITY INDEX	INTERNET SOURCES	PUBLICATIONS	STUDENT PAPERS

PRIMARY SOURCES

1	www.ncbi.nlm.nih.gov Internet Source	3%
2	www.nature.com Internet Source	3%
3	H.-Y. Shu. "Genetic diversity of capsular polysaccharide biosynthesis in Klebsiella pneumoniae clinical isolates", Microbiology, 12/01/2009 Publication	1%
4	Rebekah M. Martin, Michael A. Bachman. "Colonization, Infection, and the Accessory Genome of Klebsiella pneumoniae", Frontiers in Cellular and Infection Microbiology, 2018 Publication	1%
5	Kelly L. Wyres, Margaret M. C. Lam, Kathryn E. Holt. "Population genomics of Klebsiella pneumoniae", Nature Reviews Microbiology, 2020 Publication	1%
6	wiredspace.wits.ac.za Internet Source	
7	Submitted to University of Witwatersrand Student Paper	1%
8	Daria Artyszuk, Wojciech Jachymek, Radosław Izdebski, Marek Gniadkowski, Jolanta Lukasiewicz. "The OL101 O antigen locus specifies a novel Klebsiella pneumoniae serotype O13 structure", Carbohydrate Polymers, 2023 Publication	1%
9	Martin, Rebekah Michal. "Identification of Clinical and Bacterial Genetic Risk Factors Associated with Klebsiella pneumoniae Infection", University of Michigan, 2023 Publication	1%
10	Submitted to Higher Education Commission Pakistan Student Paper	<1%
11	Ziyaad Dangor, Nicole Benson, James A. Berkley, Julia Bielicki et al. "Vaccine value profile for Klebsiella pneumoniae", Vaccine, 2024 Publication	<1%
12	"13th European Congress of Clinical Microbiology and Infectious Diseases", Clinical Microbiology and Infection, 2003 Publication	<1%
13	coloringfolder.com Internet Source	<1%
14	Min Wu, Xuefeng Li. "Klebsiella pneumoniae and Pseudomonas aeruginosa", Elsevier BV, 2015 Publication	<1%
15	Submitted to Queen's University of Belfast Student Paper	<1%
16	Tao Chen, Liya Ying, Luying Xiong, Xueting Wang, Ping Lu, Yuan Wang, Ping Shen, Yonghong Xiao. "Understanding carbapenem-resistant hypervirulent Klebsiella pneumoniae: Key virulence factors and evolutionary convergence", hLife, 2024 Publication	<1%
17	pmc.ncbi.nlm.nih.gov Internet Source	<1%
18	www.journalijar.com Internet Source	<1%
19	docplayer.net Internet Source	<1%
20	publications.aston.ac.uk Internet Source	<1%
21	www.jazindia.com Internet Source	
22	www.scirp.org Internet Source	<1%
23	Yan, Yue. "The NOTCH-RIPK4-IRF6-ELOVL4 Axis Suppresses Squamous Cell Carcinoma", McGill University (Canada), 2024 Publication	<1%
24	sajid.co.za Internet Source	<1%
25	www.researchsquare.com Internet Source	<1%
26	www.science.gov Internet Source	<1%

Exclude quotes	On	Exclude matches	< 10 words
Exclude bibliography	On		

APPENDIX B: ETHICS CERTIFICATE: CORRELATES OF PROTECTION STUDY, HREC NUMBER: 181110

University
of the Witwatersrand,
Johannesburg

Human Research Ethics Committee: (Medical)
FWA Registered No IRB 00001223

SECRETARIAT: Suite 189, Private Bag x2600, Houghton 2041, South Africa Tel: +27-11-274 9200 Fax: +27-11-274 9281

14 February 2019

EMAILED & COURIERED

Ms C Cockrell

Ethics & Regulatory Administrator
DST/NRF - RMPRU
11th Floor, West Wing, Nurses Residence
Chris Hani Baragwanath Hospital
2013

Fax: 086 567 1104

Dear Ms Cockrell,

PROTOCOL: GBS-COP - INVESTIGATING FOR IMMUNOLOGICAL CORRELATES OF PROTECTION AGAINST INVASIVE GROUP B STREPTOCOCCUS DISEASE IN INFANTS LESS THAN 90 DAYS OF AGE

ETHICS REFERENCE NO: 181110

RE : FINAL ETHICS APPROVAL

This is to certify that the above-mentioned trial has been approved by the University of the Witwatersrand, Human Research Ethics Committee (HREC), and the Protocol/Expert Reviewer. Date of Meeting where trial was reviewed: 30 November 2018.

The University of the Witwatersrand, Human Research Ethics Committee Approval Granted for the above mentioned study is valid for five years. Where required by Sponsor to have approval on a more frequent basis it remains the responsibility of the Sponsor and Investigator to apply for continuing review and approval, or for the duration of the Trial.

1. It is the responsibility of the Sponsor and Principal Investigator to ensure, where required, that relevant approvals are in place and compliance with the following is adhered to before a trial may begin:

- If trial is being conducted in Provincial Health facilities: Approval from the Hospital CEO / Clinic Manager / District Research Committee (whichever is applicable) be obtained.
- The study is submitted onto The National Health Research Database (NHRD).
- The relevant approvals are uploaded onto the NHRD system: Ethics Approval, SAHPRA Approval, Hospital CEO / Clinic Manager / District Research Committee Approval.

* A copy of the SAHPRA Approval and/or SAHPRA Notification letter must be submitted to the Ethics Secretariat Office for record purposes (IF SAHPRA APPROVAL / NOTIFICATION IS APPLICABLE).

* The study is conducted according to the protocol submitted to the University of the Witwatersrand, Human Research Ethics Committee. Any amendments to the protocol must first be submitted to the Human Research Ethics Committee for approval.

* During the study, the University of the Witwatersrand, Human Research Ethics Committee is informed immediately of :

- Any Unexpected Serious Adverse Events or Unexpected Adverse Drug Reactions, which, in the Investigator and/or the Sponsor's opinion are suspected to be related to the study drug. (Refer to POL-IEC–001 and SOP-IEC–005, Item 3.4).
- Any data received during the trial which, may cast doubt on the validity of the continuation of the study.

* The University of the Witwatersrand, Human Research Ethics Committee is notified of any decision to discontinue the study and the reason stated.

* The Investigators authorised by this approval participate in this study. Additional Investigators shall be submitted to the University of the Witwatersrand, Human Research Ethics Committee for approval prior to their participation in the study.

* In the event of an authorised Investigator ceasing to participate in the study, the University of the Witwatersrand, Human Research Ethics Committee must be informed and the reason for such cessation given.

2. PRINCIPLES OF INFORMED CONSENT:
* The University of the Witwatersrand, Human Research Ethics Committee requires that in all studies, the Principles of Informed Consent are adhered to. This applies to volunteers as well as patients.

3. PROGRESS REPORTS:
* The University of the Witwatersrand, Human Research Ethics Committee requests that the SAHPRA Progress Reports be submitted twice a year either in March and September or six monthly from start of study to the HREC Secretariat Office - 011 274 9281 and a report of the final results, at the conclusion of the study. (IF APPLICABLE)

4. REIMBURSEMENT TO PATIENTS FOR TRANSPORT:
* The Human Research Ethics Committee: (Medical) is in agreement that reimbursement per visit is according to the South African Health Products Regulatory Authority and that reimbursement should be appropriate according to the situation.

5. TRANSPORT AND STORAGE OF BLOOD AND TISSUE SAMPLES IN SOUTH AFRICA:
* If blood specimens are to be stored for future analysis and is planned that such analysis will be done outside Wits, then the blood must be stored at a facility in South Africa agreed with the relevant IRB, with release of sub-samples only once projects have been approved by the local Research Ethics Committee applicable to where the analysis will be done as well as by the Wits Human Research Ethics Committee: (Medical).

6. GENETIC TESTING:
* The Human Research Ethics Committee: Medical; will not approve open-ended genetic testing as this does not fit the Human Research Ethics Committee criteria.

7. GOOD CLINICAL PRACTICE:
* The South African Department of Health, South African Health Products Regulatory Authority requires Good Clinical Practice (GCP) Training for all Investigators in Clinical Trials, and that GCP training be renewed every three (3) years.

As yet, there are no National Guidelines for the content of GCP courses. Until these are available the Wits Human Research Ethics Committee (Medical) will note courses completed by Investigators without approval of the content of the individual courses.

8. THE SUPPORTING APPROVAL DOCUMENTS ARE ATTACHED:

8.1 Ethics Approval Form signed by the Chairperson of the HREC - Kindly return the copy of the Approval Form signed by the Principal Investigator(s) per fax: 011 274 9281 for our records (this is applicable with the initial Approval).

8.2 List of members present at the HREC meeting held as per INDEPENDENT ETHICS COMMITTEE APPROVAL FORM

9. WE AWAIT YOUR RESPONSES AS REQUESTED: Ensure to have these documents forwarded at the earliest for the HREC records.

* SAHPRA Approval letter and/or letter of Notification before the above study may commence / or where an Amendment may be implemented (IF SAHPRA APPROVAL / NOTIFICATION IS APPLICABLE). It remains the responsibility of the Principal Investigator and/or Sponsor to ensure that the relevant approvals are in place.

* Copy of Independent Ethics Declaration Approval Form signed by the Principal Investigator. (this is applicable with the initial Approval).

* Kindly forward the above to the undersigned at fax: 011 274 9281 at your earliest convenience.

Prof S Velaphi declared a conflict of interest.

The above has been noted for the Ethics Committee information and records.

KINDLY FORWARD TO THE RELEVANT INVESTIGATORS / CRA / SPONSOR / STUDY CO-ORDINATORS - WHERE APPLICABLE

Regards,

PROF CLEMENT P[illegible]
For and on behalf of the Human Research Ethics Committee: (Medical)

PENNY

APPENDIX C ETHICS CERTIFICATE: EPIDEMIOLOGY OF COMMUNITY AND HOSPITAL-ACQUIRED INVASIVE INFECTIONS IN YOUNG INFANTS, HREC NUMBER: M200932

UNIVERSITY OF THE WITWATERSRAND, JOHANNESBURG

R14/49 Dr Fikile Cynthia Mabena

HUMAN RESEARCH ETHICS COMMITTEE (MEDICAL)

CLEARANCE CERTIFICATE NO. M200932

NAME: (Principal Investigator)	Dr Fikile Cynthia Mabena
DEPARTMENT:	Paediatrics Chris Hani Baragwanath Academic Hospital Thelle Mogoerane Hospital and Leratong Hospital
PROJECT TITLE:	Epidemiology of community and hospital-acquired invasive infections in young infants
DATE CONSIDERED:	02/10/2020
DECISION:	Approved unconditionally
CONDITIONS:	
SUPERVISOR:	Prof S. Madhi and Prof S. Velaphi
APPROVED BY:	Dr CB Penny, Chairperson, HREC (Medical)
DATE OF APPROVAL:	09/12/2020

This clearance certificate is valid for 5 years from date of approval. Extension may be applied for.

DECLARATION OF INVESTIGATORS

To be completed in duplicate and **ONE COPY** returned to the Research Office Secretary on the Third Floor, Faculty of Health Sciences, Phillip Tobias Building, 29 Princess of Wales Terrace, Parktown, 2193, University of the Witwatersrand. I/we fully understand the conditions under which I am/we are authorized to carry out the above-mentioned research and I/we undertake to ensure compliance with these conditions.Should any departure be contemplated, from the research protocol as approved, I/we undertake to resubmit the application to the Committee. I **agree to submit a yearly progress report.** The date for annual re-certification will be one year after the date of convened meeting where the study was initially reviewed. In this case, the study was initially reviewed in **October** and will therefore be due in the month of **October** each year. Unreported changes to the application may invalidate the clearance given by the HREC (Medical).

Principal Investigator Signature

11/06/2021
Date

PLEASE QUOTE THE PROTOCOL NUMBER IN ALL ENQUIRIES

APPENDIX D ETHICS CERTIFICATE: OPTIMISATION AND VALIDATION OF A NANOFLUIDIC REAL-TIME QPCR ASSAY FOR THE DETECTION AND SEROTYPING OF *KLEBSIELLA PNEUMONIAE*, (M231117).

UNIVERSITY OF THE WITWATERSRAND, JOHANNESBURG	HUMAN RESEARCH ETHICS COMMITTEE (MEDICAL)

Office of the Deputy Vice-Chancellor (Research and Innovation)

TO: Ms L van der Merwe
School of Pathology
Wits VIDA - Vaccines and Infectious Diseases
Analytics Research Unit
Medical School
University

E-mail: lara.vandermerwe@wits-vida.org

CC: Supervisor: Drs C Olwagen and V Baillie; Professor SA Madhi
Courtney.Olwagen@wits-vida.org
and <HREC-Medical Research Office@wits.ac.za>

FROM: Mr Iain Burns
Human Research Ethics Committee (Medical)
Tel: 011 717 1252

E-mail: Iain.Burns@wits.ac.za

DATE: 15 February 2024

REF: R14/49

PROTOCOL NO: **M231117** (This is your ethics application reference number. Please quote it in all enquiries, oral or written, relating to this study.)

PROJECT TITLE: *Optimization and validation of a nanofluidic real-time qPCR assay for detection and serotyping of Klebsiella pneumoniae*

Please find attached the Clearance Certificate for the above project. I hope it goes well and that an article in a recognized publication comes out of it. This will reflect well on your professional standing and contribute to Government funding of the University.

MSWorks2000/Iain0007/Clearscan.wps

UNIVERSITY OF THE WITWATERSRAND JOHANNESBURG

R49 Ms L van der Merwe

HUMAN RESEARCH ETHICS COMMITTEE (MEDICAL)
CLEARANCE CERTIFICATE NO. M231117

NAME: Ms L van der Merwe **DEGREE:** MSc (Med)
(Principal and Co-Investigators)

DEPARTMENT: School of Pathology
Wits VIDA - Vaccines and Infectious Diseases
Analytics Research Unit
Medical School
University

PROJECT TITLE: *Optimization and validation of a nanofluidic real-time qPCR assay for detection and serotyping of Klebsiella pneumoniae*

DATE CONSIDERED: 24 November 2023

DECISION: Approved unconditionally

CONDITIONS:

NOTE: If contact information regarding student study participants is required, please contact the Registrar's office <Nicoleen.Potgieter@wits.ac.za>

SUPERVISOR: Drs C Olwagen and V Baillie; Professor SA Madhi

APPROVED BY:
Ms M van Niekerk, Co-Chairperson, HREC (Medical)

DATE OF APPROVAL: 15 February 2024 **EXPIRY DATE:** 14 February 2029

This Clearance Certificate is valid for 5 years from the date of approval. An extension may be applied for.

DECLARATION OF INVESTIGATORS

To be completed in duplicate and **ONE COPY** returned to the Research Office secretariat on the 3rd floor, Phillip Tobias Building, Parktown, University of the Witwatersrand, Johannesburg.

I/we fully understand the conditions under which I am/we are authorized to carry out the above-mentioned research and I/we undertake to ensure compliance with these conditions. Should any departure be contemplated from the research protocol as approved, I/we undertake to submit details to the Committee. **I agree to submit a yearly progress report** in the format available at https://wits.ac.za/research/researcher-support/research-ethics/ethics-committees/. This report is due annually, for the duration of the Clearance Certificate, beginning on the first anniversary of Date of Approval above. Unreported changes to the study may invalidate the clearance given by the HREC (Medical).

L v.d Merwe 16/02/2024

Signature of Principal Investigator Date